

NASCI Abstracts

Published online: 17 January 2007
© Springer Science+Business Media B.V. 2007

06-A-11-NASCI

The relationship between target heart rate and ischemia in myocardial perfusion imaging using stress protocol of Treadmill exercise

Ali Gholamrezanezhad, Sahar Mirpour, Hadi Hajimohammadi
Tehran university of medical sciences, Tehran, Iran (Islamic Republic of)
e-mail: gholamrezanezhad@razi.tums.ac.ir

Background Treadmill exercise (ETT) is one of the most helpful diagnostic tools in the field of cardiology. It has been used frequently as one of the main stress protocols and the best physiological stress technique for scintigraphic assessment of ischemia and myocardial perfusion imaging (MPI). However, it has been postulated that if patients fail to achieve their age-predicted target heart rate (THR), the electrocardiographic changes following ETT stress and also scintigraphic results of this stress protocol for MPI are unreliable. We decided to assess the ability of submaximal ETT in provoking ischemia as determined by MPI.

Methodology One hundred and nine patients (60 F, 49 M) were prospectively assessed

with MPI after stress protocol of ETT. Patients were advised to discontinue Beta-blockers and nitrates before test. Forty-nine patients failed to attain THR (due to fatigue, breathlessness or other causes). MPI was performed based on 1-day protocol, using Tc-sestamibi.

Results 60 patients attained THR, of which 28 patients (46.7%) had normal myocardial perfusion pattern and 32 patients (53.3%) had scintigraphic evidences of ischemia. The remaining 49 patients had submaximal ETT, of which 15 patients (30.6%) had normal MPI and 34 patients (69.4%) had scintigraphic evidences of ischemia. The prevalence of ischemia was significantly higher in patients with submaximal ETT ($P < 0.01$).

Conclusion In our study, ischemia was more common in patients who had performed a sub-maximal ETT. It could be a logical hypothesis that ischemic heart disease limits the ability of patients to complete ETT and therefore, it would not be judged that submaximal ETT is always insufficient for MPI. In these settings, it could be possible to administer the radiopharmaceutical in the peak heart rate even if the patient fails to attain their THR (except when HR is slowed by a beta-blocking or bradycardic drug or other known nonischemic causes of slowing HR).

06-A-12-NASCI

Coronary CT angiography with 64-MSCT in ESRD patients: comparison with invasive coronary angiography

Eun Jeong Choi^{1,2}, Byoung Wook Choi², Young Jin Kim², Jae Seung Seo², Kyu Ok Choe², Beom Suk Kim²

¹Korea Univ Hospital, Seoul, Republic of Korea

²Yonsei Medical Center, Seoul, Republic of Korea
e-mail: cadpel2@naver.com

Purpose As the leading cause of death, cardiovascular disease due to coronary arterial calcification and stenosis is one of the major problems correlated with morbidity and mortality in end stage renal disease (ESRD) patients.

Material and methods From 1 May 2005 to 30 September 2005, 24 (M: F = 18:6, mean age 61.5) patients newly diagnosed as ESRD agreed to coronary evaluation. All patients were about to initiate peritoneal dialysis (PD) or had a history of PD once before CTA, free of cardiac symptoms without past history of cardiac event. All CTA were taken by 64-MSCT with informed consents before examinations. Conventional coronary angiography (CCA) was done in cases of significant coronary stenosis in CTA.

Results The results of CTA of all 24 patients were divided as 2 groups: (1) group without significant coronary luminal narrowing ($n = 6$) and (2) group with significant coronary luminal narrowing ($n = 19$). In CTA of group 2, multifocal soft and/or calcified plaques were noted with Agaston scores ranged from 0.0 to 1647.8 (mean 485.4) and 80% or more coronary arterial luminal narrowing.

Conclusion In the possibility of coronary disease, severe or not, is always considered in ESRD patients, even though they have no symptom. CTA is a very useful noninvasive tool to diagnose subclinical and not symptomatic coronary disease in ESRD patients.

06-A-13-NASCI

A large correlative study comparing current different methods of calculating left ventricular ejection fraction

Ali Gholamrezanezhad, Sahar Mirpour, Mohsen Saghari, Mohammad Eftekhari, Armaghan

Fard-Esfahani, Babak Fallahi, Davood Beiki
Tehran University of Medical Sciences, Tehran,
Iran (Islamic Republic of)
e-mail: gholamrezanezhad@razi.tums.ac.ir

Background Left ventricular ejection fraction (EF) is a major determinant of survival in patients with coronary artery disease (CAD). Comparative accuracy of current modalities in calculating EF is not well investigated.

Method We compared EF as calculated by rest and post-stress Cedars automated quantitative gated SPECT (AQGS), rest and post-stress semi-automatically processed gated SPECT (MQGS), echocardiography and contrast ventriculography (LVG) to those determined by rest and post-stress cavity-to-myocardium ratio (CMR) in 109 patients. Gated SPECT was performed based on 2-day protocol using Tc-MIBI.

Results Mean EF in LVG, echo, post-stress CMR, rest CMR, post-stress AQGS, rest AQGS, post-stress MQGS and rest MQGS were $41.8\% \pm 12.1$, $44.8\% \pm 11.8$, $38.1\% \pm 10.7$, $35.7\% \pm 12.1$, $44.5\% \pm 15.1$, $46.9\% \pm 14.7$, $40.1\% \pm 14.3$ and $43.5\% \pm 14.3$, respectively. Although significant differences were observed between some of these pairs, good and excellent linear correlations were present among values (all Pearson correlations > 0.63). Considering LVG as gold standard, we defined 2 groups: EF $< 35\%$ (class 1) and $> 35\%$ (class 2). Discriminant analysis showed SPECT has the ability to predict patient's class. In 4/18 of patients with normal SPECT (on both visual and quantitative analyses, SSS < 4), EF on QGS showed a significant drop on post-stress compared with rest (Delta EF = Rest EF - Stress EF).

Conclusion (1) Good correlation exists among different routine methods (LVG, echocardiography, gated SPECT), but the raw values of EF in different techniques are not identical and cannot be used interchangeably. (2) Adding delta EF to other quantitative ischemic indices (SSS, SDS, SRS) can increase the CAD diagnostic accuracy. Thus performing gated procedure on both phases of study may allow identification of post-stress stunning that may aid in diagnosis of CAD, particularly in multi-vessel disease. (3) In patients with SSS (Summed Stress Score) $> = 13$, post-stress gated SPECT can not predict angiographic EF as accurately as patients

with $SSS < 13$. (4) Whenever gating is impossible, calculation of LVCMR is a reliable alternative.

06-A-16-NASCI

Masses of the heart; are they true tumors or not?

Eun Jeong Choi¹, Byoung Wook Choi², Young Jin Kim², Jae Seung Seo², Kyu Ok Choe²

¹Korea Univ Hospital, Seoul, Republic of Korea

²Yonsei Medical Center, Seoul, Republic of Korea

e-mail: cadpel2@naver.com

The diagnosis of cardiac masses has been getting better because of the fast and fabulous development of CT and MR. Detection and differential diagnosis of cardiac masses is important especially when the masses are small and no definite evidence of malignancy such as metastasis or adjacent invasion. We reviewed the CT and MR images of patients diagnosed as cardiac tumor, benign or malignant.

06-A-17-NASCI

The accurate identification and evaluation of bicuspid aortic valve by cardiac magnetic resonance imaging

Imran Syed, Jerome Breen
Mayo Clinic, Rochester, MN, USA
e-mail: syed.imran@mayo.edu

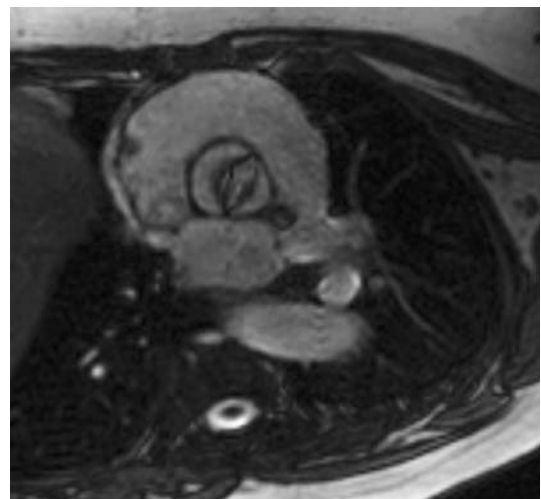
Background Bicuspid aortic valve (BAV) is a common congenital abnormality seen in 1–2% of the population. The diagnosis is usually made by echocardiography. Although there are several single case reports of BAV being visualized by cardiac magnetic resonance (CMR), the ability of this modality to accurately identify BAV in a series of patients has never been reported.

Methods A series of 27 patients with a diagnosis of BAV after transthoracic echocardiography subsequently underwent CMR with accurate positioning of the imaging plane perpendicular to

the aortic valve leaflets in order to evaluate valve morphology. The presence or absence of aortic stenosis and/or regurgitation (semi-quantitative) and any coexistent aortic pathology such as aortic dilatation or coarctation were also assessed.

Results CMR correctly identified 26 of the patients as having BAV. The one remaining patient identified as having BAV on echocardiography, appeared to have a tri-leaflet valve on CMR. A tri-leaflet valve was in fact later confirmed during surgery. There was excellent correlation with echocardiography with regard to commissural location, the presence of aortic stenosis (12 patients with both echocardiography and CMR) and aortic regurgitation (15 patients with both echocardiography and CMR). Both modalities also identified two patients as having aortic coarctation, and 16 patients with some degree of aortic dilatation.

Conclusions CMR is a highly accurate modality for the identification of bicuspid aortic valve, provided an accurate imaging plane is obtained perpendicular to the aortic valve leaflets. It offers the advantage of concomitant evaluation of associated conditions such as ascending aortic dilatation and aortic coarctation. Furthermore, CMR may be helpful in confirming the diagnosis of bicuspid aortic valve when echocardiographic assessment is hindered by poor acoustic windows.



06-A-21-NASCI

Evaluation of the optimal image reconstruction interval for coronary artery imaging using 64-slice CT

Markus Weininger, Christian Ritter, Meinrad Beer, Dietbert Hahn, Matthias Beissert
University Hospital of Wuerzburg, Wuerzburg, Germany.
e-mail: weininger@roentgen.uni-wuerzburg.de

Purpose To prospectively evaluate if there is a specific image reconstruction interval providing optimal image quality for all coronary segments and each coronary artery.

Method and materials In a clinical study 296 coronary artery segments of 20 patients (14 males, 6 females; mean age 54 ± 10 years) with a mean heart rate of 66 ± 12 beats per minute (bpm) were analyzed using a 64-slice CT scanner (Siemens) and a standardized scanning protocol. Oral β -blockers were administered to 10 patients with a baseline heart rate > 70 bpm. Data reconstruction was performed in 5% increments from 5% to 100% of the R-R interval using maximum intensity projections (slice thickness 3.0 mm, reconstruction increment 1.5 mm). Four blinded experienced observers independently evaluated image quality of the coronary arteries according to the 15 segment AHA classification. A 3-point ranking scale was applied: 1, very poor, no evaluation possible; 2, diagnostically sufficient quality; 3, highest image quality, no artifacts.

Results In the mean of all patients the best reconstruction point for all 15 segments was found to be at 65% of the R-R interval (mean 2.3 ± 0.5 ; $P < 0.05$). Divided into each coronary artery best image quality could be achieved by again referencing image reconstruction to 65% of the R-R interval: RCA, 2.1 ± 0.5 ; LCA, 2.3 ± 0.5 ; LM, 2.5 ± 0.2 ; LAD, 2.3 ± 0.4 ; LCX, 2.3 ± 0.5 . The same applied for segments 8, 9, 10, 12, 14 and 15. No significant influence of the heart rate was found for all analyzed distinctions.

Conclusions Our results show that by using a 64-slice CT scanner with a gantry rotation time of 330 ms the need for accordingly adjusting the

reconstruction point to each coronary segment might be overcome as diagnostically sufficient image quality as well as best image quality could be achieved with image reconstruction at 65% of the R-R interval for all coronary segments and each coronary artery, respectively.

06-A-22-NASCI

Variability of coronary calcium scores at different image reconstruction intervals using 64-slice CT

Markus Weininger, Christian Ritter, Meinrad Beer, Dietbert Hahn, Matthias Beissert
University Hospital of Wuerzburg, Wuerzburg, Germany
e-mail: weininger@roentgen.uni-wuerzburg.de

Purpose To evaluate the variability of coronary calcium scores depending on the image reconstruction interval using a 64-slice CT scanner with a fast gantry rotation time of 330 ms.

Method and materials In a clinical study 21 patients (12 males, 9 females; mean age 56 ± 11 years) with a mean heart rate of 68 ± 7 beats per minute (bpm) underwent coronary calcium scoring using a 64-slice CT scanner (Siemens, Germany) and a standardized scanning protocol (collimation 1.5 mm, rotation time 0.33 s, 120 kV, 190 mAs eff.). Oral β -blockers were administered to 12 patients to reduce heart rates. Image reconstruction (slice thickness 3 mm, increment 1.5 mm) was performed in 10% increments from 0% to 100% of the RR-interval. Two blinded experienced observers independently calculated Agatston (AS), calcium mass (MS) and volume scores (VS) for every reconstructed image series using syngo CaScoring software (Siemens).

Results Excellent inter-observer agreement was achieved ($K = 0.98$). Mean values and mean coefficients of variation among all patients were as follows: AS, 224 ± 396 , 77%; MS, 40 ± 68 , 70%; VS, 200 ± 362 , 81%. Image reconstruction interval dependent analysis displayed mean coefficients of variation of 81% (AS), 79% (VS) and 74% (MS), respectively. No statistical significant difference in variations depending on the image

reconstruction interval could be found for AS, VS and MS ($P > 0.05$).

Conclusions Our results show that by using a 64-slice scanner with fast gantry rotation values for VS, AS and MS display a wide range of variability depending on the image reconstruction interval. Our findings are in concordance with prior studies using 4- and 16-slice CT scanners and reporting similar results. We could not identify a specific image reconstruction interval displaying a significant lesser variability. This indicates that for accurate and reproducible quantification of coronary calcium scores still more than one reconstruction interval needs to be evaluated.

06-A-23-NASCI

Correlation between stress myocardial perfusion imaging and myocardial jeopardy score: usefulness of electrocardiographic parameters

Jyotiranjana Pradhan¹, Ashutosh Niraj², Hema Vankayala², Priya Kumaravelu², Mona Trivedi², Deepak Thatai²

¹Detroit Medical Center, Detroit, MI, USA

²Wayne State University, Detroit, MI, USA

e-mail: jspradhan@gmail.com

Background Defining the correlation between Myocardial Perfusion Imaging results and myocardial jeopardy score carries prognostic information in terms of future cardiac events. EKG parameters correlation with jeopardy score during adenosine stress Tc-99 sestamibi SPECT MPI has been evaluated in this study.

Method 88 consecutive male patients, who had positive stress SPECT MPI, were followed with coronary angiogram and classified into two groups: Cohort 1, with no significant stenosis, ($n = 34$), Duke Score = 0; and Cohort 2 ($n = 54$), with significant CAD, Duke Score ≥ 2 . Resting and stress QTc & QTd, Δ QTc (=Stress QTc-resting QTc) and Δ QTd (=Stress QTd-resting QTd) were evaluated as independent predictor for severity of CAD against baseline cardiovascular risk factors.

Results On student's *t*-test, mean resting QTd was higher in cohort 2 compared to cohort 1. During peak infusion of adenosine, QTd got

significantly prolonged in cohort 1 but remain unchanged or 'fixed' in cohort 2. In both groups, means of resting QTc were same and QTc got prolonged during stress test. Thus unlike QTd, QTc failed to differentiate the angiography findings between the study cohorts. In patient with significant CAD, resting QTd and stress QTd were positively correlated with Duke score (rho coeff. 0.4 and 0.5 respectively, $P < 0.01$) on bivariate correlation analysis. In the final model of Binomial logistic stepwise multiple regression analysis, independent predictors for significant CAD were hypercholesterolemia (OR 6.8, $P < 0.01$), Δ QTd (OR 3.7 for 1st and 2nd Quartile compared to 3rd and 4th Quartile, $P < 0.05$) and diabetes (OR 2.8, $P < 0.10$).

Conclusion Δ QTd and hypercholesterolemia, if considered as adjunctive clinical marker during stress MPI, can improve its accuracy in diagnosing significant CAD. In addition, resting QTd during stress MPI correlated with jeopardy score and therefore, carries prognostic information for cardiovascular morbidity and mortality.

06-A-26-NASCI

64-slice CT coronary angiography with ct cardiac function analysis and cardiac catheterization compared with myocardial perfusion imaging for diagnosis of functionally relevant coronary artery stenosis

Christian Thilo, Salvatore Chiaramida, Shaun Nguyen, Giancarlo Savino, Randall Goodroe, Peter Zwerner, Philip Costello, U. Joseph Schoepf MUSC, Charleston, SC, USA

e-mail: thilo@musc.edu

Purpose We compared coronary CTA (cCTA) without and with functional analysis and quantitative catheter angiography (QCA) for predicting ischemia on myocardial perfusion imaging (MPI).

Methods 33 patients with suspected CAD underwent 64-slice cCTA, QCA and gated SPECT-MPI. Two blinded observers analyzed cCTA and QCA for $\geq 50\%$ and $\geq 70\%$ stenosis. CT myocardial function was analyzed for global and regional abnormalities using a dedicated workstation. Rest and stress MPI studies were ana-

lyzed for perfusion deficits and their respective coronary territories. cCTA without and with functional analysis was compared with QCA for predicting ischemia on MPI.

Results 131 coronary arteries were analyzed. cCTA and QCA detected $\geq 50\%$ stenosis in 23 and 27 ($P = 0.95$) and $\geq 70\%$ in 18 and 17 ($P = 0.90$) vessels. Stenosis $\geq 50\%$ ($\geq 70\%$) in any vessel on cCTA predicted perfusion deficits on MPI in any region with 58% (50%) sensitivity, 79% (77%) specificity, 79% (75%) PPV, and 58% (53%) NPV. On QCA, stenosis $\geq 50\%$ ($\geq 70\%$) in any vessel predicted perfusion deficits on MPI in any region with 57% (53%) sensitivity, 50% (83%) specificity, 67% (83%) PPV, and 40% (53%) NPV. On cCTA, the location of 12/23 stenoses $\geq 50\%$ matched with perfusion deficits on MPI versus 14/27 on QCA ($P = 0.83$). For predicting matching perfusion deficits on MPI, $\geq 50\%$ ($\geq 70\%$) stenosis on cCTA had 43% (35%) sensitivity, 87% (91%) specificity, 52% (61%) PPV, and 82% (79%) NPV. On QCA, $\geq 50\%$ ($\geq 70\%$) stenosis predicted matching perfusion deficits with 45% (33%) sensitivity, 87% (94%) specificity, 54% (69%) PPV, and 82% (79%) NPV. There was excellent ($r = 0.92$) correlation between CT functional analysis and MPI for regional functional abnormalities.

Conclusion cCTA and QCA correlate only moderately with ischemia on MPI but very well with each other. CT function correlates very well with MPI. cCTA has the potential to replace catheter angiography in an MPI-based algorithm for CAD workup.

06-A-27-NASCI

Can non-calcified coronary plaques be detected on non-contrast calcium scoring studies?

Christian Thilo, Florian Mayer, Peter Zwerner, Philip Costello, U. Joseph Schoepf
MUSC, Charleston, SC, USA
e-mail: thilo@musc.edu

Purpose It has been demonstrated that contrast enhanced CT coronary angiography (cCTA) can

detect non-calcified coronary artery plaque. Depending on tissue composition, attenuation of non-calcified plaque differs significantly from non-enhanced blood and epicardial fat. We investigated, if non-calcified plaque can be detected on non-contrast calcium scoring scans.

Method and materials After IRB approval, 106 patients (40 females, 66 males, mean age 58.5 years, range 27–79 years) underwent non-contrast calcium scoring scans, contrast enhanced 64-slice (Siemens) cCTA and quantitative cardiac catheterization angiography (QCA). The calcium score (Agatston, Volume) was determined in each patient. Two blinded observers independently reviewed the non-contrast calcium scoring scans for findings suggestive of non-calcified plaque. Criteria included features of vascular remodeling and detection of hypo-attenuating areas within the vessel wall, not explained by volume averaging or blooming artifact from adjacent calcifications. Findings at non-contrast calcium scoring scans were then compared with lesion morphology at cCTA and QCA.

Results The mean Agatston score was 379, with a mean Volume score of 457. Interobserver variability for identification of suspicious lesions was excellent ($\kappa = 0.83$). Observer 1 and observer 2 identified 19 and 21 patients, respectively, with a total of 37 and 35 suspicious lesions suggestive of non-calcified plaque. Contrast enhanced cCTA confirmed presence of non-calcified plaque in 32/37 (observer 1) and in 29/35 (observer 2) lesions ($P = 0.89$). Thus, in this cohort, the overall positive predictive value for the correct identification of non-calcified plaque on non-contrast calcium scoring scans was 0.86. 12 (38%) and 13 (45%) of the detected lesions showed stenosis $\geq 50\%$ on QCA.

Conclusion Non-calcified plaque can be detected with fairly high positive predictive value and inter-reader reproducibility based on non-contrast enhanced calcium scoring scans. Calcium scoring scans should be reviewed for features of non-calcified plaque. This may allow identification of patients with more active disease and significant coronary artery stenosis.

06-A-28-NASCI**Coronary artery calcium: correlation of calcification patterns with non-calcified plaque and stenosis**

Florian Mayer, Christian Thilo, Shaun Nguyen, Peter Zwerner, Philip Costello, U. Joseph Schoepf
 MUSC, Charleston, SC, USA
 e-mail: mayerflo@musc.edu

Purpose It has been shown that there is no one-on-one relationship between the overall coronary artery (CA) calcium score (CS) and stenosis. We investigated, whether regional calcification patterns correlate better with stenosis and non-calcified plaque.

Methods 106 patients underwent quantitative catheter angiography (QCA), non-contrast CS and contrast enhanced 64-slice coronary CTA. In each patient, a global CS was calculated as well as regionally for each vessel. Based on the CS scan, two blinded observers noted the location of each calcified plaque and classified the calcification pattern as calcified nodule (punctate), shell-like (eccentric) or diffuse (circumferential). CTA studies were then evaluated for the presence and location of non-calcified plaque, with or without association with calcified plaque. The global CS, the regional CS and the calcification pattern were correlated with stenosis at QCA.

Results CA calcium was found in 93 patients. 56/106 patients had stenosis at QCA. The average global CS was 457.1 ± 59.8 . The average CS for the major coronary arteries were LM 31.2 ± 17.21 , LAD 258.7 ± 57.69 , Cx 43.36 ± 12.43 , RCA 190.1 ± 58.44 . On a per-patient basis there was no good correlation ($r = .36$) of the global CS with the presence and degree of stenosis. Correlation was somewhat better (LM $r = 0.56$, LAD $r = 0.61$, Cx $r = 0.55$, RCA $r = 0.67$) on a per-vessel basis. Calcified nodules did not correlate ($r = -0.002$) with stenosis, while shell-like calcifications ($r = 0.61$) and diffuse calcifications ($r = 0.69$) showed good correlation with stenosis. Shell-like calcifications ($r = 0.57$) and diffuse calcifications ($r = 0.51$) were also frequently associated with non-calcified plaque,

while this was not true for calcified nodules ($r = 0.28$).

Conclusion As shown before, the global CS does not correlate well with CA stenosis. Calcified nodules are generally not associated with stenosis. Shell-like and diffuse calcifications are frequently associated with non-calcified plaque and stenosis. These findings may help improve the specificity of CA calcium scoring for identifying individuals with CA stenosis.

06-A-29-NASCI**Triphasic contrast injection improves diagnosis of the right heart at coronary CT angiography**

Christian Thilo, Matthias Kerl, James Ravenel, Shaun Nguyen, Corey Jensen, Philip Costello, U. Joseph Schoepf
 MUSC, Charleston, SC, USA
 e-mail: thilo@musc.edu

Purpose At coronary CTA, a saline chaser is ordinarily used for reducing streak artifacts from dense contrast in the superior vena cava and the right heart. In many cases, however, the void of contrast precludes right heart analysis. We aimed at improving right heart diagnosis by using a triphasic injection protocol with a contrast/saline mixture during the second phase of injection.

Methods Seventy-five patients underwent contrast enhanced 64-slice coronary CTA: 25 with a monophasic iodine-only protocol using a single-syringe injector; 25 with a biphasic protocol (iodine bolus followed by a saline chaser) using a dual-syringe injector; and 25 with a triphasic protocol using Dual Flow (Medrad) technology with simultaneous injection from two syringes to achieve a 70%/30% mixing ratio of saline and contrast (50 cc volume), also followed by a saline chaser. Two radiologists rated the visualization of right and left heart structures and the degree of streak artifacts. One observer performed attenuation measurements of the left and right heart and of the coronary arteries.

Results Contrast attenuation (mean \pm SE) in the right heart was significantly [$P < 0.05$] higher in the triphasic group (225.04 ± 46.74) than in the biphasic group (143.00 ± 83.321) but signifi-

cantly [$P < 0.05$] lower than in the monophasic group (320.72 ± 114.68). For the left heart and the coronary arteries there were no significant differences between the three groups. Artifacts occurred less frequently [$P < 0.05$] in the biphasic and triphasic groups in comparison to the monophasic group. Right heart structures were rated significantly [$P < 0.05$] better in the triphasic group compared to the two other groups while left heart structures showed no difference between the groups.

Conclusion Dual flow injection provides sufficient enhancement for assessing the right heart while streak artifacts from dense contrast material can generally be avoided. This approach appears recommendable for coronary CTA, as right heart pathology (thrombo-emboli, tumors, etc.) can be reliably detected.

06-A-30-NASCI

Extra-cardiac findings at cardiac CT: experience in 1,000 patients

Florian Mayer, U. Joseph Schoepf, Shaun Nguyen, Philip Costello, James Ravenel
MUSC, Charleston, SC, USA
e-mail: mayerflo@musc.edu

Purpose To investigate incidental findings at cardiac CT and their frequency based on indication for study.

Material and methods We retrospectively reviewed the reports of 964 cardiac studies over a 2 year period including 241 calcium scorings (CS), 425 coronary CTAs (CTA), 176 evaluations for pulmonary vein stenosis following radiofrequency ablation (PVS) and 122 evaluations of bypass grafts (CABG). The incidental cardiac findings were classified in (1) requiring immediate clinical evaluation (emergent) including acute aortic dissection, pulmonary embolism, and pneumonia; (2) requiring urgent follow-up; (urgent) including pulmonary nodule > 1 cm, aortic aneurysm and other lesions suspicious for neoplasm; (3) important, but non-urgent including pulmonary nodules < 1 cm, interstitial lung disease, pleural effusion and indeterminate liver or

adrenal lesions; and (4) incidental lesions requiring no specific follow-up including emphysema, benign liver or adrenal lesions and subsegmental atelectasis. Multiple linear regression and correlation were calculated to determine relationship between the indication and findings.

Results There were 323 extra-cardiac findings in 291 patients (30.2%). Of these, 190 patients (19.7%) had a finding in groups 1–3. By group, there was at least one extra cardiac finding in 27/241 CS (11.2%); 156/425 CTA (36.7%); 54/176 PVS (30.7%); 54/122 CABG (44.3%). Extra cardiac findings occurred significantly more frequently with CTA vs. Calcium scoring ($P < 0.001$) and significantly less with CTA vs. CABG ($P = 0.03$). Findings considered emergent/urgent occurred in 0.8%/6.8%/1.7%/4.1% of patients, respectively, while other important findings occurred in 8.3%/17.6%/15.5%/23.8% of patients. There were no significant relationships between the indication and specific findings.

Conclusion Important extra-cardiac findings are documented in up to 20% of cases. These occur more frequently in groups undergoing contrast enhanced studies compared with calcium scoring.

06-A-31-NASCI

Improved reliability of MRI measurements of carotid artery wall thickness with contrast enhancement

Saurabh Malhotra¹, Shenghen Lai², Harikrishna Tandri³, Ernesto Castillo⁴, Gilberto Szarf⁴, Bruce Wasserman¹

¹Division of Neuroradiology, Johns Hopkins University, Baltimore, MD, USA

²Bloomberg School of Public Health, Johns Hopkins University, Baltimore, MD, USA

³Division of Cardiology, Johns Hopkins University, Baltimore, MD, USA

⁴Department of Radiology, Johns Hopkins University, Baltimore, MD, USA

e-mail: drsmalhotra@hotmail.com

Purpose To compare the reliability of contrast-enhanced (CE) and T2-weighted (T2 W) black blood magnetic resonance imaging (BBMRI) for measuring carotid artery wall thickness.

Methods BBMRI images were acquired through carotid plaque using double inversion recovery fast spin-echo T2W and CE (0.1 mmol/kg gadolinium) T1-weighted sequences at corresponding locations in four subjects on a 1.5 T scanner. The image pair showing the thinnest wall was analyzed. MR parameters were: slice thickness, 2 mm; FOV, 14 cm; matrix, 256x256; 1 nex. Three trained analysts drew lumen and outer wall contours. The four vessel pairs were analyzed three times at intervals of at least 48 h. Intraclass correlation coefficient (R) and coefficient of variance (CV) were calculated for wall thickness measurements based on CE and T2W images.

Results There was no significant difference in carotid wall thickness measured by CE and T2W MRI for each vessel wall. Inter- and intra-observer R for CE images were 0.95 and 0.93, respectively, as compared to 0.69 and 0.53 for corresponding T2W images. The CV was 0.13 and 0.17 for CE and T2W images, respectively.

Conclusion CE BBMRI shows greater reliability for wall thickness measurements than T2W BBMRI. This reinforces the value of gadolinium administration for MRI measurements of the carotid wall.

06-A-38-NASCI

The analysis of pixel intensity (myocardial signal density) data: the quantification of myocardial perfusion by imaging methods

William McCarthy, Douglas Thompson
Maryland Medical Research Institute, Baltimore,
MD, USA
e-mail: wmccarthy@mmri.org

This paper describes a number of important issues in the quantification and analysis of myocardial perfusion data. We particularly emphasize the issue of clustering, which may be ubiquitous in studies of myocardial perfusion data. Clustering can take many forms, e.g., measurements of different sections of a heart or repeated measurements of the same research participant. Clustering typically has an effect on variance estimates. If clustering is not taken into account, with

positive intracluster correlations, the estimated variance can be smaller than it actually is and the opposite is true if there is a negative intracluster correlation. We illustrate several possible approaches to account for clustering, including adjusting standard errors for design effects and modeling the covariance structure within clusters using mixed models. These methods offer great flexibility for dealing with a wide variety of research designs and include the capability for adjusting for covariates. Similar methods can be used to account for clustering in both superiority and method comparison (equivalence) analyses.

06-A-39-NASCI

Likelihood of critical angiographic coronary artery disease in intermediate risk patients presenting to the emergency room utilizing resting myocardial perfusion imaging and cardiac biomarkers

Marcos Daccarett, Mouhanad Freih, Jessica Ottino, Ayad Jazrawi, Christian Machado, Souheil Saba
Providence Heart Institute, Southfield, MI, USA
e-mail: mdaccarett@yahoo.com

Background Chest pain remains one of the most common presenting complaints in emergency rooms. Despite optimal guidelines, intermediate risk patients receive unnecessary imaging testing prior to discharge. We conducted a prospective trial evaluating the feasibility of resting Myocardial Perfusion Imaging (MPI) combined with cardiac biomarkers as predictors of critical coronary artery disease (CAD).

Methods Patients classified as intermediate clinical risk according to the American College of Cardiology guidelines were included. Samples for troponin I, Brain Natriuretic Peptide (BNP), C-Reactive Protein (CRP) and Myeloperoxidase levels (MPO) were taken. Resting and stress MPI images with Technetium Tc99m Sestamibi were taken shortly after blood draws. A blinded reader reviewed the resting studies. Critical (> 70% stenosis) CAD was documented by selective quantitative coronary angiography.

Results A total of 23 patients were included, 14 of them females. The mean age was 63 ± 15 . Of the 23 patients, six (26%) had angiographically documented CAD, 50% of them with abnormal resting MPI. Of the patients with documented CAD, 67% had abnormal MPO levels (> 150 pg/ml), 17% abnormal troponin I levels (> 0.4 ng/ml) and 50% abnormal CRP levels (> 4 ng/ml). None of the CAD patients had abnormal BNP levels. In the patients without CAD, 23% had abnormal MPI, 41% abnormal MPO levels and 18% abnormal CRP levels. The BNP and troponin I levels were normal among all those without CAD. The negative likelihood ratio of CAD using all five diagnostic tests was 0.167 [CI95% 0.1–0.4] (Neg LR = 0.25 without resting imaging). Compiling all five diagnostic tests, the sensitivity and negative predictive value to detect CAD were 94% and 93%, respectively.

Conclusions In patients with intermediate risk presenting the ER due to chest pain, normal levels of specific cardiac biomarkers along with a normal resting MPI carry a very low likelihood of angiographically critical coronary artery disease.

06-A-40-NASCI

Coronary atherosclerotic plaque burden on computed tomographic arteriograms: correlation with Framingham and National Cholesterol education program risk estimates

Kevin Johnson¹, Jolanta Dennis¹, Wayne Martyn², David Dowe²

¹Yale University, New Haven, CT, USA

²Atlantic Medical Imaging, Galloway, NJ, USA
e-mail: kevin.johnson@yale.edu

Background It is unknown to what extent conventional coronary atherosclerosis risk estimates reflect the total burden of coronary plaque. Coronary computed tomographic arteriography for the first time allows a noninvasive approach to this question in a broad spectrum of patients.

Methods and results 510 outpatients presenting to a general radiology practice between February 2005 and March 2006 because of concern for elevated risk of coronary disease were

studied. Plaque burden was estimated on a per segment basis then summed. This total plaque burden score correlated moderately with Framingham risk estimates ($r^2 = 0.38$ for unmodified FRE, $r^2 = 0.43$ for modified FRE). For the unmodified FRE, 64.5% of all cases fell outside the matching quartiles (kappa = 0.14), and for the modified FRE 54% of cases (kappa = 0.26). For NCEP core risk categories, 54.2% of patients fell outside the diagonal (kappa = 0.16). Age and gender were most strongly correlated with total plaque burden (both $P < 0.0001$). Systolic blood pressure ($P < 0.001$), diabetes ($P = 0.002$), smoking history ($P = 0.01$) and history of non-coronary atherosclerosis ($P = 0.04$) all were associated with total plaque burden. Serum HDL cholesterol levels were negatively correlated ($P = 0.001$). Plaque burden showed a smooth upward trend with increasing total cholesterol/HDL ratio. Interestingly, no detectable trend of plaque burden with increasing levels of serum total cholesterol was seen.

Conclusions Conventional risk estimates correlate with total plaque burden in the coronary arteries, but the variation within individuals is wide, so that for many patients their risk estimate does not accurately reflect their plaque burden. Some individual factors correlate much more strongly with plaque burden than do others.

06-A-41-NASCI

Pitfalls in vessel selective visualization of coronary CTA

Peter van Ooijen, Riksta Dijkers, Gonda de Jonge, Matthijs Oudkerk

University Medical Center Groninge, University of Groningen, Groningen, The Netherlands

e-mail: p.m.a.van.ooijen@rad.azg.nl

Introduction The constant improvement in CT technique has enabled the visualization of the coronary arteries in an adequate way with high image quality. Besides this, the advancements in image processing techniques have enabled to visualize and segment the acquired data fast and easy. One of the main algorithms used nowadays

is the vessel selective segmentation of the coronary artery tree. Although this method is frequently used, it also has some major pitfalls.

Methods and materials 20 patients were scanned using a dual source MDCT (Definition, Siemens, Forchheim, Germany) using a standard protocol. Post-processing was performed on an AquariusWorkstation (TeraRecon, San Mateo, CA).

Results Vessel selective visualization is possible for all patients and requires approximately 3 min for full segmentation of all three major branches. Pitfalls are found in the apparent stenoses introduced by different artefacts. Furthermore, the algorithms used have many difficulties with segmentation of stents and other high contrast structures (e.g. calcified plaques). Static instead of dynamic viewing of the reconstructions could complicate the correct interpretation.

Conclusion Segmentation for vessel selective visualization is adequate in all cases. However, one should be aware of the pitfalls presented in this work and evaluate the data dynamically to obtain a correct diagnosis based on these visualizations.

06-A-42-NASCI

Multidetector-row CT coronary angiographic finding of myocardial bridging

SungMin Ko, JoongHyuk Kwon
Department of radiology, Dongsan Medical Center, Daegu, Republic of Korea
e-mail: ksm9723@yahoo.co.kr

Myocardial bridging is caused by muscles overlying the intramyocardial course of an epicardial coronary artery. The middle segment of the left anterior descending artery (LAD) is the most common site to be involved. Myocardial bridging is divided into superficial and deep type. While generally benign, myocardial bridges can cause angina, myocardial ischemia, myocardial infarction, left ventricular dysfunction, myocardial stunning, paroxysmal AV blockade, exercise-induced ventricular tachycardia, and sudden cardiac death. The diagnosis of myocardial bridging is made possible with the tunneled segment and

its systolic compression on the catheter angiogram, intravascular ultrasound, intracoronary Doppler ultrasound. But these modalities are invasive. MDCT coronary angiography enables to assess the length, depth, and precise location of the tunneled coronary segment. The phasic change of the luminal diameter of the intramyocardial segment can be assessed by comparing systolic and diastolic images. Also, MDCT coronary angiography may be helpful to avoid further invasive procedures in asymptomatic patients. In our study, among the 265 patients with chest pain examined with MDCT coronary angiography, 20 cases (7.5%) of myocardial bridging were detected. All cases of myocardial bridging were located at the middle third of the LAD. Superficial bridging was identified in 13 cases and deep bridging in seven cases. The length of tunneled artery was between 5 mm and 25 mm, with a mean of 15.6 mm, and the depth of tunneled artery was between 1.0 mm and 6.2 mm, with a mean of 3.1 mm. In 5/20 cases, bridges were clearly associated with chest pain. Eight patients had multifocal atherosclerotic stenosis of the coronary arteries with sparing the tunneled segment. The exhibit will demonstrate typical findings, classification, and complication of myocardial bridging with MDCT angiography as a reliable and noninvasive imaging technique.

06-A-43-NASCI

Radiologic features of cardiogenic pulmonary edema: focused on cardiac MDCT findings of underlying causes

SungMin Ko, JinSoo Choi, YoungHwan Kim
Department of Radiology, Dongsan Medical Center, Daegu, Republic of Korea
e-mail: ksm9723@yahoo.co.kr

Cardiogenic pulmonary edema (CPE) is a common and potentially fatal condition frequently encountered in emergency medicine. CPE is caused by pulmonary venous hypertension and is most commonly the result of left ventricular failure. The diagnosis of CPE is usually based on clinical information, chest radiographic findings,

and response to treatment. Regardless of the underlying cause of CPE, prompt diagnosis and management are very important in patients with CPE because of quickly developing respiratory failure. Mortality may be higher when the condition is associated with acute myocardial infarction or acute valvular dysfunction. Knowledge of the cause of CPE has important implications for treatment. Transthoracic echocardiography can evaluate myocardial and valvular function and can help identify the cause of pulmonary edema. Contrast-enhanced cardiac multidetector-row computed tomography (MDCT) has allowed assessment of the detailed cardiovascular morphology and can demonstrate cause of CPE. In this presentation, we show the characteristic MDCT features of various causes of CPE (acute myocardial infarction [AMI] with septal perforation, AMI with mitral regurgitation, Marfan syndrome with aortic regurgitation [AR], severe aortic and mitral valvular heart disease, prosthetic mitral valve dysfunction, leaflet escapes of prosthetic mitral valve, cardiomyopathy, severe left ventricular dysfunction, AR secondary to back-and-forth intimal flap movement of acute type A dissection, and cardiac tumor).

06-A-45-NASCI

ECG-correlated cardiac scanning with a 64-slice Dual Source CT (DSCT) system

Herbert Bruder¹, Rainer Raupach¹, Karl Stierstorfer¹, Martin Petersilka¹, Stefan Ulzheimer¹, Christoph Suess¹, Cynthia McCollough², Thomas Flohr¹
¹Siemens Medical Solutions, Forchheim, Germany
²Mayo Clinic, Rochester, MN, USA
 e-mail: herbert.bruder@siemens.com

In cardiac CT temporal resolution is directly related to the gantry rotation time of 3rd generation CT scanners which cannot be substantially reduced below current standards of 0.33–0.35 s due to mechanical limitations. We developed a dual-source-detector 3rd generation CT scanner (Siemens SOMATOM Definition) to overcome these limitations. The tube-detector pairs are

mounted on the gantry with an angular distance of 90°. Images are reconstructed using complementary data from each stream of detector data. Due to the mechanical configuration these data are acquired at the same temporal position in cardiac cycle. The benefits of the dual source-detector device are:

1. exposure time for a cardiac image is reduced by a factor of two, and
2. consequently, the temporal resolution is increased by the same factor of two.
3. Faster volume coverage in cardiac spiral imaging is achieved, because multi-segment reconstruction techniques often applied in single source cardiac CT, that limit the table feed, are not needed any more.

In contrast to single source cardiac CT the temporal resolution does not depend on the heart rate. An immediate consequence of 1. and 3. is an significant reduction of patient dose. For the dual source scanner with 330 ms rotation time a robust temporal resolution of 83 ms is established. The new scanner design shows significantly higher image quality in phantom measurements compared to a conventional multi-slice scanner with multi-segment cardiac reconstruction. The evaluation of clinical images from the recently introduced DSCT scanner demonstrates excellent image quality in coronary CTA examinations independent of the patient's heart rate at pitch values of typically 0.25–0.5. Due to the robust temporal resolution below 100 ms, coronary CTA exams can be performed without administration of β -blockers. Fast volume coverage combined with efficient mA modulation enable examination with half the dose compared to single source CT.

06-A-47-NASCI

Coronary ostium—straight tube or funnel-shaped? A computerized tomographic coronary angiography study

Galit Aviram, Haim Shmilovich,
 Ariel Finkelstein, Galia Rosen,

Moshe Graif, Shmuel Banai, Gad Keren
Tel-Aviv Medical Center, Tel-Aviv, Israel
e-mail: aviramgalit@hotmail.com

Background The 3D configuration of the aortic-coronary junction is decisive in stenting ostial coronary lesions. We hypothesized that it varies from straight to funnel-shaped tubes and studied arterial orifices using cardiac-gated computerized tomographic coronary angiography (CTCA).

Methods Axial and sagittal 2D and volumetric 3D reconstructions of the aorto-coronary junction were performed in 25 patients who underwent CTCA. The following measurements of the left main (LM) and right coronary (RCA) arteries' ostia were obtained: the coronary orifice broad-base diameter, the diameter of the coronary vessel most proximal segment, the distance between these two lines, and the angles of the aortic-coronary junction. The aortic-coronary junction was defined as "funnel-shaped" when the orifice diameter was $\geq 50\%$ larger than the diameter of the vessel's most proximal segment, and "asymmetric" when the difference between the two measured angles at the aortic-coronary junction was ≥ 20 degrees.

Results All patients exhibited a funnel-shaped aortic-coronary junction in at least one plane. The RCA take-off had symmetric angling in both the axial and sagittal planes in only one patient, while the LM did not have a symmetric origin in either plane in any patient. The mean coronary orifice funnel depths in the axial and sagittal planes were 2.7 ± 1.5 mm and 2.1 ± 0.8 mm for the LM and 2.4 ± 0.8 mm and 2.1 ± 0.6 mm for the RCA. The mean ostial cross-sectional diameters in the axial and sagittal planes were 9.6 ± 1.8 mm and 8.6 ± 1.8 mm for the LM and 9.4 ± 2.2 mm and 9.1 ± 1.7 mm for the RCA. The LM diameters in the axial and sagittal views were 5.1 ± 0.8 mm, 4.3 ± 0.6 mm, and the RCA diameters were 4.4 ± 0.9 mm and 4.3 ± 1 mm.

Conclusion The frequency of funnel-shaped and asymmetric shapes of the aortic-coronary junction configuration needs to be considered in designing stents for aortic-ostial coronary lesions in order to achieve optimal results and reduce ostial stent thrombosis and restenosis.

06-A-48-NASCI

64-Detector CT imaging in the evaluation of adult congenital heart disease

Amgad Makaryus, Sonia Henry, John Makaryus, Lawrence Boxt
North Shore University Hospital, Manhasset, NY, USA
e-mail: amakaryu@nshs.edu

Background Congenital heart defects (CHD) are the most common birth defects, occurring in about 1% of live births. Today, most infants born with CHD live into adulthood. The number of adults with CHD now exceeds the number of children with CHD. As a result, patients with CHD represent a large and steadily growing sub-population of patients that require specialized diagnostic and therapeutic management. We examined the utility of 64-detector CT (64-CT) in identifying and assessing CHD in referred patients.

Methods From April 2005 to April 2006, 1,317 patients were consecutively investigated for the presence of CAD using cardiac 64-CT (GE LightSpeed VCT™, GE Healthcare). All patients with identified CHD were further examined.

Results 38 patients (2.9%; 22 men; 16 women; ages 48 ± 16 years) were identified with CHD. CHD was correctly identified and examined in all cases. Of these, three (0.23%) patients had tetralogy of Fallot with repair, three (0.23%) patients had a persistent left superior vena cava, one (0.08%) patient had situs inversus, and one (0.08%) patient had Ebstein's anomaly. A total of 16 (1.21%) patients had anomalous coronary arteries, four (0.30%) patients had an ASD status-post repair, three (0.23%) patients had a VSD not related to a tetralogy of Fallot, and four (0.30%) patients had coarctation of the aorta which had been repaired. Two (0.15%) patients had anomalous pulmonary venous return with one of these being a Scimitar syndrome. The final three patients (0.23%) had aberrant subclavian arteries. One of these originated from a right-sided arch and the other patients originated from a left-sided arch.

Conclusion 64-CT is an accurate diagnostic tool for the assessment of adults with CHD. It gives an accurate assessment of structural anomalies due to its superior spatial resolution and three-dimensional reconstruction abilities.

06-A-49-NASCI

Contrast-induced nephropathy (CIN) in risk patients: a double blind comparison of iopamidol and iodixanol

Dushyant Sahani¹, Brendan Barrett², Richard Katzberg³, Henrik Thomsen⁴, Gilles Soulez⁵

¹Massachusetts General Hospital, Boston, MA, USA

²Memorial University of Newfoundland, St. John's, NF, Canada

³University of California, Davis Medical Center, Sacramento, CA, USA

⁴Copenhagen University Hospital at Herlev, Herlev, Denmark

⁵Centre Hospitalier de l'Université de Montréal, Montreal, PQ, Canada

e-mail: dsahani@partners.org

Purpose To prospectively compare the effects on renal function of iopamidol-370 and iodixanol-320 in renally impaired patients undergoing contrast-enhanced multidetector CT (CE-MDCT) examinations using a multicenter, double-blind, randomized, parallel-group design.

Method and materials 166 patients with stable moderate-to-severe renal impairment (screening and baseline serum creatinine, SCr, ≥ 1.5 mg/dl and/or creatinine clearance, CrCl, ≤ 60 ml/min) undergoing CE-MDCT of the liver or peripheral arteries were randomized to receive equi-iodine IV doses (40 gI) of either iopamidol-370 (370 mgI/ml, 796 mOsm/kg) or iodixanol-320 (320 mgI/ml, 290 mOsm/kg) at 4 ml/s. SCr and CrCl were obtained at screening, baseline, and at $48\text{--}72 \pm 6$ h postdose (mean: 57.4 h). CIN was defined as an absolute increase ≥ 0.5 mg/dl and/or a relative rise in SCr $\geq 25\%$ from baseline. CrCl decreases $\geq 25\%$ from baseline were also assessed.

Results 153 patients were included in the final analysis (13 patients excluded because of lack of

follow-up, hemodialysis to remove contrast, average daily CrCl variation $> 1\%$ at screening). The two study groups were comparable with regard to age, gender distribution, presence of diabetes, concomitant medications, hydration and contrast dose. Mean predose SCr was 1.6 ± 0.4 mg/dl in both groups ($P = 0.9$). An absolute increase ≥ 0.5 mg/dl in SCr was observed in none of the patients receiving iopamidol-370 and in 2.6% (2/76) of patients receiving iodixanol-320 (95% CI $[-6.2, 1.0]$, $P = 0.2$). A relative increase $\geq 25\%$ in SCr occurred in 3.9% (3/77) of patients receiving iopamidol-370 and in 4% (3/76) of the patients receiving iodixanol-320 (95% CI $[-6.2, 6.1]$, $P = 1.0$). A relative decrease $\geq 25\%$ in CrCl occurred in none of the patients receiving iopamidol-370 and in 1.3% (1/76) of patients receiving iodixanol-320 (95% CI $[-3.9, 1.3\%]$, $P = 0.5$).

Conclusions The rate of CIN was low and not statistically different in risk patients after administration of iopamidol-370 or iodixanol-320 for CE-MDCT.

06-A-50-NASCI

The role of cardiac MRI and cardiac CT in the diagnosis of myocarditis

Orly Goitein, Oren Agranat, Shlomi Matezky, Guy Rozen, Ariel Bentancur, Eli Konen
Sheba Mediacal Center, Ramat Gan, Israel
e-mail: Orly.Goitein@sheba.health.gov.il

The purpose of this work is to describe the role of cardiac MRI (CMR) and cardiac CT angiography (CCTA) in the diagnosis of acute myocarditis.

Patients and methods Twenty two sequential patients (pts) (all males) with clinically suspected myocarditis, were enrolled in the study (average age 33 years, range 21–53). Presenting signs and symptoms included chest pain, fever, high Troponin and CPK levels, decreased left ventricular (LV) function and LV hypokinesis. All pts underwent CMR, and 13/22 pts underwent CCTA, within 36 h of presentation. CMR was performed using a 1.5 Tesla scanner (Excite General Electric); Cine sequences were acquired

in the short axis and the axial planes using steady state free precession. Contrast enhanced CMR was performed in the short axis 6–10 min following the administration of Gadolinium DTPA (0.02 mmole/kg; Soreq Radiopharmaceuticals) using segmented inversion recovery gradient echo (IR-GRE) sequence to null the normal myocardium.

Results Abnormal patchy epicardial areas of delayed enhancement were seen in 15/22 (68%) patients. In all these cases the inferolateral segments were involved. Average LV ejection fraction was 55% (range: 38–67%). All CCTA's were normal.

Conclusions Combined evaluation using CCTA and CMR offers comprehensive evaluation of patients with suspected myocarditis. CCTA can exclude ischemic etiology, while CMR may have a confirmatory role for the diagnosis of myocarditis by demonstrating a typical pattern of epicardial delayed enhancement in the inferolateral segments.

06-A-51-NASCI

Cardiac contrast-enhanced MRI for non-invasive detection of myocardial fibrosis in patients with aortic valve stenosis

Markus Weiningers, Christian O. Ritter, Frank Weidemann, Joerg S. Strotmann, Herbert Koestler, Dietbert Hahn, Meinrad Beer
University Hospital of Wuerzburg, Wuerzburg, Germany
e-mail: weininger@roentgen.uni-wuerzburg.de

Introduction Several invasive studies implicate that myocardial fibrosis is closely associated with aortic valve stenosis. Furthermore, the degree of valvular stenosis seems to influence the degree of fibrosis.

Purpose Our goal was to investigate whether contrast-enhanced MRI (ceMRI) can non-invasively detect myocardial fibrosis in patients with aortic stenosis.

Methods 11 patients (mean age 70 ± 9 years, 6 males, 5 females) with valvular aortic stenosis (AHA classification; mild: $n = 1$; moderate: $n = 3$;

severe: $n = 7$) according to echocardiography were examined using a 1.5 T MR scanner. In all patients cine-MRI (SSFP), flow quantification (SSFP) and late enhancement imaging (PSIR) were performed. In the same MRI exam both, degree of stenosis and impairment of ventricular function were determined as well. Prior to MRI, coronary artery disease was ruled out in five patients by conventional coronary angiography. Presence and absence of late enhancement (LE) as parameter for myocardial fibrosis was correlated to left ventricular morphological and functional data. According to the presence of LE patients were divided into two groups (G1, LE; G2, no LE).

Results In 73% of our patients LE was detected (G1; 8/11; 5 males, 3 females), ranging from small focal spots to larger areas with a preference for basal segments. Mean value for left ventricular mass was 165 ± 52 g (G1, 168 ± 59 g; G2, 157 ± 27 g), for ejection fraction $58 \pm 18\%$ (G1, $54 \pm 19\%$; G2, $67 \pm 13\%$), for orifice area 0.8 ± 0.5 cm² (G1, 0.8 ± 0.6 cm²; G2 0.8 ± 0.1 cm²). Additional findings included significant aortic regurgitation (G1, $n = 4$; G2, $n = 2$) and mitral regurgitation (G1, $n = 2$; G2, $n = 1$).

Conclusions Our results show that a high percentage of patients with aortic stenosis display myocardial fibrosis, which can be detected non-invasively using ceMRI. Furthermore, our data indicate that myocardial fibrosis is associated with a clear tendency to left ventricular functional impairment and additional valvular diseases.

06-A-52-NASCI

Extreme lipomatous hypertrophy of the interatrial septum mimicking right atrial myxoma

Rishi Kad, Mohammad Abdul Waheed, Brahma Sharma, Aashish Dua, Alan Gradman
Western Pennsylvania Hospital, Pittsburgh, PA, USA
e-mail: mwaheed@wpahs.org

Background Lipomatous hypertrophy of the interatrial septum is a rare, benign condition of the heart that needs to be differentiated from an

atrial tumor. The management modalities of these two conditions are at two extremes of the spectrum and hence a precise diagnosis is obligatory. We present to you a case of an unusual lipomatous hypertrophy of the interatrial septum that was misdiagnosed to be an atrial myxoma by echocardiography. Adjunctive imaging modalities prevented an unwarranted surgical intervention. *Case report* A 75-year-old female with history of hypertension, diabetes, obesity and right breast cancer presented to the hospital with two weeks of fatigue and exertional dyspnea. She was found to be in atrial fibrillation. A transthoracic echocardiogram revealed a mass in the right atrium attached to the interatrial septum. A diagnosis of atrial myxoma was made and surgery was consulted for resection of the mass. A cardiac catheterization revealed a “tumor blush” typical for an atrial tumor. A pre-operative transesophageal echocardiogram revealed a dumb-bell shaped hypertrophy of the interatrial septum with sparing of the fossa ovalis and a well circumscribed, mobile mass protruding into the right atrial cavity. This unusual anatomy prompted a cardiac MR which showed a diffuse lipomatous infiltration of the interatrial septum with focal infiltration at the junction of the inferior vena cava and the right atrium. A portion of this focal infiltration appeared endophytic and protruding into the right atrial cavity. The patient was eventually diagnosed with extreme lipomatous hypertrophy of the interatrial septum and was managed conservatively.

Conclusions The above case represents an unusual appearance of lipomatous hypertrophy of the interatrial septum with focal endophytic protrusion into the right atrial cavity. A timely use of noninvasive imaging modalities in conjunction with conventional assessment prevented an unnecessary surgical intervention in this patient.

06-A-53-NASCI

Multiple factors may play a role in heart rate during coronary CT angiography

Donna S. Lesniak, Brian A. Seeck, Michael O. Barry, Joseph A. Craft, Timothy W. Schloss,

Robert J. Gropler, Pamela K. Woodard
Washington University School of Medicine, St. Louis, MO, USA
e-mail: cassadyd@mir.wustl.edu

Background It is generally accepted that heart rates (HR) increase during injection of iodinated contrast media, with the hypothesis that iso-osmolar contrast agents cause less of a HR increase in comparison to low-osmolar agents. While conducting coronary CT angiography (CCTA) studies at our institution we determined average HR during acquisition of a non-contrast calcium score and CCTA.

Method Between August 2005 and May 2006, 127 patients with and without known CAD were enrolled and underwent 64-slice CT (Sensation 64, Heartview, Siemens). Eighty-six patients received a low-osmolar agent, (792 mOsm/kg water). The remainder ($n = 41$) received iso-osmolar contrast, (290 mOsm/kg water). Intravenous metoprolol was administered to all participants with HRs > 65 bpm prior to both scans. Average HR was recorded from the Heartview workstation after confirming there were no gating errors. Both scans were performed during inspiration breathhold. The pre-contrast scan and breathhold were obtained simultaneously. The CCTA was performed 5-s after start of breathhold.

Results Mean HR declined pre and post contrast agent for both the low-osmolar group, 64.0 (SD 8.9) and 61.2 (SD 8.8) bpm $P < 0.001$ m and for the iso-osmolar group, 62.5 (SD 7.9) and 57.6 (SD 8.2) bpm, $P < .001$. Mean difference in pre-post contrast HR was greater for the iso-osmolar group 7.8 (SD 6.6) bpm compared with the low-osmolar group 3.9 (SD 10.8), $P = 0.03$. HR's increased in 20/86 and 1/41 patients administered low- and iso-osmolar agent, respectively. Administered metoprolol dose was similar between the 2 groups ($P = \text{NS}$).

Conclusion Despite the administration of iodinated contrast agent, HR generally decreased during CCTA. HR of patients who received iso-osmolar contrast agent had a small but statistically significant greater decrease than those who received a low-osmolar agent. Other factors, such as scan delay during the Valsalva maneuver of

breathholds, may effect a greater role in HR regulation during CCTA and warrant further investigation.

06-A-54-NASCI

Effects of nonionic iodinated contrast media on heart rate in patients undergoing multidetector ct exams: comparison of iopamidol-370 and iodixanol-320

Dushyant Sahani¹, Ke-min Chen², Luigi Lepanto³, Jian-rong Xu⁴, Rendon Nelson⁵, Jay P. Heiken⁶
¹Massachusetts General Hospital, Boston, MA, USA

²Rui Jin Hospital, Shanghai, China

³Centre hospitalier de l'Université de Montréal (CHUM) Hospital of St. Luc, Montreal, PQ, Canada

⁴Ren Ji Hospital, Shanghai, China

⁵Duke University Medical Center, Durham, NC, USA

⁶Mallinckrodt Institute of Radiology, St. Louis, MO, USA

e-mail: dsahani@partners

Purpose We conducted a prospective study of heart rate (HR) changes in patients undergoing multidetector CT (MDCT) exams with either iopamidol (370 mgI/ml, 796 mOsm/kg) or iodixanol (320 mgI/ml, 290 mOsm/kg).

Method and materials 166 patients undergoing MDCT of the liver or peripheral arteries were randomized to receive equi-iodine (40 gI) iopamidol-370 or iodixanol-320 intravenously via power injector (4 ml/s). HR was measured in a supine position before and for 5 min after contrast medium (CM) administration. Mean and peak increases in HR were calculated and compared in the two populations by ANCOVA analysis using baseline as covariate. The proportion of subjects in each group with pre-defined increases in HR (> 5 to < 10; 10 to < 15, 15 to < 20, > 20 bpm) was compared using a Chi square test.

Results 84 subjects received iopamidol-370; 82 received iodixanol-320. Mean age, gender distribution, weight, total iodine dose, dose/body weight, concomitant medications, and presence

of hypertension were comparable in both groups. Mean baseline HR was similar in both groups (iopamidol-370: 72.3 ± 12.5 bpm, range 47–101 bpm; iodixanol-320: 74.5 ± 11.9 bpm, range 47–114 bpm). HR increased slightly in both groups following CM administration: mean change from baseline to peak post dose HR was 8.0 ± 9.34 after iopamidol and 8.4 ± 14.69 after iodixanol, $P = 0.72$ ANCOVA). Peak post-dose HR ranged from 51 bpm to 112 bpm in the iopamidol group and 53–164 in the iodixanol group. The proportion of subjects in each group having increases of > 5 to < 10, 10 to < 15, 15 to < 20, or > 20 bpm was comparable ($P = 0.87$). No subject in the iopamidol group and two subjects in the iodixanol group (2.4%) experienced post-contrast tachycardia (> 120 bpm) following CM administration (peak HR of 146 and 164 bpm).

Conclusion The effects of iopamidol-370 and iodixanol-320 on HR were similar in patients undergoing MDCT. Concerns that low osmolar CM may have more effects on HR during intravenous injection than isotonic CM are not justified.

06-A-55-NASCI

Feasibility of myocardial delayed enhancement techniques in evaluation of vasculitis

David Stanley¹, James Glockner²

¹GE Healthcare, Proctor, MN, USA

²Mayo Clinic, Rochester, MN, USA

e-mail: david.stanley@med.ge.com

Purpose Current techniques to evaluate vasculitis include CT, MRI, PET and conventional angiography (CA). CT provides high resolution images of vessel wall thickening and vascular stenosis or occlusion, but also involves use of iodinated contrast media and ionizing radiation. CA is an invasive technique also requiring iodinated contrast and radiation, with superb spatial resolution but no depiction of the vessel wall. Common MRI techniques include 3D CE-MRA, black blood imaging of vessel walls, and post contrast T1-weighted images to demonstrate vessel wall enhancement.

Myocardial delayed enhancement techniques have recently been applied to vessel wall imaging. The inversion time (TI) is chosen to null the signal of the normal vessel wall, emphasizing enhancement in patients with vasculitis. We evaluated the feasibility of this technique in several patients with known or suspected vasculitis involving the thoracic aorta, performing single shot MDE sequences following contrast administration for 3D CE-MRA.

Methods Single shot MDE (sshmde) is a cardiac gated fast gradient recalled echo technique in which all data for a single slice is acquired in 3 R/R intervals. TI was selected using a multi TI cine sequence performed in a sagittal projection through the thoracic aorta to determine the optimal TI. Axial black blood imaging was performed using a cardiac gated double inversion recovery sequence. 3D MRA was then performed and followed by sshmde acquisitions 5–10 min following contrast injection.

Results Vessel wall enhancement was well seen with the MDE sequences in patients with vasculitis and vessel wall thickening on black blood sequences. The image contrast was higher but SNR lower in comparison to the non-gated post contrast fast SPGR sequences. **Discussion** Preliminary results are promising using sshmde to evaluate vasculitis. Improved conspicuity of vessel wall enhancement may allow detection of subtle vascular inflammation, and more accurate assessment of the activity of treated vasculitis.

06-A-56-NASCI

In vivo MRI of injected mesenchymal stem cells in myocardial infarction; simultaneous tracking and functional measurement

Young Jin Kim¹, Eun Jeong Choi², Yong Min Huh¹, Byoung Wook Choi¹, Jin Suk Suh¹, Kyu Ok Choe¹

¹Yonsei University College of Medicine, Seoul, Republic of Korea

²Korea University Hospital, Seoul, Republic of Korea

e-mail: dryj@yumc.yonsei.ac.kr

Purpose The purpose of this study was to determine if magnetically labeled mesenchymal stem cells could be imaged in vivo in a rat model of myocardial infarction and cardiac function could be simultaneously evaluated using MRI.

Methods and materials Myocardial infarction was induced in rat myocardium ($n = 14$, male SD rat) by cryoinjury. Human mesenchymal stem cells (MSC) were labeled with superparamagnetic iron oxide particle (SPIO, Feridex®) and injected into the infarcted myocardium three weeks after the injury. In control group ($n = 5$), cell-free media was injected three weeks after cryoinjury. In vivo MRI was serially performed before and after cell injection during three months using 47 mm microcoil and 1.5 T clinical scanner. For in vivo cell trafficking, gradient echo sequence with EKG gating was used. For evaluation of cardiac function, ejection fraction (EF) was measured using cine MRI.

Results SPIO-labeled mesenchymal stem cells were visualized on in vivo MRI until 10 weeks after injection. On serial follow-up MRI, ejection fraction was significantly higher in MSC injection group ($EF = 55.3 \pm 9.2\%$) than in control group ($EF = 32.7 \pm 3.1\%$) ($P < 0.0001$).

Conclusion These findings support the ability of MRI to track injected cells in vivo as well as evaluate long term therapeutic potential of mesenchymal stem cell in the setting of myocardial infarction.

06-A-57-NASCI

Assessment of diastolic dysfunction: usefulness of velocity encoded MR during Valsalva maneuver and tissue velocity MR

Young Jin Kim, Byoung Wook Choi, Ji Eun Nam, Kyu Ok Choe

Yonsei University College of Medicine, Seoul, Republic of Korea

e-mail: dryj@yumc.yonsei.ac.kr

Purpose In the assessment of diastolic dysfunction, mitral flow velocity data by velocity encoded magnetic resonance (VE-MR) is comparable to echocardiography. However, pseudonormalization is difficult to differentiate from normal pattern by mitral flow velocity, because mitral flow is preload-dependent. We hypothesized that VE-MR during Valsalva maneuver and tissue velocity MR enables to discriminate pseudonormalization from normal pattern. **Methods and materials** A total 53 subjects (42 males, 57 ± 13 years) underwent VE-MR after Echo. Underlying diseases were myocardial infarction ($n = 32$), hypertrophic cardiomyopathy ($n = 5$), dilated cardiomyopathy or congestive heart failure ($n = 5$), atypical chest pain ($n = 6$), and other diseases ($n = 5$). Routine VE-MR for mitral flow velocity was obtained at the level of mitral valve (40 phase per cardiac cycle, $V_{ENC} = 100$ cm/s). Valsalva VE-MR was acquired at the same level during Valsalva maneuver. Tissue velocity MR was obtained at the same level ($V_{ENC} = 50$ cm/s) and tissue velocity was measured in the posterior basal septum. Pattern of diastolic dysfunction (normal, relaxation abnormality, pseudonormalization, and restrictive physiology) was analyzed by VE-MR and compared with Doppler echocardiography.

Results Based on routine VE-MR data, 30 patients were normal pattern, 21 were relaxation abnormality and two were restrictive physiology. Among the 30 patients showing normal pattern on routine VE-MR, conclusion of 21 patients was changed from normal pattern to pseudonormalization, who demonstrated reversal of E/A ratio on Valsalva VE-MR or reversed pattern of E' and A' on tissue velocity. Pattern of diastolic dysfunction by VE-MR was mismatched with Echo in eight patients, however, five of whom were pseudonormalization pattern by VE-MR and relaxation abnormality by Echo.

Conclusions In the evaluation of diastolic dysfunction, VE-MR during Valsalva and tissue velocity MR are useful methods to differentiate pseudonormalization from normal pattern.

06-A-58-NASCI

Multislice computed tomography evaluation of left ventricular ejection fraction in patients without structural heart disease: comparison with echocardiography and nuclear imaging

Gaurav Aggarwala, Nikhil Iyengar, Kimberly Staffey, Stephen Burke, Brad Thompson, Edwin vanBeek, Dinesh Jagasia
University of Iowa, Iowa City, IA, USA
e-mail: gaurav-aggarwala@uiowa.edu

Background Echocardiography (ECHO), Nuclear Imaging (NI) including Gated SPECT/MUGA and Cardiac MRI (CMR) are used to assess Left ventricular ejection fraction (LVEF). Multislice Computed Tomography (MSCT) is a reliable diagnostic tool to exclude CAD. The aim of the study is to compare MSCT derived LVEF with LVEF assessed by ECHO and NI.

Methods Medical records of 67 patients without structural heart disease, who underwent MSCT, were reviewed. Retrospective reconstruction was performed for acquisition of phase images from early systole to end diastole using 10% increments. LVEF obtained through ECHO and NI were recorded and compared to MSCT derived LVEF. The agreement between the LVEF obtained by NI, ECHO and MSCT was assessed by Bland-Altman method. Estimate of mean bias as measured by the mean of paired differences between the two methods was obtained and one sample t -test was performed to test if the mean bias was significantly different from zero.

Results Among the 67 patients, 35 patients (52.2%) also underwent ECHO assessment while 29 patients (43.3%) had NI. MSCT could not evaluate LVEF in seven patients (10.4%). In patients who had an ECHO and MSCT, LVEF by MSCT was $67.1 \pm 9.8\%$ compared to $61.7 \pm 9.6\%$ by ECHO. In patients who underwent NI and MSCT, LVEF by MSCT was $70.2 \pm 10.3\%$ compared to $59.3 \pm 9.2\%$ by NI. There was a bias in

the LVEF measurement by MSCT. MSCT overestimated LVEF when compared to NI by +10.9% ($P < 0.0001$) and LVEF measurement by MSCT when compared to LVEF by ECHO of +5.4% ($P = 0.0002$).

Conclusion We observed in patients without structural heart disease, MSCT overestimated LVEF when compared to Gated SPECT / MUGA and ECHO. In 10% of patients, LVEF could not be assessed by MSCT due to difficulty with segmental reconstruction. Larger studies comparing MSCT derived LVEF with CMR in patients with/without structural heart disease are needed.

06-A-59-NASCI

Evaluation of Patients With Congenital Coronary Anomalies with Cardiac CT Angiography, South Florida Medical Imaging, Boca Raton, Florida, University of Texas Health Science Center at San Antonio, Texas

Claudio Smuclovsky, Baum S., Dhir M., Arora U.K., McInnis P.

South Florida Medical Imaging, Boca Raton, FL, USA

e-mail: drs@sfmipa.com

Introduction Invasive coronary angiography has been the gold standard for the diagnosis of coronary anomalies (CA). Cardiac computed tomographic angiography (CTA) provides the ability to non-invasively detect, evaluate and follow patients (pts) with CA. Additionally, cardiac morphology and function can be reliably

assessed to determine the functional significance of these lesions.

Methods Non-ionic contrast enhanced CTA using 16 and 64 MSCT was performed in 1,084 consecutive patients in the last 12 months (February 2005 to January 2006) of whom 11 (1%) were diagnosed with coronary artery anomalies.

Results Of the 11 pts with CA, 7 were men (64%) and the age range was 17–80 years. The left main was anomalous in four pts, the left circumflex was anomalous in three pts, four pts had an anomalous RCA. The entire course of all coronary arteries could be identified in all 11 patients. Three pts were previously known to have coronary anomalies. Six pts were being evaluated for chest pain, one presented with cardiomyopathy, three pts had abnormal stress tests and one pt was referred for preoperative evaluation. Two pts needed CABG and one needed surgical repair based on the cardiac CTA findings. Extracardiac pathology was seen in 4/11 (36%) pts and most commonly represented post inflammatory lung disease. Ventricular function, prior infarction, regional wall motion, chamber size and other cardiac anomalies could additionally be reliably assessed.

Conclusions Cardiac CTA is a reliable, accurate non invasive tool to assess coronary anomalies in adult patients and may be used as the preferred initial imaging modality. Potentially lethal anomalous course between the two great arteries is easily identified contrary to coronary angiography. Thus, CTA can be used as the primary diagnostic test to diagnose, evaluate the need for coronary bypass surgery, and follow up of these patients.

Table 1 Stenosis and plaque burden measurements. Data = mean \pm SD

AHA class.	No. of subjects	Percentage stenosis (%) as measured by ECST MRA	Percentage stenosis (%) as measured by NASCET MRA	Percentage stenosis (%) as measured by NASCET combi	Plaque index (volume wall/vessel) (%)	Max–Min wall thickness (maximum) (mm)
0–I	4	2.13 + 1.61	1.51 + 1.30	1.05 + 0.23	42.69 + 2.79	1.01 + 0.07
I–II	6	7.41 + 4.01	5.09 + 1.57	5.20 + 4.31	44.17 + 6.69	1.05 + 0.13
III	5	15.70 + 7.16	9.40 + 5.94	10.65 + 7.63	45.00 + 5.97	1.92 + 0.47
IV–VI	7	50.03 + 26.04	31.35 + 31.49	35.56 + 21.14	58.37 + 7.05	2.33 + 0.74

06-A-60-NASCI**An automated integrated analysis method for quantifying vessel stenosis and plaque burden from carotid MR images based on MRA and vessel wall MR**

Isabel Maria Adame¹, Rob J van der Geest¹, Patrick J. H. de Koning¹, Bruce A. Wasserman², Johan H. C. Reiber¹, Boudewijn P. F. Lelieveldt¹
¹Leiden University Medical Center, Leiden, The Netherlands

²The Russell H. Morgan Department of Radiology and Radiological Sciences. The Johns Hopkins Hospital, Baltimore, MD, USA
 e-mail: rvdgeest@lumc.nl

Introduction Our purpose was to evaluate the benefits of combining contrast-enhanced MRA (CE-MRA) and vessel wall MRI for automated assessment of stenosis severity and plaque burden in atherosclerotic carotid arteries.

Methods An automated method was used for the detection of luminal contours in CE-MRA, and lumen and outer wall contours in post-contrast T1-weighted MR (PC-T1W MR). Different measurements of lumen diameter were derived from those contours to evaluate the accuracy of CE-MRA alone, and that of the combined approach of CE-MRA and PC-T1W MR (*combi*). The NASCET and the ECST criteria were used to measure the degree of stenosis. Minimum diameters were measured at the point of greatest narrowing based on CE-MRA and PC-T1W MRI. For NASCET, the reference diameter was measured immediately distal to the narrowing beyond any poststenotic dilatation based on CE-MRA. For ECST, the diameter at the point of greatest narrowing was also extrapolated to its estimated size before narrowing occurred based on CE-MRA. To estimate plaque burden, plaque index and vessel wall thickness were estimated in the PC-T1W images. Data from 22 subjects (352 PC-T1W cross-sections and 3D CE-MRA) that presented high cardiovascular disease risk factors were used to validate the new approach.

Results The average paired difference in percent stenosis between the ECST/NASCET *combi* measurement pairs was 7.428.71%

($P = \text{NS}$) and between the ECST/NASCET CE-MRA, 7.5811.14% ($P = \text{NS}$). In cases with almost no stenosis, analysis of PC-T1W MR showed an abnormal vessel wall (outward remodelling) (Table 1).

Conclusions CE-MRA is capable of estimating the location and degree of stenosis, and high resolution vessel wall MR permits analysis of plaque burden and more accurate estimation of the stenosis percentage.

06-A-62-NASCI**Carotid plaque instability as assessed by mri: importance of size and location of the hemorrhagic necrotic core**

Wei Yu, Hunter R. Underhill, Minako Oikawa, Baocheng Chu, Marina S. Ferguson, Thomas S. Hatsukami, Chun Yuan

University of Washington, Seattle, WA, USA
 e-mail: yuwei2@u.washington.edu

Purpose High-resolution MRI has proven to be capable of quantifying carotid plaque components. Previous prospective studies suggest that intraplaque hemorrhage (IH) may stimulate progression of carotid atherosclerosis by increasing the lipid rich necrotic core (LRNC) size and total plaque volume. However, the role volume and spatial location of the hemorrhagic necrotic core play in the advanced lesion has not been studied. We hypothesize that necrotic core size, content and location are significant factors in the development of carotid related neurological symptoms.

Methods 24 consecutive symptomatic subjects scheduled for carotid endarterectomy were compared to a group of 24 randomly selected asymptomatic individuals matched for degree of stenosis by duplex ultrasound. All participants were imaged using multi-sequence, high-resolution carotid MRI protocol on a 1.5 T scanner. Two experienced reviewers, blinded to symptom status, interpreted each scan by reaching a consensus opinion. A custom designed image analysis tool obtained area and location measurements of the lumen, wall, LRNC and IH. Size was recorded in 10% increments and the highest spatial resolution (0.6 mm) of MRI was used as criteria for

distance. LRNC and IH size measurements were compared using Pearson's correlation. An independent Chi-square test was used to assess between-group differences.

Result In review of all 276 locations, a significant correlation existed between IH size and NC size ($R = 0.705$, $P = 0.001$). More importantly, we found that symptoms were strongly associated with the presence of large hemorrhagic (> 20% of the wall volume) LRNC (> 40% of the wall volume) located adjacent to the lumen (86.7% vs. 13.3%, $P = 0.006$).

Conclusion The relative amount, location and content of the hemorrhagic necrotic core are significantly associated with the presence of previous symptoms of the atherosclerotic carotid patient. These findings warrant further investigation in prospective studies.

06-A-64-NASCI

Evaluation of chest pain in the emergency department with 64-slice MDCT coronary angiography: initial experience at a community hospital

Brian Ghoshhajra, Sanjeev Katyal, Rishi Kad, Scott Beasley, Susanj Patel, Richard Kaplan, Venkatraman Srinivasan

The Western Pennsylvania Hospital, Pittsburgh, PA, USA

e-mail: ghoshhajra@yahoo.com

Objective To determine whether initial 64-MDCT chest CTA can provide a reliable, comprehensive evaluation of both cardiac and noncardiac causes of chest pain in Emergency Department patients deemed at low or intermediate risk for Acute Coronary Syndrome (ACS) in a community hospital setting.

Methods IRB approval was obtained prior to enrollment. Hundred adult patients (males over 40, females over 40) presenting to our ED with chest pain were assessed clinically and stratified into three groups (definite, intermediate, or low risk for ACS). Patients deemed low to intermediate risk were assessed and recruited immediately by the ED physician for possible chest CTA. Consenting and eligible patients underwent an ECG-gated 64-MDCT of the chest.

Image acquisition and interpretation All patients were scanned on a 64-MDCT scanner. Retrospective ECG-gated images were obtained through the entire chest during a single breath-hold. Beta blockade was used as indicated after a discussion between the Radiology and ED staff. Images were initially evaluated for emergent non-cardiac causes of chest pain (pulmonary embolus, aortic dissection, pneumothorax, pneumonia, etc.), and a preliminary radiographic diagnosis was determined, and communicated to the ED Physician. Post processing was performed on a separate workstation, and complete coronary angiographic evaluation and cardiac assessment was then reported to the ED Physician.

Clinical follow-up ED data and all available medical records were reviewed for each patient between 1 month and 2 months after the ED visit. Further relevant diagnostic testing was recorded, within 1 month of presentation to the emergency department. A consensus group (Radiologist, ED Physician, Cardiologist) adjudicated each case to determine the final diagnosis.

Statistical analysis Sensitivity, specificity, positive predictive value and negative predictive value were calculated for the chest CTA using the final clinical diagnosis as the reference standard. A cost analysis and time to discharge between the chest CTA and conventional workup was performed.

06-A-65-NASCI

Coronary calcification with multislice CT in patients with acute coronary syndrome and its relation to angiographic disease

Tarun Mittal, John Partridge, Mahmud Barbir, Mark Mason, Andrew Mitchell, Charles Ilsley
Harefield Hospital, London, UK

e-mail: mittaltk@msn.com

Purpose The aim of this study was to determine the degree of calcification in the culprit and all the coronary arteries and correlate this with angiographic stenosis in patients presenting with acute coronary syndrome using retrospectively gated MSCT.

Methods 238 patients presenting with whole spectrum of acute coronary syndromes were enrolled over a 2 year period. CT coronary calcifica-

tion was performed using 4×2.5 mm collimation, retrospective gating and ECG tube modulation. Images were reconstructed with a slice width and increment of 3/1.5 mm and lesion with three contiguous pixels of more than 130 HU considered as calcification. Two-hundred and ten patients underwent both MSCT and catheter coronary angiogram. Patients with STEMI had the MSCT after thrombolysis. Patients with previous MI, stent insertion or CABG were excluded from the study.

Results There were 150 men (72.8%) and 60 women (27.2%) with total AS (Agatston score) ranging from 0 to 4,209 (median = 560) and 0 to 3,328 (median = 99), respectively. Thirty-nine patients had STEMI, 130 NSTEMI and 41 UA as per ACC criteria. 22 patients had no calcification of which only two had significant angiographic disease warranting percutaneous intervention. Of the 178 patients with known culprit artery, 28 had no calcification in the culprit artery but 15 of these had calcification in other coronary arteries. Using Mann–Whitney test, there was significantly higher values of calcium ($P < 0.0001$) in both the culprit artery and overall in patients with significant stenosis ($> 50\%$).

Conclusions Calcification as detected with retrospectively gated MSCT is common in the culprit artery in patients presenting with acute coronary syndromes with degree of AS significantly related to angiographic stenosis. Absence of calcium has a low probability of significant coronary artery disease.

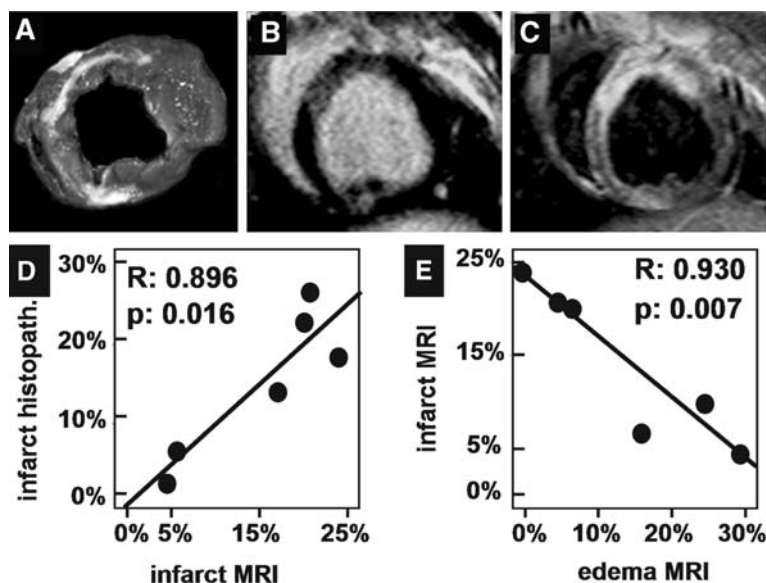
06-A-66-NASCI

Cardiac magnetic resonance imaging (MRI) is a useful tool for the evaluation of post-ischemic stunned myocardium. Histopathological validation in a porcine model

Borja Ibanez, Gemma Vilahur, Susanna Prat, Javier Sanz, Walter S Speidl, M. Urooj Zafar, Brian G Choi, Giovanni Cimmino, Gregg Goldschlager, Valetin Fuster, Bernardo Nadal-Ginard, Juan J. Badimon
Mount Sinai School of Medicine, New York, NY, USA

e-mail: borja.ibanez@mssm.edu

MRI is the gold-standard for *in vivo* infarct area assessment. Canine data suggest that early peri-infarct edema by MRI represents the non-infarcted area at risk (stunned-myocardium); however, frequent collateralization in dogs may confound interpretation. Since the porcine MI model is the large-animal gold standard, we compared MRI and histopathologic necrotic area and stunned-myocardium in the pig to test the hypothesis that MRI is effective in depicting the area of post-ischemic stunned myocardium in a model more similar to humans. Six pigs underwent closed-chest 90 min occlusion of middle-LAD. MRI studies were performed 4 and 20 days post-MI. After second MRI, animals were sacri-



ficed for histopathological analysis (TTC necrotic area staining). Contiguous short-axis MRI slices were acquired with steady-state-free-precession cine imaging for the evaluation of cardiac function, T2W triple-inversion-recovery-turbo-spin echo for edema, and delayed-enhancement (15 min post 0.2 mmol/Kg Gd-DTPA) imaging for necrotic area. Edema and infarction areas were defined as those with signal intensity > 3 SD of remote normal myocardium. At days 4 and 20, LVEF was $39 \pm 12\%$ and $49 \pm 1\%$, respectively. LV infarct area on MRI was $14 \pm 9\%$ and $15 \pm 8\%$, respectively. Infarct area on pathology was $15 \pm 9\%$. MRI edema areas were $18.8 \pm 11\%$ and $7 \pm 1\%$ on days 4 and 20. Panels A–C (A: histol; B: delayed enh; C: edema) show images from the same animal. Correlation between infarct areas on MRI/histology is shown on panel D. Inverse correlation between MRI areas of infarct/edema on day 4 is on panel E. MRI is a useful tool for non-invasive assessment of post-ischemic stunned myocardium. Four days after reperfused-MI there is a wide LV hypo-akinetic area showing edema on T2W-MRI, which disappears at day 20 coinciding with LVEF improvement, while the area of necrosis remains unaltered.

06-A-67-NASCI

Epidemiology of coronary artery calcification (CAC) detected by multi-slice computed tomography (MSCT) in an asymptomatic population of adults

Sanjaya Viswamitra, Sharp Malak, Whitney Goodwin, Ernest Ferris
University of Arkansas for Medical Sciences,
Little Rock, AR, USA
e-mail: ViswamitraSanjaya@uams.edu

Purpose (1) Characterize the prevalence and distribution of CAC among a population of asymptomatic adults. (2) Investigate associations between CAC and coronary artery disease (CAD) risk and determine whether CAC is associated with increased mortality.

Method and materials 3,198 asymptomatic adults were prospectively enrolled and interviewed to assess medical history and CAD risk factors: age,

sex, hyperlipidemia (HLP), hypertension (HTN), family history (FH), smoking, and Diabetes Mellitus (DM). Assignment of a coronary artery calcium score (CACS) via MSCT was performed at a single center, and patients were followed to ascertain mortality.

Results The mean age of patients was 55 ± 0.2 , range 21–90 years; 1,495 (47%) were female. CAC prevalence, i.e. $CACS > 0$, was 56%. Mean CACS was 123 ± 329 , range 0–5,319 with 18% 11–100, 11% 101–400, 9% > 400. CAD risk factors were associated with $CACS > 400$ in multivariate analysis: increasing age, male sex, and positive FH ($P < 0.001$); HTN, smoking, DM ($P < 0.01$) and HLP ($P < 0.05$). Subgroup analysis of females < 55 and males < 45 revealed a high prevalence of CAC, 207/693 (30%) and 112/276 (42%), respectively. Among females < 55 CACS were 21% 11–100, 9% 101–400, and one case > 400. Thirty percent of men < 45 had a CACS of 11–100, 10% 101–400, and 2% > 400. DM, HTN, FH, HLP were associated ($P < 0.05$) with $CACS > 0$ in women < 55, but no CAD risk factor was associated with $CACS > 0$ among men < 45. Analysis of mortality data is ongoing.

Conclusion Using MSCT, we identified an alarming prevalence of clinically relevant CAC in an asymptomatic population. An elevated prevalence of CAC, even among younger patients who would otherwise be considered to have lower risk using traditional CAD risk stratification, was observed. CAD risk factors were significantly associated with CAC in all subgroups of the cohort except among men < 45.

06-A-69-NASCI

Coronary fly-through or virtual angiography using dual source MDCT data

Peter van Ooijen, Matthijs Oudkerk
University Medical Center Groningen, University
of Groningen, Groningen, The Netherlands
e-mail: p.m.a.van.ooijen@rad.azg.nl

Introduction Coronary fly-through, or virtual angiography (VA), has been studied ever since its invention in 2000. However, application was limited because of the requirements for an opti-

mal CT scan and time consuming post-processing. Recent advances in post-processing software facilitate easy construction of VA but until now, image quality was insufficient in most patients. The introduction of dual source MDCT could prove to enable VA in all patients.

Methods and Materials Sixteen patients were scanned using a dual source MDCT (Definition, Siemens, Forchheim, Germany) using a standard coronary artery protocol. Post-processing was performed on an AquariusWorkstation (Tera-Recon, San Mateo, CA). Length travelled per major branch was recorded in mm together with the time required in minutes.

Results VA could be performed in every patient for each of the major coronary arteries. The mean (range) length of the automated fly-through is 82 (32–107) mm for the left anterior descending, 74 (21–116) mm for the left circumflex artery, and 112 (21–183) mm for the right coronary artery. Calcifications and stenoses are visualized, as well as most side branches. Mean time required was 3 min for LAD, 2.5 min for LCx, and 2 min for the RCA.

Conclusion Dual source MDCT allows for high quality visualization of the coronary arteries in every patient because scanning with this machine is independent of the heart rate. This is clearly shown by the successful virtual angiography in all patients. Potential clinical value of the VA should be determined in the near future.

06-A-71-NASCI

Integration of coronary computer tomography angiography and cardiovascular magnetic resonance information by post processing and software fusion of images

Marcin Basiak, Jolanta Misko, Barbara Paraniak, Jacek Brzezinski, Marek Konopka
HELIMED Silesian Centre of Diagnostic Imaging, Katowice, Poland
e-mail: marcin.basiak@helimed.pl

Introduction Currently new techniques of cardiac imaging, coronary computer tomography angiography (CTA) and cardiovascular magnetic resonance (CMR) are undergoing rapid technological devel-

opment with constantly growing usefulness of both methods in diagnosis of coronary artery disease (CAD). However, CTA and CMR are not widely available and each of them has its own limitations the combination of imaging of coronary arteries by CTA and myocardial viability by CMR could be a noninvasive and highly effective way of the assessment of CAD patients before revascularization. We hypothesize that post processing and software fusion of CTA and CMR images has the potential for better visualisation and analysis of viability and necrosis in myocardial areas supplied by stenotic coronary artery.

Methods For evaluation of potential role of image fusion of CTA and CMR we used software program for post processing and image fusion—P-MOD. CTA (16-slices CT) with standard protocol for coronary arteries imaging and CMR (1.5 T scanner) with protocol for myocardial viability imaging were performed in seven patients with CAD before planned revascularization. CTA images were used as reference data, CMR images were processed and two and three dimensional color-coded maps of myocardial viability as input data were coregistrated with CTA images.

Results All fused CTA and CMR images in two versions (two dimensional and three dimensional reconstruction) were analyzed by two cardiac surgeons. Three dimensional reconstructions were considered to be more easy for reading for surgeons before revascularization planning but two dimensional fused images were more precise in describing viability in myocardial segments.

Conclusion Combination of two noninvasive imaging techniques; coronary CTA and CMR viability imaging seemed to have specific role in the assessment of patients with CAD before revascularization.

06-A-72-NASCI

Clinical experience with 64-multidetector computed tomography in the assessment of coronary bypass grafts and in detecting stenosis >50%

Gudrun Maria Feuchtner, Guy Friedrich, Thomas Schachner, Andrea Klauser, Johannes Bonatti, Dieter zur Nedden

Innsbruck Medical University, Innsbruck, Austria
e-mail: Gudrun.Feuchtner@uibk.ac.at

Purpose To evaluate the clinical performance of 64-multidetector computed tomography (64-MDCT) in the assessment of coronary bypass graft stenosis <50% in comparison with interventional angiography.

Methods 53 patients were examined with 64-multidetector CT (Sensation 64TM, Siemens): 64 × 0.6 mm; 0.33 s; 120 kV; 700–850 mA s; eff. sl. 0.75 mm, inc. 0.4, B20f; retrospective ECG-gating (30–40% at >65 bpm/55–70% < 65 bpm); 120 ml Iodixanol (Visipaque 320TM) or Iomeprol (Iomeron 400TM) after conv. or minimal invasive CABG surgery. A beta-blocker was given if the heart rate was > 85 bpm (5 mg i.v., BelocTM).

Results 117 grafts (58 arterial; 49 venous) (53 IMA, 5 RA; 47 aortocor., 2 axillocor.) were assessed. Eighteen grafts (15.4%) were correctly found occluded with 64-MDCT. Visualization of grafts was good in 103/109 (94.5%) but limited in 6/109 (5.5%) (e.g. weak opacification of distal target vessel, clips); anastomosis stenosis was falsely suspected in two grafts. 64-MDCT correctly identified six of eight graft stenosis, two distal stenosis were missed (sensitivity 75%, specificity 98%, PPV 75%, NPV 96%). 64-MDCT performed better if stenosis >50% and occlusion were pooled together (sensitivity 92%, specificity 97%, PPV 92%, NPV 97%). Venous graft disease was detected in 15/42 (35.7%) patent vein conduits (age 13.6 ± 5.4). Non-obstructive vein graft disease was found in 19% (non-calcifying plaque = 53%; mixed non-calcifying/calcifying = 47%). Proximal LIMA course was median-retrosternally (>1 cm depth) in 26%, paramedian-retrosternally in 26% and non-retrosternally in 48%.

Conclusion 64-MDCT performs well in assessing bypass patency and may be used for the exclusion of stenosis > 50%. Vein graft disease can be detected before graft obstruction develops. Proximal LIMA course should be evaluated in relation to the sternum which is a crucial information before Redo-CABG. Visualization of the distal target vessel is improved with 64-MDCT (94.5%) when compared with literature (74%) [1]. However, detection of distal

anastomosis stenosis is still limited reflecting the demand of further technical improvements. [1] Schlosser. JACC 2004;44:1224–1229.

06-A-73-NASCI

First clinical experience with a new image integration module (CartoMergeTM): 3-D fusion of 64-slice computed tomography and electroanatomical mapping data for navigation of atrial catheter ablation

Gudrun M. Feuchtner, Florian Hintringer, Wolfgang Dichtl, Markus Stühlinger, Thomas Berger, Dieter zur Nedden
Innsbruck Medical University, Innsbruck, Austria
e-mail: Gudrun.Feuchtner@uibk.ac.at

Purpose Fusion of multislice computed tomography (CT)-derived anatomic models of the left and right atrium with electroanatomical mapping data could help to identify anatomy and navigate ablation catheters in patients with atrial flutter and fibrillation. The objective was to validate alignment and show the influence of adding CT data on the ablation procedure.

Methods 17 patients underwent 64-slice CT (Sensation 64TM, Siemens) (64 × 0.6 mm; 0.33 s; 120 KV, 600–800 mA s; 100–150 ml Iodixanol (VisipaqueTM320); retrospective ECG-gating at 60%; eff. sl. 0.75 mm, inc. 0.4, B20f) before left atrial (LA) ($n = 6$) or right atrial (RA) ($n = 9$) radiofrequency- or kryoablation. For LA, bolus tracking (ascending aorta; 100 HU; 5 ml/s) and for RA, delayed scan 70 s p.i. (biphasic: 5 ml/s, 1.5 ml/s) was performed. EsophagocatTM was given for delineation of the esophagus. Using the CARTOMergeTM Image Integration Module (Biosense WebsterTM), CT and electroanatomical mapping data (40–100 endocardial surface points) were aligned. A statistical algorithm provided information about the accuracy of the fusion process.

Results In 16/17 patients, CT images could be fused with the electroanatomical map. 8/17 patients were in sinus rhythm. A beta blocker i.v. was given in 6/15. The average alignment error was 2.2 ± 0.7 mm. Contrast attenuation of RA and LA were 220.7 HU ± 34.6 and 352.6 HU ± 38, resp. In 8/8 patients with LA fibrillation, CT added relevant

anatomical information to the electroanatomical map influencing the ablation line or strategy: position of esophagus ($n = 2$); aberrant right middle PV mistaken as superior right PV ($n = 1$); position of PV's ($n = 3$). In 3/8 (38%) patients with RA flutter CT was useful: coronary sinus aneurysm ($n = 1$), prominent Eustachian ridge ($n = 1$), RCA attached to the atrial wall ($n = 1$).

Conclusion 3-D Fusion of CT with electroanatomical mapping data is feasible to navigate ablation catheters in the atria. CT added relevant morphological information about the right atrium in 38% and about left atrium/PV's in 100% of patients influencing the ablation strategy.

06-A-74-NASCI

64-slice computed tomography for the evaluation of ventricular function using an automated contour tracking algorithm (Circulation™) and the aortic valve orifice area in aortic stenosis

Gudrun M. Feuchtner¹, Wolfgang Dichtl¹, Guy Friedrich², Silvana Müller³, Dieter zur Nedden⁴

¹Department of Radiology, Innsbruck Medical University, Innsbruck, Austria

²Department of Cardiology, Innsbruck Medical University, Innsbruck, Austria

³Innsbruck Medical University, Innsbruck, Austria

⁴Department of Radiology II, Innsbruck Medical University, Innsbruck, Austria

e-mail: Gudrun.Feuchtner@uibk.ac.at

Purpose To evaluate measurement of [1] left ventricular function and [2] the aortic valve orifice area (AVA) with 64-slice computed tomography (CT) in patients with aortic stenosis in comparison to the diagnostic standard trans-thoracic echocardiography (TTE).

Methods 16 patients with aortic stenosis were examined with 64-slice CT (Sensation 64, Siemens) (64×0.6 mm; 0.33 rot.; 120 KV; 800–900 mA s; 100 ml iodixanol (Visipaque 320); 5 ml/s flow; retrospective ECG-gating). [1] For the assessment of left ventricular function, images were reconstructed at every 10% of RR-interval (eff.s 1.1.5 mm; inc.1.2; B 30 f). LV-EF, LV-EDV and LV-ESV were calculated by two independent

observers. Post-processing was performed with a dedicated software using an automated contour-tracking algorithm (Circulation™, Siemens). [2] For planimetry of the AVA, images were reconstructed at 12%; eff. slice 0.75 mm, inc.0.4; B 25 f+). All patients underwent TTE including measurement of LV-EF, LV-EDV and LV-ESV (Simpson's rule) and calculation of the AVA by using Continuity Equation (Doppler VTI-integral).

Results [1] LV-EF, LV-ESV and LV-EDV by 64-MSCT were significantly correlated with TTE ($P = 0.004$; $P = 0.002$; $P < 0.001$). On Bland-Altman plot, LV-EF was slightly overestimated (+0.7%) by using CT and LV-EDV and LV-ESV were slightly underestimated (−3.9; −3.3 ml). Mean LV-EF;-ESV;-EDV were $60.1\% \pm 8.9$; $38 \text{ ml} \pm 14$; $95 \text{ ml} \pm 29$ by CT, respectively. Interobserver variability was 2.6%(LV-EF);4.1%(LV-ESV);3.6%(LV-EDV). Mean time for post-processing was 5.3 min [2] Planimetric measurement of the AVA by CT (mean $1.07 \text{ cm}^2 \pm 0.38$) was significantly ($r = 0.82$; $P = 0.0003$) correlated with TTE (mean $1.02 \text{ cm}^2 \pm 0.37$).

Conclusion 64-slice CT may provide a promising non-invasive diagnostic approach in patients with aortic stenosis. 64-slice CT shows promising results in the assessment of left ventricular function and allows an accurate planimetry of the AVA. In patients in whom coronary artery disease is a differential, 64-slice CT might be the imaging modality of first choice because coronary arteries can be evaluated simultaneously in a non-invasive fashion.

06-A-75-NASCI

Initial diagnosis of presence, location and transmural extension of myocardial infarction based on electrocardiographic method, compared with delayed enhancement magnetic resonance findings

Marcin Basiak¹, Jolanta Misko¹, Barbara Paraniak¹, Anna Wycisk², Jacek Brzezinski¹, Marek Konopka¹

¹HELIMED Silesian Centre of Diagnostic Imaging, Katowice, Poland

²3rd Division of Cardiology, Silesian School of Medicine, Katowice, Poland

e-mail: marcin.basiak@helimed.pl

Purpose Initial diagnosis of myocardial infarction (MI) in patients with acute coronary syndrome (ACS) is assessed by measurement of cardiac markers and ECG changes. Myocardial dysfunction detected by echocardiography could be the effect of necrosis but also stunning or hibernation. Recently delayed-enhanced cardiovascular MR (DECMR) has become the “gold standard” method for imaging and quantification of necrotic myocardial tissue. The aim of this study was to evaluate the concordance between assessment of presence, location and transmural extension of MI based on ECG and DECMR.

Material and methods Our study group consisted of 25 patients (pts) after ACS; 14 pts with known chronic MI and 11 pts without defined MI based on conventional methods. Presence of MI was determined upon elevation in enzyme levels during the acute phase of ACS and/or typical ECG changes. Location and transmural-ity of MI was defined by ECG (Q-wave or non-Q). To correlate DECMR and ECG evaluation of MI we divided the left ventricle into three regions: 1—typically supplied by LAD (anteroseptal, anterior, anterolateral wall) 2—LCx (lateral, inferolateral wall) and 3—RCA (inferoseptal, inferior wall). Transmural extension of MI was defined as < 50% involvement of myocardial wall thickness—subendocardial and > 50%—transmural.

Results In 2/11 pts without previous MI we found subendocardial necrosis on DECMR. In pts with known MI there was mismatch in location between ECG and DECMR in 8/14 pts: concerning myocardial walls in the same coronary artery territory in 5/14 pts and walls which belong to different coronary artery territories in 3/12 pts. Transmural extension of MI differed in 7/14 pts.

Conclusion In pts with a history of ACS, the use of DECMR enables more accurate assessment of presence, location and transmural extension of MI than ECG, which could be useful in choosing the revascularization strategy.

06-A-76-NASCI

Frequency of significant incidental findings in routine renal MRI/MRA examinations performed for suspected renovascular hypertension

Rajiv Agarwal¹, Raja Muthupillai², Scott D. Flamm³

¹University of Texas Health Science Center Houston, Houston, TX, USA

²Philips Medical Systems, Cleveland, OH, USA;

³St. Lukes Episcopal Hospital/Texas Heart Institute, Houston, TX, USA

e-mail: agarwalheart@yahoo.com

Introduction Renovascular hypertension remains a common and treatable diagnosis, and is commonly diagnosed by renal MRI/MRA. Significant extra-renal findings may supersede the primary intent of the study. The frequency of significant incidental findings necessitating further attention and diagnostic workup is unknown.

Purpose The aim of this study was to quantify the frequency of significant incidental findings in routine renal MRI/MRA examinations performed for suspected renovascular hypertension.

Methods From January 2002 to November 2005, 1050 patients underwent MRI/MRA on a 1.5 T Philips MR system for suspected renovascular hypertension. T1 and T2 weighted axial and coronal images were obtained pre and post gadolinium administration. Additionally, non-ECG gated contrast enhanced MRA, and 3D phase contrast MRA were performed. All clinically relevant incidental findings were divided into two categories: Grade I (changes management and needs immediate attention) and Grade II (may change management).

Results A total of 278 Grade I findings were detected (Table 1) in 228 patients (21.7%). A total of 552 Grade II findings were detected (Table 2) in 414 patients (39.4%). **Conclusions** Incidental findings necessitating further attention and diagnostic workup (Grade I) were frequently encountered in patients undergoing renal MRI/MRA for suspected renovascular

hypertension. The majority of such findings were unrelated to the renovascular system yet well within the image purview, highlighting the critical importance for complete anatomic and functional evaluation to facilitate optimal patient care and management.

Table 1 Grade I incidental findings

Incidental finding	N	% of 1,050	Incidental finding	N	% of 1,050
Masses suspicious for cancer	35	3.3	Severe stenosis, occlusion, or aneurysm of mesenteric or pelvic arteries	107	10.2
Liver pathology (ascites, portal hypertension, hemosiderosis)	38	3.6	Infra-renal aortic aneurysm	24	2.3
Adrenal adenoma	24	2.3	Other aortic pathology (Le Riche Syndrome, dissection, A-V fistula)	3	0.2
Gall bladder and bowel pathology (cholecystitis, colitis, ileus)	9	0.9			
Kidney pathology (Staghorn Calculus, PCKD)	4	0.4	Large pleural or pericardial effusion	2	0.2
Other masses including adenopathy	4	0.4	Moderate to severe splenomegaly	28	2.7

06-A-77-NASCI

Automated vessel segmentation from MRA using a three-dimensional tubular model

Piotr Makowski, Patrick de Koning, Emmanuelle Angelié, Jos Westenberg, Rob van der Geest, Hans Reiber
Leiden University Medical Center, Leiden, The Netherlands
e-mail: rvdgeest@lumc.nl

Introduction Three-dimensional (3D) patient specific vessel models are needed in many appli-

Table 2 Grade II incidental findings

Incidental finding	N	% of 1,050
Mild to moderate mesenteric or pelvic artery stenosis	208	19.8
Liver pathology (hepatomegaly, cysts, hemangiomas)	112	10.7
Renal pathology (horseshoe, angiomyolipoma, ectopic, dilated ureter)	33	3.1
Adrenal hyperplasia	68	6.5
Gallstones	93	8.9
Thoracic pathology (moderate pleural or pericardial effusion, cardiomegaly, large hiatal hernia)	35	3.3
Chronic pancreatitis	2	0.2
Spinal fracture	1	0.1

cations such as for the assessment of the stenosis severity or the definition of boundary conditions for Computational Fluid Dynamics (CFD) calculations.

Material and method We developed a computer model of bifurcated vessels consisting of two overlapping tubes. Each tube was implemented as a cylindrical B-spline surface, so its shape is determined by the location of a number of control points. Our model was organized as rings of control points located in planes perpendicular to the vessel axis. We used 7–11 control points per ring in 30–50 rings depending on the vessel length. The 3D model was fit to the MRA data in an iterative process involving around 30 iterations. Validation of the method was based on nine CE-MRA patient studies of carotid arteries and one phantom dataset. Area's of manually drawn contours (M) were compared to contour area's obtained from cross-sections of the 3D model (S).

Results Automated vessel wall segmentation was successful in all clinical cases and the phantom study. The automated method demonstrated a small underestimation of the area. For the phantom data the mean difference between actual physical lumen area and the area of segmented contour was 1.73 mm^2 . Evaluation results for nine studies involving 450 contour pairs showed a mean difference of $4.32 \pm 5.97 \text{ mm}^2$. Figure 1 presents the differences versus their mean. We applied one of the resulting 3D models for CFD calculations in FIDAP software (Fluent Inc.) as presented in Fig. 2.

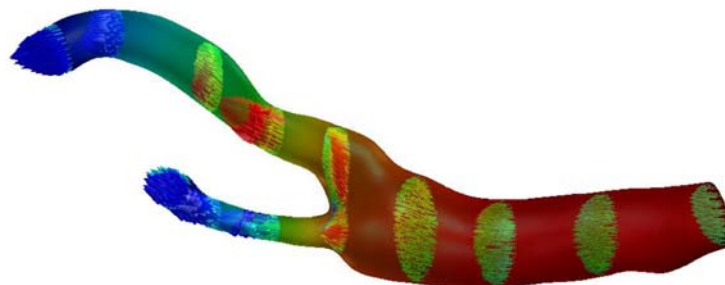
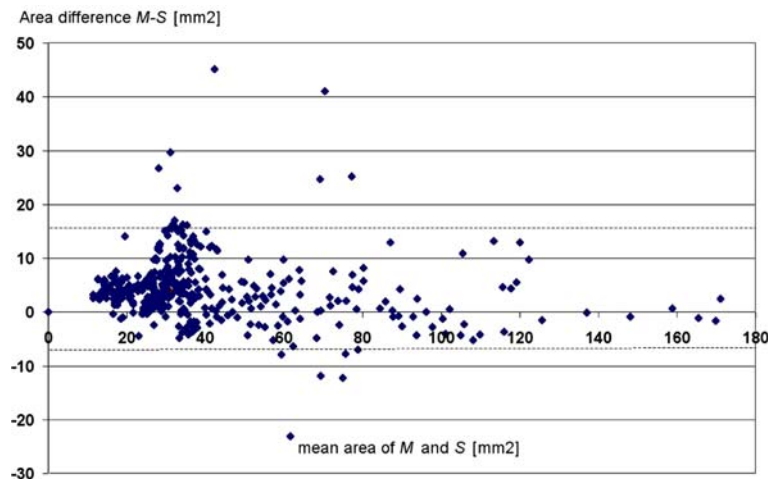
06-A-78-NASCI

Development and application of a quantitative approach to myocardial perfusion imaging and potential indications for clinical use

Christopher Klassen, Alan Siuciak, Minh Nguyen, Norbert Wilke
 University of Florida Health Science Center,
 Jacksonville, FL, USA
 e-mail: christopher.klassen@jax.ufl.edu

The University of Florida Health Science Center Jacksonville operates a busy cardiac imaging program. Since its inception over 600 patients have been scanned. Most of these exams evaluate chest pain using myocardial perfusion scans. These are initially interpreted by Radiologists and Cardiologists using a qualitative approach. In certain cases this was found to be inadequate and that more additional information could be derived from applying a quantitative approach. Our purpose was to develop a quantitative method for myocardial perfusion scans and determine

what cases this would be indicated. Myocardial perfusion scans are acquired at rest and during stress using Adenosine (140 mg/kg/min). The first pass of an 0.03 mmol/kg bolus injection of Gadolinium-DTPA is captured using a Turbo-Flash sequence on a 1.5 T Siemens Sonata. Post-processing consists of placing regions of interest around epicardial and endocardial surfaces. Signal intensity curves are calculated for the myocardium and left ventricular blood pool. The myocardial tissue curve can be represented as a convolution of the tissue impulse response with the left ventricular blood pool. The measured signal intensities of the myocardial tissue and LV blood pool are convolved with the tissue impulse response (Fermi function). A Marquardt-Levenburg fitting algorithm is used so that convolution yields absolute myocardial blood flow and perfusion reserve numbers. In our experience, the quantitative approach is useful if not indicated in at least six categories. (1) Cases with apparent perfusion artifacts. (2) Cases with multiple coronary vessel disease where quantiation may differ-



entiate and map affected coronary territories. (3) Cases with coronary artery stenosis in general, where quantitation can assist in determining the degree of stenosis and possible need for intervention. (4) Patients with microvascular disease. (5) Follow up cases. (6) Finally, it is anticipated that quantitative perfusion results will be used prognostically to determine cardiac risk.

06-A-79-NASCI

Computed tomography angiography of coronary arteries (CCTA). Assessment of images quality in correlation with coronary artery calcium score

Barbara Paraniak, Marcin Basiak, Jolanta Misko, Jacek Brzezinski, Marek Konopka, Dorota Sojka, Piotr Dziurkowski
Silesian Center of Diagnostic Imaging, Katowice, Poland
e-mail: barbara.paraniak@helimed.pl

Computed tomography angiography of coronary arteries has high accuracy and sensitivity in detection stenosis in comparison to results of conventional coronary angiography. Not only heart rate during scan is crucial for good image quality but also amount of coronary artery calcium (CAC). The goal of this study was to assess influence of coronary artery calcium volume on image quality. Sixty-five consecutive patients, aged 34–75; 35 men and 30 women with suspected and confirmed coronary artery diseases were examined. In all cases the MSCT was performed using 16 row CT scanner. Scans before and after contrast enhancement were obtained in all patient; the following settings were applied: slice thickness in pre-contrast scan 2,5 mm, post-contrast 0,625 mm with automatic mAs selection. In all cases nonionic contrast medium was administered in 20 cases using single and in 45 cases dual barrel injector, with flow rate 3.5–5 ml/s, with 2-phase injection protocol. Reformatted images, 3D and volume rendering models were obtained. In all patients Smart Score software was used to assess volume calcium score. Evaluation of the coronary arteries was done in accordance to the AHA classification which distinguishes 15

different coronary segments. Each scan was independently evaluated for by two radiologists. Six-hundred and twenty-four artery segments were assessed. Ninety-four segments were excluded because of superimposing motion artifacts. All patients were divided into groups:

- I—patients with $CS = 0$
- II—patients with $0 < CS < 400$
- III—patients with $400 < CS < 1000$
- IV—patients with $CS > 1000$

In all patients we assessed image quality according to the following pattern:

- good image quality, was defined as sharp delineation between vessel and surrounding structures, good differentiation between vascular lumen and wall
- unsatisfactory was defined as not fulfilling conditions above

There is no significant difference in image quality among each I–IV groups, however the best image quality was observed in cases with $ASE < 400$.

06-A-80-NASCI

Computing effective doses from dose-length products in cardiac CT

Rolf Grage, Walter Huda, Jasjeet Saluja, Kent Ogden, Jennifer Caldwell
Upstate Medical University, Syracuse, NY, USA
e-mail: rgrage@yahoo.com

Purpose CT scanners from all major vendors display the dose length product (DLP) at the completion of each examination; 600 mGy-cm is typical for cardiac CT examinations. We investigated how to convert DLPs into an effective dose, which quantifies the patient stochastic risk (i.e., carcinogenesis and induction of genetic effects).

Method Three CT dosimetry software packages (ImpACT CT Patient Dosimetry Calculator; Scanditronix Wellhofer Impact; CT-expo) were used to compute patient effective doses (E) and the corresponding DLP values for representative

cardiac CT examination (12 cm scan length). We investigated how the E/DLP conversion ratio depends on: (i) CT manufacturer; (ii) scanner model; (iii) X-ray tube voltage (kV); (iv) software package; and (v) patient sex.

Results The average E/DLP ratio was 19 $\mu\text{Sv}/\text{mGy cm}$. Little difference ($< 10\%$) was found in the computed E/DLP ration between four major vendors, or between five models from one vendor manufactured over a 20 year period. E/DLP ratios using all three software packages gave very similar results with differences less than 10%. Increasing the X-ray tube voltage from 80 kV to 140 kV increased the E/DLP ratio by $\sim 25\%$. Female E/DLP ratios in cardiac CT are $\sim 40\%$ higher than for males, due to high breast doses.

Conclusion For cardiac CT examinations, dose length product data can be converted into effective doses using a value of 19 $\mu\text{Sv}/\text{mGy cm}$. A typical cardiac CT study requires $\sim 600 \text{ mGy cm}$, corresponding to a patient effective dose of $\sim 11 \text{ mSv}$.

06-A-81-NASCI

Correlation of emerging risk factors and total coronary atherosclerotic burden using coronary artery calcium scoring

Alireza Zarrabi^{1,2}, Reza Mazraeshahi^{2,3},
Lorraine Frazier¹, Ward Casscells^{1,2}

¹University of Texas – Houston Health Science Center, Houston, TX, USA ²Texas Heart Institute, Houston, TX, USA

³Weill Medical College of Cornell University, The Methodist Hospital, Houston, TX, USA
e-mail: azarrabi@uth.tmc.edu

Background In recent years a number of new markers have been proposed as significant predictors of coronary artery disease (CAD) and its complications. The objective of the study was to examine the correlation of traditional and emerging risk factors with coronary artery calcium (CAC) score a surrogate of coronary atherosclerotic burden.

Methods and results In a prospective cohort, data for 64 patients (41 males and 23 females)

aged between 45 years and 88 years who were followed by cardiology clinic were obtained. Clinical, laboratory, and multi-detector computed tomography (MDCT) data including age, gender, family history of CAD, systolic blood pressure, CRP, homocysteine, fibrinogen, D-dimer, total cholesterol, LDL, HDL, triglyceride (TG), serum creatinine, WBC count, and CAC score were collected. Univariate and multivariate regression analyses were performed. In univariate analysis, there was significant correlation between total CAC score and HDL (negative), TG, systolic blood pressure, creatinine, fibrinogen, and CRP. In multivariate analysis, only fibrinogen level was significantly correlated with total CAC score ($P = 0.03$, $\beta = 3.2$, $\text{CI} = 0.19\text{--}6.23$)

Conclusions Our data suggest that in a multivariate comparison of traditional and new CAD markers, serum fibrinogen is associated with total coronary atherosclerotic burden.

Table 1 Univariate analysis

Risk factors	$\beta \pm \text{SE}$	P Value
CRP	0.57 ± 0.28	0.049
Fibrinogen	4.825 ± 1.612	0.004
D-Dimer	0.107 ± 0.371	0.7
Homocysteine	1.22 ± 0.977	0.2
Creatinine	2.18 ± 0.96	0.02
Total cholesterol	0.016 ± 0.012	0.1
LDL	-0.019 ± 0.016	0.2
HDL	-0.05 ± 0.02	0.004
TG	1.287 ± 0.635	0.04
SBP	0.076 ± 0.023	0.001
WBC	2.18 ± 2.12	0.3
Platelets	0.006 ± 0.005	0.2
Age	0.06 ± 0.03	0.06
Family history of CAD	1.5 ± 0.74	0.04
Smoking history	1.68 ± 1.89	0.3
Treadmill stress test	1.71 ± 0.97	0.08
ASA therapy	0.49 ± 0.69	0.5
<hr/>		
Statin therapy	0.34 ± 0.67	0.6
<hr/>		
Gender (male)	1.41 ± 0.66	0.03

06-A-82-NASCI**Role of emerging risk factors for predicting major adverse cardiovascular events**

Alireza Zarrabi^{1,2}, Reza Mazraeshahi^{2,3}, Lorraine Frazier¹, Ward Casscells^{1,2}

¹University of Texas – Houston Health Science Center, Houston, TX, USA

²Texas Heart Institute, Houston, TX, USA

³Weill Medical College of Cornell University, The Methodist Hospital, Houston, TX, USA

e-mail: azarrabi@uth.tmc.edu

Background Current risk stratification systems for predicting coronary heart disease events are not optimal. The objective of this study was to examine the role of new emerging risk factors for predicting major adverse cardiovascular events (MACE). **Methods and results** A prospective cohort study with a 5 year follow-up of 64 patients was performed. Clinical and laboratory data were collected from 41 males and 23 females patients aged between 45 years and 88 years who were followed at cardiology clinic in University of Texas-Houston. Major cardiovascular events included were cardiovascular-related death, non-fatal heart attacks or stroke, resuscitated cardiac arrest, percutaneous transluminal coronary angioplasty/stent (PTCA), and unstable angina. In a 5-year follow-up period, there were 5 MACEs (two events in females and three events in males) including two PTCAs in females, two PTCAs and one unstable angina in males. Clinical and laboratory data, including new emerging risk factors and coronary calcium score (using GE 16 slice multi-detector computed tomography scan), were compared among patients who experienced a MACE and those who did not (Table 1). Among clinical, traditional, and emerging risk factors, fibrinogen level ($P = 0.001$) and positive treadmill stress test ($P < 0.001$) were the only significant predictor of MACE in our cohort.

Conclusions In a cohort of patients evaluated with traditional and new biomarkers plus coronary calcium scoring, coronary events were best predicted by fibrinogen and perfusion stress testing.

Table 1

Characteristics	CHD Events (N = 5)	No CHD Events (N = 59)	P value
Age (years), SD	69 ± 8	66 ± 9	0.3
Ln (Coronary Artery Calcium +1), SD	6.1 ± 3.1	4.2 ± 2.5	0.1
CRP, SD	1.04 ± 0.26	1.67 ± 1.8	0.6
Homocysteine, SD	11.7 ± 4	10.8 ± 3.6	0.6
D-Dimer, SD	0.56 ± 0.66	0.39 ± 0.27	0.22
Total cholesterol, SD	192 ± 24	180 ± 27	0.31
LDL, SD	78 ± 18	83 ± 21	0.59
HDL, SD	49 ± 18	57 ± 16	0.31
Triglyceride, SD	191 ± 131	135 ± 66	0.1
Fibrinogen, SD	411 ± 120	311 ± 53	0.001
SBP, SD	136 ± 12	126 ± 13	0.08
WBC, SD	5.5 ± 1.2	4.8 ± 0.75	0.062
Platelets, SD	299 ± 87	261 ± 71	0.26
Creatinine, SD	0.90 ± 0.14	0.94 ± 0.33	0.74
Male (%)	3 (60%)	38 (64%)	0.88
DM (%)	0 (0%)	4 (7%)	0.54
HTN therapy (%)	3(60%)	24 (40%)	0.64
Smoker (%)	0 (0%)	2 (3.4%)	0.84
ASA therapy (%)	4 (80%)	38 (64%)	0.65
Statin therapy (%)	3 (60%)	35 (59%)	0.67
Positive Treadmill stress test (%)	5 (100%)	4(10%)	<0.001
Family history (%)	3 (60%)	13 (22%)	0.095

06-A-84-NASCI**A new method of measuring non-calcified coronary atherosclerotic disease by MDCTA**

Melvin Clouse

Beth Isreal Deaconess Hospital, Boston, MA, USA

e-mail: mclouse@bidmc.harvard.edu

A new method of measuring non-calcified coronary atherosclerotic disease by MDCTA.

Purpose To evaluate a new method for quantifying non-calcified atherosclerotic plaque in coronary arteries using voxel histogram analysis.

Methods MDCTA and CCA were performed on 40 patients. Ten with non-calcified plaque by MDCTA and < 50% stenosis by CCA were selected for analysis. Eight equally spaced radial lines, each consisting of seven isotropic voxels (A–G) were drawn across 41 normal and seven abnormal cross-sections (Fig. 1). Voxels A and B

were in epicardial fat, C at fat/wall interface, D and E in arterial wall, F at wall/lumen interface, and G within lumen. 2,292 voxels in normal and 392 voxels in abnormal cross-sections were measured. Plaque volume was calculated by digitally subtracting the voxels representing the normal arterial wall and lumen. A phantom was created for verification.

Results In normal sections, HU values were 2 ± 19 for epicardial fat and outer-arterial wall interface (voxel C). Voxels D and E spanned the wall (D: 65 ± 36 HU and E: 141 ± 53 HU); F at the arterial wall-lumen interface (206 ± 59 HU); G within lumen (249 ± 58 HU). A significant increase in HU value occurred at epicardial fat and outer-arterial wall and inner-arterial wall and lumen interfaces ($P < 0.05$). Mean attenuation values were 30 ± 25 HU (outer-arterial wall) and 175 ± 50 HU (inner-arterial wall), suggesting an average wall thickness of two voxels (0.8 mm). Mean attenuation values were significantly lower in plaque-containing segments: voxel E (83 ± 41), F (115 ± 54), G (139 ± 61) ($p < 0.05$). Two observers measured plaque volumes independently with excellent correlation ($R^2 = 0.968$). MDCT overestimated luminal diameter by 10.3%.

Conclusion Voxel profile analysis is an accurate and reproducible method of quantifying the entire atherosclerotic process (plaque, arterial wall, adventitial thickening) and may be useful in following patients for progression, regression or stabilization of atherosclerosis.

06-A-85-NASCI

Pulmonary vein enlargement detected by magnetic resonance angiography is associated with early recurrence after catheter ablation of atrial fibrillation

Bryan Yoo, Howard Dinh, Deborah Budge, Kalyanam Shivkumar, Paul Finn
David Geffen School of Medicine at UCLA,
Los Angeles, CA, USA
e-mail: byoo@ucsd.edu

Purpose The pulmonary veins (PV) have been implicated in atrial fibrillation (AF). PVs are

enlarged in patients with AF, but whether their size affects recurrence after ablation is unknown. We assessed whether PV diameters measured from pre-ablation magnetic resonance angiography (MRA) is associated with early recurrence after catheter ablation of AF.

Methods Consecutive patients ($n = 68$) underwent MRA prior to ablation procedure for symptomatic, drug refractory AF. Early recurrence was defined as the presence of AF and/or flutter on ECG at the most recent follow-up after ablation. PV diameters were measured using coronal MRA reconstructions. Receiver operating characteristics (ROC) were generated to assess accuracy in predicting AF recurrence.

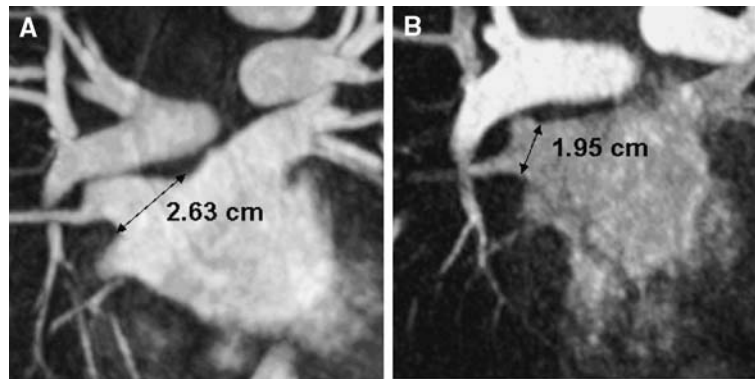
Results There were 12 patients who were lost to follow-up. Of the remaining 56 patients, 22 (39%) had early recurrence of AF. The diameter (cm) for the bilateral superior PVs (RSPV, LSPV) when compared between those who had AF recurrence vs. those who remained in sinus reached the following values: RSPV 2.63 ± 0.86 vs. 2.23 ± 0.42 ($P = 0.03$), LSPV 2.20 ± 0.42 vs. 2.05 ± 0.37 ($P = 0.17$). The diameter for the bilateral inferior PVs (RIPV, LIPV) for AF recurrence vs. sinus were RIPV 2.21 ± 0.47 vs. 2.01 ± 0.34 ($P = 0.07$), LIPV 2.15 ± 0.60 vs. 1.91 ± 0.32 ($P = 0.07$). See figure for example of RSPV measurements (A, recurrence, B, sinus). ROC analyses were performed for all four PV diameters to assess accuracy in detecting recurrent AF. The RSPV diameter had the highest area-under-the-curve (0.682, $P = 0.025$).

Conclusion Increased PV diameter is associated with higher recurrence of AF after ablation, with the RSPV size being the most accurate of the four PVs.

06-A-86-NASCI

Value of MSCT (multislice CT) plus cardiac magnetic resonance imaging (CMRI) for the acute coronary syndrome exclusion

Miguel Orejas¹, Antonia Arjonilla¹,
Borja Ibanez², Antonio Pinero¹, Felipe Navarro¹,
Jose Manuel Rubio¹, Pedro Marcos-Alberca¹,
Angeles Franco¹, Jeronimo Farre¹
¹Fundacion Jimenez Diaz-Capio, Madrid, Spain



²Mount Sinai School of Medicine, New York, NY, USA

e-mail: ibanez_borja@yahoo.es

Introduction ACS-diagnose is based on chest pain+enzyme rise+ECG-changes. However, there are patients, especially young with prior flu-like-symptoms, which fulfil these criteria but have no coronary-artery-disease(CAD). Currently the gold standard technique to rule out ACS is the invasive-coronary-angiography. MRI-delayed-enhancement has been recently reported to show a different pattern in ACS(sub-endocardial enhancement) and in myocarditis(sub-epicardial enhancement). In addition MSCT has emerged as a promising tool for CAD evaluation. **Hypothesis** The combination of CMRI and MSCT can accurately rule out ACS in patients with ACS-criteria and infectious-symptoms.

Methods Eight consecutive patients (26 ± 6 years) with flu-like-symptoms prior to the onset of “ACS-like” criteria were included. MSCT and CMRI (after MSCT) were performed within 48 h after admission. Coronary 40-slice-CT was performed under ECG-gating with 40×0.625 mm collimation and after 75 cc injection of iodinated-contrast-media. CMRI-study included cine-gradient-echo-sequences (first pass [perfusion study] and delayed enhancement 15 min post 0.2 mmol/kg Gd-DTPA). Second CMRI was performed four months after discharge in 50%.

Results CMRI segmental-wall-motion-abnormalities were seen in 7/8 patients. CMRI perfusion-study was normal in all eight cases. Seven patients showed Gadolinium delayed-enhancement in different segments. In six of these, the delayed-

enhancement pattern was sub-epicardial, being subendocardial in the remaining case. On coronary-MSCT study, 7/8 patients showed no significant CAD lesions and one presented severe stenosis in the circumflex-coronary-artery. This patient presented with sub-endocardial CMRI-delayed-enhancement pattern. In one case, coronary angiography showed a critical stenosis on left circumflex (confirming CMRI and MSCT data) that need percutaneous transluminal coronary angioplasty. Follow-up CMRI showed complete resolution in both delayed enhancement and segmental wall motion abnormalities except in the ischemic patient.

Conclusions Combination of two non-invasive imaging-techniques(MSCT and CMRI) is extremely accurate in the exclusion of CAD in patients with “ACS-criteria” and infectious symptoms prior to the onset of symptoms. This approach avoids the need of invasive procedures to rule out an ACS.

06-A-88-NASCI

Comparison between tissue doppler imaging and velocity-encoded MRI for the assessment of left ventricular dyssynchrony

Jos Westenberg, Hildo Lamb, Rob van der Geest, Gabe Bleeker, Eduard Holman, Martin Schalij, Albert de Roos, Ernst van der Wall, Johan Reiber, Jeroen Bax

Leiden University Medical Center, Leiden, The Netherlands

e-mail: r.j.van_der_geest@lumc.nl

Introduction A mechanical delay between septum and lateral wall contraction (i.e., LV dyssynchrony (LVD)) may be the main predictor of response to cardiac resynchronization therapy (CRT). LVD can be adequately assessed with tissue Doppler imaging (TDI), but this has not been validated by other imaging modalities. Velocity-encoded (VE) MRI allows direct myocardial wall motion measurement similar to TDI.

Methods Twenty patients (15 men, mean age 57 ± 15 years) with heart failure, QRS-duration > 120 ms and interventricular conduction delay were included, as well as 10 healthy volunteers (8 men, mean age 57 ± 9 years) with QRS-duration < 85 ms and normal LV function. TDI was acquired on a Vingmed Vivid Seven (GE, Milwaukee, WI). Times of peak systolic velocities (PSVs) were assessed in septum and lateral wall at basal level, and the difference (i.e., septal-to-lateral delay) defines LVD. MRI was performed on a 1.5 T ACS-NT15 Gyroscan (Philips Medical Systems, Best, The Netherlands). Three-directional VE MRI (velocity sensitivity 20 cm/s) was performed in a four-chamber orientation. Similar to TDI, the difference in times of PSVs in septum and lateral wall defines LVD. Correlation between both modalities was investigated.

Results None of the volunteers showed LVD (mean -2 ± 15 ms on TDI; mean -5 ± 17 ms on MRI, $p =$ non-significant (NS)). In patients, mean LVD was 55 ± 37 ms on TDI and 49 ± 38 ms on MRI ($p =$ NS). Figure 1 shows LVD by MRI versus TDI. Good correlation between both modalities is observed (linear

regression $Y = aX + b$, with a (\pm standard error SE) = 0.99 ± 0.04 and $b \pm$ SE = -5 ± 2 , $n = 30$, $r = 0.98$, $P < 0.01$). MRI showed a small, non-significant underestimation of 5 ± 8 ms compared to TDI.

Conclusion Very strong correlation between MRI and TDI for LVD assessment, with both modalities producing similar results.

06-A-89-NASCI

Characterization of non-calcific coronary plaques using high-resolution MR imaging at 3 T: comparison with MDCT

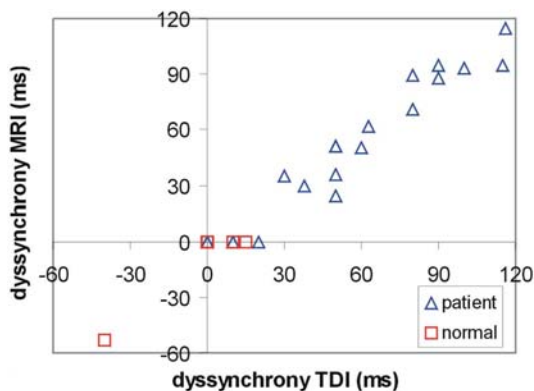
Yeon Hyeon Choe¹, Min Hee Jeon¹, Jin Ho Choi²
¹Department of Radiology, Samsung Medical Center, Sungkyunkwan University School of Medicine, Seoul, Republic of Korea

²Division of Cardiology, Department of Internal Medicine, Samsung Medical Center, Sungkyunkwan University School of Medicine, Seoul, Republic of Korea

e-mail: yhchoe@smc.samsung.co.kr

Purpose To evaluate the feasibility of detection and characterization of non-calcific coronary artery plaques in vivo using high-resolution MR imaging at 3 T.

Materials and methods Coronary artery MRA was performed 10 patients with non-calcific components of coronary artery lesions detected at MDCT. Twelve non-calcified stenotic segments were targeted for plaque imaging at 3 T (Intera Achieva, Philips). T1-, T2-weighted double inversion recovery imaging (slice thickness, 1.5 or 2 mm; FOV, 22 cm or 30 cm; in-plane resolution, $0.98 \text{ mm} \times 1.08 \text{ mm}$ or $1.17 \text{ mm} \times 1.18 \text{ mm}$) was performed in contiguous short-axial planes of proximal and mid-segments of coronary arteries. A TFE sequence (2 mm thickness; resolution, $0.9 \text{ mm} \times 0.9 \text{ mm}$) was applied in the same planes. Postcontrast T1-weighted images were also obtained. In two cases, intracoronary US was performed. Plaques with low signal intensity area more than 50% plaque area on T2-weighted and T1-weighted postcontrast MR images and with mean attenuation value of less than 30 H.U. at CT were considered as vulnerable plaques. Results:



MR image quality was diagnostic without significant artifacts in all patients. Significantly heterogeneous signal intensity on MR images of various sequences was found in 9 of 12 soft plaques (75 %). Six plaques were classified as vulnerable ones by CT findings and four plaques by MR findings. Two of six vulnerable plaques at CT showed no evidence of vulnerability on MR images. Mean plaque areas determined by MR and CT were $6.61 \pm 2.65 \text{ mm}^2$ and $5.34 \pm 2.17 \text{ mm}^2$ respectively with modest correlation ($r = 0.53$) and without significant difference ($P = 0.14$). Findings of intracoronary US correlated well with MR findings in visualization of plaque components.

Conclusion Coronary artery plaque characterization is feasible using 3 T MR imaging. 3-T MR imaging may provide more information than MDCT in coronary plaque imaging.

06-A-90-NASCI

Quantitative evaluation of the severity of aortic regurgitation using MDCT: Comparison with echocardiography

Min Hee Jeon, Yeon Hyeon Choe
Department of Radiology, Samsung Medical Center, Sungkyunkwan University School of Medicine, Seoul, Republic of Korea
e-mail: yhchoe@smc.samsung.co.kr

Purpose To evaluate the severity of aortic regurgitation (AR) quantitatively using MDCT.

Methods and materials 23 patients with AR underwent electrocardiography (ECG) gated 40-slice MDCT (Philips Brilliance 40) and transthoracic or transesophageal echocardiography. CT data sets were reconstructed during mid-systole, mid-diastole, end-systole, and end-diastole phases. The abnormally opened aortic valve area in the end-diastole (AR area) was planimetrically measured on CT reformatted images. We compared AR area on CT (ARACT) with severity of AR (mild, moderate, or severe) estimated at echocardiography. The depth, width, intensity, and pressure half time of the aortic regurgitant jet in the parasternal and apical views were considered for echocardiographic grading of AR. Valve morphology on reformatted and volume-ren-

dered CT images were also assessed. Five patients with severe AR at echocardiography underwent aortic valve replacement surgery.

Results In seven patients with mild AR, ARACT was $0.14 \pm 0.04 \text{ cm}^2$ (mean \pm 1 SD; range, 0.09 ~ 0.21). In eight patients with moderate AR, ARACT was $0.44 \pm 0.19 \text{ cm}^2$ (range, 0.26–0.81). In eight patients with severe AR, ARACT was $1.1 \pm 0.45 \text{ cm}^2$ (range, 0.5–1.83). With a cutoff value of 0.70 cm^2 for significant or severe AR, sensitivity, specificity, and diagnostic accuracy of MDCT as compared echocardiographic severity were 88%, 93%, and 95%, respectively. In five surgically treated patients, mean ARACT was 1.00 cm^2 (range, 0.5–1.49).

Conclusion Planimetric measurements of the AR area using MDCT is useful in quantitative evaluation of the severity of aortic regurgitation.

06-A-91-NASCI

Usefulness of volume-rendered virtual CT angiography in the evaluation of valvular heart diseases

Min Hee Jeon, Yeon Hyeon Choe
Department of Radiology, Samsung Medical Center, Sungkyunkwan University School of Medicine, Seoul, Republic of Korea
e-mail: yhchoe@smc.samsung.co.kr

Purpose To evaluate the usefulness of virtual CT angiography in patients with valvular heart diseases.

Methods and materials 29 patients with valvular heart diseases underwent 40-slice MDCT (24 aortic valve diseases, six mitral valve diseases, two pulmonary valve diseases, one tricuspid valve diseases, four aortic and mitral valve diseases). The volume-rendered virtual CT angiography (VCTA) were generated with Advantage workstation (Version 4.1, GE Medical systems). Two radiologists compared virtual CT angiographic images with multiplanar reformatted images (MPR). VCTA quality was graded in five scales. We evaluated CT images regarding to the distribution of the valve calcifications, shape of the valves, valve thickening, pannus at the mechanical valve, vegetations, and valve areas.

Results Average grade of VCTA quality was 3.78 (range, 2–5). VCTA provided similar information to that of MPR in 16 patients (55%). VCTA of the eight patients (28%) provide more information than MPR. In five patients (17%), MPR provide more information. Distribution of the valve calcifications, shape of the valve, valve thickening, pannus at the mechanical valve, and vegetations were better visualized on virtual CT angiography, when left ventricle cavity was homogeneously enhanced. However, the degree of aortic valve stenosis was overestimated on VCTA than on MPR image.

Conclusion Volume-rendered virtual CT angiography is useful in the evaluation of valvular heart disease. It offers more realistic information on the architecture of the valves and soft tissue lesions such as pannus and vegetations.

06-A-92-NASCI

Detection of regional circumferential strain and strain rate heterogeneity in heart failure by 2D SPAMM MRI

Juan C. Alvergue, Howard V. Dinh, Gregg Fonarow, Kalyanam Shivkumar, Paul Finn
UCLA, Los Angeles, CA, USA
e-mail: jalvergue@mednet.ucla.edu

Introduction Strain is depressed in heart failure (HF), and its magnitude displays greater regional variance in the setting of dyssynchrony. This study implements 2D MR tagging to derive regional circumferential strain (Ecc) and strain-rate ($dEcc/dt$) in HF versus healthy controls.

Methods HF patients being considered for cardiac resynchronization therapy ($n = 18$, age 49.8 ± 13.5) and age-matched controls ($n = 20$, age 43 ± 14) were scanned with a 1.5 T MRI using 2 D-FLASH spatial modulation of magnetism sequence with grid tags (1 mm diameter, 7 mm space) and temporal resolution of 46 ms. The basal, mid and apical short axes were imaged with Ecc and $dEcc/dt$ (measured for all 16 segments of the LV) assessed off-line by analysis software (Cardiac Imaging Modeler V5). Regional heterogeneity indices (Ish) were also calculated and defined as the standard deviation at the

peak average Ecc (or $dEcc/dt$)/average Ecc (or $dEcc/dt$) $\times 100\%$.

Results Strain Ish values were higher for HF compared to controls at the apex (-61 ± 76 vs. -14 ± 7.5 , $P < 0.05$), mid (-36 ± 32 vs. -20 ± 32 , $P < 0.05$), and base (-63 ± 64 vs. -28 ± 25 , $P < 0.05$). Peak diastolic strain-rate Ish values in the apex and mid regions were greater in the HF group compared to controls (-39 ± 19 vs. -18 ± 6.3 , $P < 0.001$, and -28 ± 17 vs. -18 ± 9.5 , $P < 0.01$).

Conclusions Ecc magnitude is depressed and regional Ecc heterogeneity is increased in HF. Similarly, regional $dEcc/dt$ heterogeneity is also increased in myopathic hearts, which may indicate regional delayed systolic or diastolic dyssynchrony.

06-A-94-NASCI

Coronary CT arteriographic plaque burden: correlation with past coronary events

Kevin Johnson¹, Jolanta Dennis¹, David Dowe²
¹Yale University, New Haven, CT, USA
²Atlantic Medical Imaging, Galloway, NJ, USA
e-mail: kevin.johnson@yale.edu

Background If coronary artery atherosclerotic plaque burden reflects the risk of a coronary event, several predictions should hold. Plaque burden should track past coronary events. If there is no plaque, there should have been few if any past events. Plaque burden scores should distribute between the sexes in the same proportion as do past events. Plaque burden should increase with age at the same rate as events. Plaque topography should agree with the known topography of culprit lesions.

Methods and results 2,032 outpatients presenting to a general radiology practice because of concern for elevated risk of coronary disease were studied. Of these, 220 gave a history of past coronary events including infarction, CABG, stent or angioplasty. Plaque burden was estimated on a per segment basis using a 5 point scale then summed. The area under the receiver operating characteristic curve for “prediction” of past coronary events (retrodiction) was 0.84. Only five cases out of 220 occurred in patients with no visible plaque, and several of these apparently repre-

Baseline global cardiac function

	HF (<i>n</i> = 18)	Controls (<i>n</i> = 20)	<i>P</i>
EF(%)	26 ± 14	63 ± 7	≤ 0.001
Ecc Apex	-11 ± 5	-23 ± 3.6	≤ 0.001
Ecc Mid	-10 ± 4	-21 ± 5	≤ 0.001
Ecc Base	-8.8 ± 4	-16 ± 5	≤ 0.001

sented spurious histories. One was a spontaneous coronary artery dissection. The mean plaque burden in males was 6.91 (95% C.I. 6.53–7.30) and in females 3.63 (95% C.I. 3.21–4.1), for a ratio of 1.90. Males had 154/220 past events and females 66/220, for a ratio of 2.33. Plaque burden tracked the expected increase in events with age as seen in the Framingham population, and the topology of plaque was similar to previously described distributions of culprit lesions.

Conclusions The retrospective “predictions” described above were all found to hold true for the present data. Prospective studies of coronary events are needed to determine if these attributes of coronary CTA are in fact predictive.

06-A-95-NASCI

Comparison of cardiac ejection fraction analysis packages for computed tomography

Joseph Blechinger, Milan Pantelic, Khaled Abdul-Nour, Tina Nelson
Henry Ford Hospital, Detroit, MI, USA
e-mail: josephb@rad.hfh.edu

A comparison of post-processing software packages for calculation of left ventricular volumes from 64 slice CT. Patients were scanned with a Siemens Sensation scanner, using beta blockers for a target heart rate of 60 beats per minute injected tieh 350 contrast using a Medrad injector with mixing to reduce the artifacts from the right heart. Analysis was performed using the Circulation package on a Siemens Leonardo, the Vitrea 2 from Vital Images, and the GE Healthcare AW.

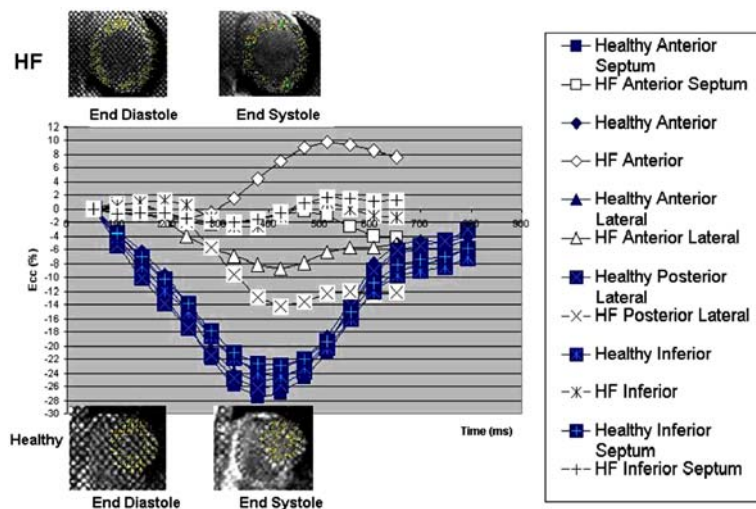
06-A-96-NASCI

Analysis of thoracic aortic dynamics and compliance by ECG-gated 64-Slice MDCT

Benoit Desjardins
University of Michigan, Ann Arbor, MI, USA
e-mail: benoitd@umich.edu

Introduction Thoracic aorta imaging with multi-detector computed tomography (MDCT) consists primarily of anatomic imaging. We evaluated the feasibility of assessing aortic compliance by MDCT, and assessed its clinical usefulness at evaluating aortic pathology.

Method and materials 25 subjects (11 with aneurysm, four with dissection, five post-grafting, five controls) underwent MDCT imaging of the thoracic aorta. Blood pressure information was measured immediately prior to the scan. MDCT was performed with ECG-gating using a 64-slice scanner, 0.4 s rotation time, 1.25 mm collimation



and intravenous contrast during a single breath-hold. Images were reconstructed at 5% increments of the RR interval. Post-processing was performed to determine changes in the thoracic aorta throughout the cardiac cycle, using a three step process: (1) a level set deformable surface algorithm to extract the thoracic aorta and branches, (2) a Voronoi diagram algorithm to compute the aortic centerline, and (3) additional processing to compute the compliance from local changes in cross sectional area.

Results Dynamic imaging of the thoracic aorta in human subjects is feasible. MDCT clearly shows changes in aortic cross sectional area with cardiac contraction. For every point along the centerline, a compliance value is computed and a global compliance curve over the entire length of the aorta is generated for each subject. Computed compliance in normal subjects matches expected normal aortic physiology. In older normal subjects, a decrease in compliance is noted. Compliance curves in subjects with aneurysms, dissection and grafts differ from those found in normal subjects, with local decrease in compliance in the areas of pathology.

Conclusions Thoracic aorta dynamic imaging by MDCT is technically feasible, and provides important information on aortic compliance in aortic pathology, such as atherosclerotic disease, aneurysm and dissection, as well as for post-surgical assessment of the aorta. This information is not provided by anatomic imaging alone.

06-A-97-NASCI

Usefulness of delayed enhancement CMR in visualization and differentiation of subendocardial infarction

Marcin Basiak, Jolanta Misko, Maria Dziubinska-Basiak, Marek Konopka, Barbara Paraniak, Marcin Hartel, Aleksandra Kieltyka
HELIMED Silesian Centre of Diagnostic Imaging, Katowice, Poland
e-mail: marcin.basiak@helimed.pl

Introduction Cardiovascular Magnetic Resonance makes possible complex imaging of myocardium function, viability and perfusion in patients

after cardiac infarction. Delayed enhancement effect is specially useful tool in assessment of extent and volume of necrotic myocardial tissue.

Materials and methods CMR examinations were performed in last 6 months in 23 patients with aggravation of Coronary Artery Disease symptoms. Eleven patients with confirmed myocardial infarction and 12 without confirmation were included in the study. In all patients MR examination was recorded using CINE option, First Pass and Delayed Enhancement –15 min after administration of contrast agent in 2- and 4-ventricular projection and in short axis of the heart. Scans were post-processed using Mass Application obtaining information about morphology, function, vitality and perfusion of LV myocardium according to AHA segmentation into areas of coronal arteries blood administration.

Results Delayed Enhancement effect imaging enabled to define very accurate presence, extent and localization of post-infarctal scar myocardial tissue. In 8 out of 23 patients extensive infarctal subendocardial necrosis were affirmed. In four patients transmural necrosis was imagined.

Conclusion MR enables evaluation of myocardial function, vitality and perfusion improving and facilitating cooperation of radiologist and cardiologist or cardiothoracic surgeon. Using Delayed Enhancement Method makes possible very accurate imaging of non-transmural myocardial infarction, that has great meaning to following therapeutic process (PCI/CABG)

06-A-99-NASCI

Magnetic resonance imaging as an essential tool for emerging and infradiagnosed pathologies

Marina Huguet¹, Cristina Moure², Gustavo Avegliano², Jose Luis Dolz¹, Pilar Lozano¹, Joan Llevadot², Guillermo Oller², Enrique Delgado¹

¹Cetir-sant Jordi, Barcelona, Spain

²Centro Cardiovascular Sant Jordi, Barcelona, Spain

e-mail: mhuguet@cetir.es

The high resolution of magnetic resonance, the absence of radiation and the technological devel-

opment, have increased substantially the number of cardiac MRI exams. Now, is an imaging modality essential in the diagnosis of some pathologies as apical hypertrophic cardiomyopathy, non-compaction cardiomyopathy and myocarditis. These entities are infradiagnosed because the limitations of other imaging modalities. We present a total of 36 studies. Eight patients with apical hypertrophic cardiomyopathy (wall thickness greater than 15 mm), five non-compaction cardiomyopathy (thickened wall with multiple prominent ventricular trabeculations and deep intertrabecular recesses, relation 2.3 with normal myocardium) and 23 myocarditis (outer myocardial layers focal enhancement with clinical features of myocarditis). We have performed cine MRI, using b-SSFF technique and CE-IR MRI with late imaging. Cardiac MRI permits a precise anatomical diagnosis of these entities, assessing functional information and the prognosis of the patients. With this technique, less known pathologies as non-compaction cardiomyopathy have emerged. Also, with cardiac MRI the diagnosis of apical hypertrophic cardiomyopathy and myocarditis has resurged.

06-A-100-NASCI

64-Slice MDCT angiography of coronary arteries: an effective filter before catheter angiography

Ralph Haberl, Doreen Voss, Juergen Buck, Eike Boehme
Klinikum Munich-Pasing, Munich, Germany
e-mail: haberlralph@t-online.de

Background Multislice CT-angiography (MD-CT-A) allows to visualize coronary arteries with impressive image quality, however, it is unclear, if it may act as an effective filter before catheter angiography (Cath-A) in patients with suspected coronary artery disease (CAD).

Methods We therefore enrolled 122 consecutive patients with de novo suspected CAD (chest pain and signs of ischemia in conventional stress tests) and performed contrast enhanced MDCT-A (Philips Brilliance 64, effective acquisition time 110–210 ms, collimation 64×0.625 mm, retrospective gating) and Cath-A in all of them.

Patients with acute coronary syndromes, a history of CAD and patients with a calcium volume score $> 1,000$ were excluded. MDCT-A and Cath-A were read by different investigators using the AHA 15-segments model. Stenosis was defined as $> 50\%$ luminal obstruction.

Results Total scan time was $9 \text{ s} \pm 3.4$. Ninety-two percent of all segments had diagnostic image quality. MDCT-A predicted exclusion of stenosis in 52 patients and this was confirmed by Cath-A in 48 patients (negative predictive value 92%, four patients missed with stenoses in side branches not requiring intervention). About 69 of 73 stenoses were correctly identified with MDCT-A (sensitivity 94%, specificity 85%, all per patient) and no stenosis requiring intervention was missed. Seven stenoses—all detected with MDCT-A—occurred in patients without any coronary calcium. MDCT-A false positively diagnosed stenosis in nine patients due to misclassification of nonobstructive plaque as stenosis (positive predictive value 87%).

Conclusion MDCT-A with the 64-slice scanner allowed to assess 96% of coronary segments relevant for coronary interventions. It proved sensitive to detect stenosis, and was accurate to exclude stenosis. Thereby this scanner generation for the first time may be accurate and robust enough to be used as a noninvasive filter before Cath-A in clinical practice. This approach has the potential to save $> 30\%$ of diagnostic invasive procedures.

06-A-101-NASCI

Significant radiation dose reduction possibilities using EKG gated high pitch helical acquisitions for gated chest exams in CT

Melissa Vass, Uri Shreter, John Londt
GE Healthcare, Waukesha, WI, USA
e-mail: Melissa.Vass@med.ge.com

Purpose Reduction of dose in EKG gated helical CT acquisitions is desired due to the low helical pitch, typically less than 0.25. Alternately a fast, ungated helical pitch could be used without EKG gating at a reduced dose, but significant

image quality loss due to cardiac induced motion in the organs of the chest may result. An advanced high pitch helical acquisition technique with EKG gating was assessed to provide a lower dose scan while maintaining image quality benefits of a gated acquisition.

Method EKG gated helical CTA parameters were assessed for heart rates in the range of 30–80 beats per minute. Heart rate dependent helical pitch values were varied over a range of low and high pitches. DLP values were evaluated from phantom scans acquired with a multi detector-row CT scanner (GE LightSpeed VCT, USA) in 64×0.625 mm mode with the advanced high pitch gated reconstruction technique at pitch values above the 0.25 range. These values were compared to DLP for equivalent typical low pitch gated acquisitions. IQ was qualitatively reviewed in comparison to the clinically accepted low pitch exams. Results were tracked to assess percentage of dose savings applicable with the high pitch EKG gated acquisition technique.

Results Over the BPM range analyzed with the high pitch gated acquisitions and image reconstruction, dose savings up to 46% were achieved with clinically acceptable image quality.

Conclusion High pitch EKG gated CT acquisitions at pitch values above the 0.25 low pitch range in clinical use today can provide gated imaging at a lower dose. Initial clinical data supports the findings. More extensive clinical evaluations are underway to assess radiation dose savings for various aspects of chest imaging.

06-A-102-NASCI

Evaluation of coronary stents with 64-slice multislice computed tomography: ready for prime time?

Franz von Ziegler^{1,2}, Carsten Rist³,
Becker Alexander², Alexander Leber²,
Janine Tittus², Norbert Wilke^{1,4},
Christoph Becker³, Andreas Knez²

¹Department of Cardiology, University of Florida, Shands, Jacksonville, FL, USA

²Department of Cardiology, University of Munich, Grosshadern Campus, Munich, Germany

³Department of Clinical Radiology, University of Munich, Grosshadern Campus, Munich, Germany

⁴Department of Radiology, University of Florida, Shands, Jacksonville, FL, USA

e-mail: Franz.Ziegler@jax.ufl.edu

Evaluation of coronary stents by multislice computed tomography (MSCT) was limited in the past by artifacts due to beam hardening and limited spatial and temporal resolution. The introduction of 64-slice MSCT technology seems to overcome these restrictions. Aim of the present study was to evaluate its diagnostic accuracy for determination of coronary artery stent patency compared to quantitative coronary analysis (QCA). Twenty male patients (age 63 ± 11.7 years) undergoing 6-month coronary angiography (CA) follow-up after directional stent implantation were included. Non-invasive angiography was acquired with 64-slice-MSCT (Sensation 64, Siemens, Germany) using a standardized protocol 1 ± 2 days within CA. QCA analysis and MSCT analysis were performed by two experienced and blinded readers. In addition to in-stent-restenosis (ISR) quantification stentlength was measured and compared to manufacturing details. 9 patients received orally Betablocker treatment one hour before the CT-scan due to heart rates > 70 bpm. Therefore, good diagnostic image quality was achieved in all cases (heart rate: 62 ± 8 bpm) so that an overall of 32 stents could be analyzed. Out of 22 stents showing no significant stenosis in CA, CTA correctly identified 18. Four stents were misclassified as mildly stenotic ($< 50\%$ luminal diameter stenosis). All totally occluded stents were correctly detected by CTA (6/32) as opposed to 1/4 significant obstructed stents ($> 70\%$). Therefore, a sensitivity of 70% (7/10) and a specificity of 82% (18/22) for the whole study group was calculated. Diagnostic accuracy for detecting significant ISR was 78% (25/32). Stentlength measurement showed no significant differences between the manufacturing details and the CTA results [13.4 ± 3.8 mm vs. 13.6 ± 3.8 mm ($P < 0.05$)]. Pearson-correlationcoefficient was 0.99. MSCT offers the ability to detect total occluded stents with a high diagnostic accuracy. Mild and significant ISR often were misclassified. Above all

stentstruts and in-stent calcium deposits due to their blooming artifacts were the most limiting factors for a correct classification.

06-A-103-NASCI

64-Detector coronary angiography for the quantification of acute angle take-off and narrow ostial areas in patients with anomalous coronary arteries

Keyoor Patel, Amgad Makaryus, Perwaiz Meraj, Lawrence Boxt
North Shore University Hospital at Manhasset, Manhasset, NY, USA
e-mail: keyletap@yahoo.com

Background Sudden cardiac death has been attributed to the presence of acute angle take-off (AAT) and narrow ostial areas of the coronaries in patients with anomalous coronary arteries (ACA). We quantified the take-off angles and ostial areas of anomalous coronaries among patients with ACA using 64-detector CT angiography (64-CT).

Methods Between April 2005 and May 2006, 1,465 consecutive patients were evaluated using 64-CT (GE Light Speed VCT™). The take-off angles and the ostial areas of the ACA were compared with the coronary arteries of 12 control patients.

Results Nineteen patients (1.3%; 11 men; 8 women; ages 47–60 years) were identified with ACA. Six (32%) patients had a separate origin of the left anterior descending artery and the circumflex artery (LCX) both originating from the left sinus of valsalva (LSOV). Five (26%) patients had a single coronary artery originating from the right sinus (RSOV) and thereby forming the right coronary artery (RCA) and the left coronary artery (LCA). Four (21%) patients had the origination of the RCA and LCA from the LSOV. The remaining four (21%) had individual anomalies: LCX originating from the RCA, the RCA originating above the RSOV, the LCA off the right lateral-most aspect of LSOV, and the LCA arising posterior at the junction between the left-coronary cusp and the non-coronary cusp. The mean take-off angles of RCA of ACA were

found to be significantly smaller than normals (23.7° vs. 61.5°, $P < 0.0001$). The mean take-off angles of the LM of the ACA were more acute than normals (24.4° vs. 63.2°, $P = 0.0002$). The mean ostial areas of the RCA of the ACA were smaller than normals (13.1 mm² vs. 19.5 mm², $P = 0.13$). The mean ostial areas of the LCA of the ACA were narrower than normals (13.07 mm² vs. 20.77 mm², $P = 0.0063$).

Conclusion 64-CT is an accurate and effective non-invasive method for the quantification of the take-off angles and ostial areas in patients with ACA. Patients with ACA have AAT and narrower ostial areas than normal patients.

06-A-104-NASCI

Evaluation of the effectiveness of oral beta blockade in patients for cardiac CT

Harpreet pannu, Elliot fishman, Johns Hopkins
Baltimore, MD, USA
e-mail: hpannu1@jhmi.edu

Purpose To determine the effectiveness of oral beta blockers in lowering the heart rate for cardiac CT.

Methods Nursing records were retrospectively reviewed in 200 consecutive patients having cardiac CT over six months. 11 patients were excluded – 5 for lack of iv access, two for pacemakers, four for incomplete nursing records. The heart rate on arrival to CT and approximately 30 min and 60 min after oral beta blocker administration was noted and the change in heart rate after medication calculated.

Results For the 189 patients, mean heart rate was 70.9 ± 12.1 bpm on arrival to CT. Eighty-five patients had a mean heart rate of 60.8 ± 6.0 bpm and did not receive beta blockers. One-hundred and four patients had a mean heart rate of 79.1 ± 9.5 bpm and 96 patients were given 50 mg metoprolol po, 7 got 100 mg metoprolol po and the dose was unavailable in 1. Approximately 30 min after metoprolol, the mean heart rate was 68.8 ± 7.6 bpm and mean change in heart rate from baseline was 10.3 ± 6.3 bpm. Of the 104 patients receiving beta blockers, 53 patients went to CT 30 min after metoprolol. In

these patients, the average heart rate was 73.3 ± 5.0 bpm on arrival to CT, 63.4 ± 3.9 bpm 30 min after metoprolol and average change from baseline was 9.9 ± 4.5 bpm. The remaining patients required additional monitoring prior to CT and their average heart rate was 85.1 ± 9.3 bpm on arrival to CT and 67.2 ± 6.3 bpm 60 min after metoprolol with average change from baseline of 17.3 ± 6.6 bpm ($n = 49$). Fourteen patients required iv metoprolol. No adverse events were recorded.

Conclusion Oral beta blockers given within one hour of CT are a satisfactory technique for optimizing the heart rate for cardiac CT in most patients without adverse events.

06-A-105-NASCI

Relief of migraine headaches associated with closure of patent foramen ovale

Farhan Aslam, James Blankenship, Leo Iliadis
Geisinger Medical Center, Danville, PA, USA
e-mail: farhan.dr@gmail.com

Objective The incidence of patent foramen ovale (PFO) in migraine patients is at least twice that of the general population. However, few reports demonstrate the impact of PFO closure on the relief of migraine headaches. We retrospectively surveyed PFO closure patients to determine if those with migraines were improved after PFO closure.

Method Between Jan 2001 and Dec. 2004 52 PFOs were closed percutaneously using the Cardioseal or Amplatzer devices for patients with a history of prior TIA or stroke. At a mean of 28 months post PFO closure all patients were called to identify the presence, frequency and type of migraine headache (MH) episode occurring pre- and post-procedure. MH and associated aura were defined according to the criteria of the International Headache Society. Patients were not informed that PFO closure might have any impact on MH.

Results Among total of 52 PFO closure patients, 22 (42%) had MH and 12/22 had aura. The average age of MH patients was 44 years and 55% were female. Follow-up trans-thoracic echo

showed complete PFO closure in all patients. Eight out of 22 (36%) had complete relief of MH and 8 (36%) had partial relief. There was a cumulative reduction in the frequency of MH from 3.06 episodes/patient/month to 0.05 episodes/patient/month.

Conclusion This observational study demonstrated that PFO closure can reduce, and frequently eliminate, migraine episodes and suggests that in some patients with MH, PFOs may have a role in the genesis of the headache.

06-A-106-NASCI

Impact of cardiac resynchronization on mortality from progressive heart failure

Farhan Aslam

Geisinger Medical Center, Danville, PA, USA
e-mail: farhan.dr@gmail.com

Background Cardiac resynchronization improves cardiac function, exercise capacity and quality of life among heart failure patients. The effect of cardiac resynchronization mortality from progressive heart failure, however, is uncertain. To determine whether cardiac resynchronization decreases mortality from progressive heart failure, we conducted a meta-analysis of randomized trials.

Methods Medline, Embase, and the Cochrane Controlled Trials Register (CCTR) were searched for reports of randomized controlled trials of cardiac resynchronization for the treatment of chronic symptomatic left ventricular dysfunction among patients with prolonged QRS intervals. Eligible studies had at least three months of follow-up. Reports of crossover trials were excluded if the first randomized crossover phase was less than three months. Trials were reviewed independently by two investigators. Trial data were pooled using random effects statistical model.

Results Outcomes from trials with 1634 total patients were included in the meta-analysis. Baseline patient characteristics were similar in the included trials, and the majority of patients were men with moderate severe heart failure symptoms at baseline (New York Heart Associ-

ation functional class 111 and 1V) and prolonged QRS intervals. Pooled data showed that progressive heart failure mortality was 1.7% for cardiac resynchronization patients and 3.5% for controls over three to six months of follow-up. Cardiac resynchronization reduced death from progressive heart failure by 51% relative to control ($P = 0.029$). There was no evidence of quantitative heterogeneity by a chi-square ($P = 0.85$), suggesting a consistent effect cross trial. **Conclusions** Cardiac resynchronization appears to reduce mortality from progressive heart failure over three to six months of follow-up in patients with symptomatic left ventricular dysfunction and prolonged QRS intervals. This finding suggests that cardiac resynchronization may have a positive impact on the most common mechanism of death among patients with advanced heart failure.

06-A-107-NASCI

Acetylcysteine prevents contrast-induced nephropathy after coronary angiography in patients submitted to low osmolar contrast media but not in patients submitted to iso-osmolar contrast media and in higher risk patients—a meta-analysis

Farhan Aslam
Geisinger Medical Center, Danville, PA, USA
e-mail: farhan.dr@gmail.com

Objective Contrast induced nephropathy related to coronary intervention has been shown to be a strong predictor of increased all cause mortality and morbidity. Clinical trials evaluating the efficacy of *N*-Acetylcysteine in preventing contrast induced nephropathy have yielded conflicting results.

Methods We analyzed the databases from MEDLINE, PUBMED and CENTRAL (January 1980 to August 2005) in all languages as well as conference proceedings from several professional societies from the years 1997 to 2005. Risk ratios and the corresponding tests for homogeneity were combined using the Mantel–Haenzel method.

Results Out of 18 trials that addressed the efficacy of *N*-Acetylcysteine in prevention of contrast-induced nephropathy in patients under-

going coronary angiography, 10 trials with a total of 141 patients met our inclusion criteria for quality and homogeneity. Administration of *N*-Acetylcysteine with peri-procedural hydration with 1/2 normal saline significantly reduced the incidence of contrast-induced nephropathy in patients undergoing procedures using low osmolar contrast media by 60% (RR 0.408, 95% CI 0.251–0.663, $P < 0.0001$). In patients undergoing procedures using the iso-osmolar contrast media, with administration of *N*-Acetylcysteine, and the same peri-procedural hydration, there was no reduction in the incidence of contrast-induced nephropathy (RR 1.129, 95% CI 0.643–1.983, $P = 0.6755$).

Conclusion *N*-Acetylcysteine with peri-procedural hydration with 1/2 normal saline prevents contrast-induced nephropathy in patients undergoing coronary interventions using low osmolar, nonionic contrast media but not in patients undergoing procedures using iso-osmolar contrast media. Studies with a higher proportion of elderly individuals or diabetic patients or studies that used a relatively high osmolality agent were associated with a change in the estimated risk difference in a direction favoring *N*-Acetylcysteine. Thus it is conceivable that the effectiveness of *N*-Acetylcysteine may be greatest among a population of individuals with a high baseline risk of developing radiocontrast induced nephropathy.

06-A-108-NASCI

Effect of intravenous glycoprotein 11b/111a receptor antagonists on survival in percutaneous coronary interventions: a meta-analysis

Farhan Aslam
Geisinger Medical center, Danville, PA, USA
e-mail: farhan.dr@gmail.com

Background Several randomized trials have shown that intravenous antagonists of the platelet glycoprotein 11 b/111 a receptors reduce the incidence of myocardial infarction (MI), and composite cardiac outcomes (death, MI, or revascularization in patients undergoing percutaneous coronary intervention (PCI). However, individual studies have not had adequate power to examine differences in mortality.

Methods We performed a meta-analysis of 19 randomized placebo-controlled trials (20 comparisons, $n = 20, 137$) of intravenous glycoprotein 11b/111a receptor antagonists in patients undergoing PCI. Death was the primary outcome.

Results Mortality was significantly reduced at 30 days (risk ratio (RR) 0.69 (95% CI, 0.53–0.90), 6 months (RR 0.79 (95% CI, 0.64–0.97), and including longer follow up (RR 0.79 (95% CI, 0.66–0.94)) with no significance between-study heterogeneity. The relative risk reduction was largely similar in trials on patients with or without acute MI: in trials continuing or discontinuing heparin after the procedure; and in trials using stents or other PCIs as the intended primary procedure. At 30 days and 6 months, MI and composite outcomes were significantly reduced ($P < 0.001$ for all). Major bleeding was significantly increased only in trials where heparin infusion was continued after the procedure (RR 1.70 (95% CI, 1.36–2.14)), while there was no excess bleeding when heparin was discontinued (RR 1.02 (95% CI, 0.85–1.24)).

Conclusion In patients undergoing PCI, glycoprotein 11b/111a receptor antagonists confer significant and sustained decrease in the risk of death.

06-A-109-NASCI

Pilot study of triple rule out protocol using CT

Kelley Branch¹, Lee Mitsumori¹,
James Caldwell¹, Adam Alessio¹,
William Warren¹, Joshua Busch¹, Grace Chen¹,
Steve Kohlmyer², William Shuman¹

¹University of Washington, Seattle, WA, USA

²GE Healthcare, Waukesha, WI, USA

e-mail: kbranch@u.washington.edu

Multislice computed tomography (CT) may be used to diagnose life-threatening diseases such as pulmonary embolism (PE), acute aortic syndrome (AAS), and coronary artery disease (CAD) in one “Triple Rule Out” (TRO) scan. No data is currently available on a true 64-slice CT for TRO evaluation.

Methods Seventeen patients referred for TRO scans were reviewed retrospectively. Cardiopulmonary risk factors included hypertension ($n = 5$),

hypercholesterolemia (4), known CAD (3), family history of premature CAD (3), and smoking (1). CT imaging was performed using a 64-slice Light-Speed VCT with a triple-phase contrast bolus. CAD was defined by $\geq 50\%$ stenosis by quantitative coronary angiography (QCA). A final diagnosis for chest pain was obtained from 1 month followup and medical records. Cost-benefit assessment was calculated by comparing CT cost to a theoretic nuclear stress test or cardiac catheterization.

Results Mean TIMI Unstable Angina Risk Score was 0.9 ± 1.1 . No cardiopulmonary disease was seen in 76% of patients. CAD was identified in four patients and only one previously unknown stenosis was identified (50% stenosis). Acute PE or AAS was not observed, but pulmonary fibrosis ($n = 1$) and a chronic PE (1) was identified. Two coronary angiograms were obtained to correlate CT findings, but without revascularization. No cardiopulmonary events occurred at followup. Chest pain diagnoses included non-intervenable CAD ($n = 1$), asthma (1), old PE (1), gastrointestinal disease (4), musculoskeletal disease (1), pleuritis (1), and unknown (3). The TRO CT was estimated to save 14 nuclear stress tests and two cardiac catheterizations while resulting in two catheterizations. Net savings was \$6,850, or an average of \$403 per patient. **Conclusions** This pilot study shows that 64-slice CT TRO protocol can be used in acute chest pain patients with good 1 month prognosis. TRO CT may also offer cost-savings compared to the traditional clinical pathways. Larger, prospective studies are underway to test these assertions.

06-A-110-NASCI

Evaluation of Pulmonary Arteries, Coronary Arteries, and Thoracic Aorta With One CT Angiographic Acquisition

Minh Nguyen, Christopher Klassen, Kiran Kareti,
Ivan Ayala, Norbert Wilke

University of Florida, Jacksonville, Jacksonville,
FL, USA

e-mail: mxnguyen@hotmail.com

Purpose We present a methodology for simultaneous optimal contrast enhancement of pulmo-

nary arteries, coronary arteries, and thoracic aorta in one CT acquisition to evaluate the three most dangerous causes of acute chest pain (PE, coronary stenosis, thoracic aortic dissection).

Method and materials KG-gated thoracic CT using a 64 slice CT scanner (Siemens Sensation 64). Collimation 64 × 0.6 mm; rotation time 0.33 s; tube voltage 120 kV; CareDose 4D effective exposure 500–600 mA s; pitch 0.3; scan range 25–30 cm from lung apices to diaphragm cranial-caudally; bolus trigger region of interest at left atrium with threshold 120 HU and 5 s delay to allow for table repositioning and patient breath-hold. Contrast injection protocol: Ultravist 370 (Berlex) using a dual syringe injector (Stellant D) via 18 G needle at antecubital vein: 80 cc contrast, followed by 50 cc of equal mixture of contrast and saline, followed by 50 cc of saline. Infusion rate for all volumes: 5 cc/s.

Results Anova analysis of 11 consecutive studies using the above protocol showed no significant difference in the average Housfield value of the main pulmonary artery (PA) (HU 380), left PA (HU 382), right PA (HU 381), distal PA (354), proximal LeftMain (HU 410), proximal RCA (HU 382) ($P = 0.014$). Wilcoxon unpaired test showed *no significant difference* in average Housfield value of Main PA (HU 375), distal PA (HU 356) between the 11 studies using the new protocol versus three studies using a traditional pulmonary CTA protocol (HU 368), (HU 362). Additionally, there is *no significant difference* in average Housfield value of proximal LeftMain (HU 412), proximal RCA (HU 398) between the 11 studies using the new protocol versus three studies using a traditional coronary CTA protocol (HU 416), (HU 411).

Conclusion Optimal simultaneous enhancement of the pulmonary arteries, coronary arteries, and thoracic aorta is possible using the new CT protocol

06-A-111-NASCI

Coronary and thoracic aorta CT-angiography: frequency and spectrum of collateral findings in 194 patients

Carlo Liguori, Giancarlo Savino, Pierluigi Rinaldi, Marco Politi, Riccardo Marano, Lorenzo

Bonomo

Universita' Cattolica-Roma, Roma, Italy
e-mail: cliguori@sirm.org

Purpose To retrospectively evaluate frequency and spectrum of collateral findings depicted with coronary and thoracic aorta CTA scans. **Material and methods** 194 consecutive CT Angiography exams (95 coronaries, 99 thoracic aorta) performed from October 2005 to April 2006 were reviewed by two different readers (one junior and one senior radiologist). Scans were obtained with a 16 slices MDCT scanner during intravenous contrast material injection. All collateral findings depicted were tabulated and pooled by type (lung parenchyma, pleura, mediastinum, pulmonary vessels, thoracic vessels, other). To evaluate data descriptive statistics (means, standard deviations, and percentages) were used and k statistic was performed to assess inter-observer agreement.

Results By 194 patients (138 M; 56 F; median age: 63), 111 (57%) showed at least 1 finding (total findings: 243, 1.25/patient). 173/243 were clearly benign, 70/243 were of uncertain malignant nature requiring further investigations. Findings were described most frequently in the superior abdomen viscera (88), lung parenchyma (72) and pulmonary arteries (38), less frequent were pleural and mediastinal findings.

Conclusion With coronary and thoracic aorta CT-Angiography, findings were detected in a large number of subjects, and many findings were elicited recommendations for additional evaluation showing the importance to evaluate all the visualized structures by the radiologist.

06-A-112-NASCI

A 64-channel validation study in the treatment of peripheral vascular disease from “Head-to-Toe” utilizing a low contrast volume protocol

David Allie¹, Chris Hebert¹, Mitchell Lirtzman¹, Charles Wyatt¹, V. Antoine Keller¹, Peter Fail², Krishnamoorthy Vivekananthan¹, Elena Mitran¹, Gary Chaisson², Samuel Stagg, III², Michael

McElderry¹, Jason Hebert², Gerald Laurich¹, Kurt Broussard¹, Craig Walker²

¹Cardiovascular Institute of the South, Lafayette, LA, USA

²Cardiovascular Institute of the South, Houma, LA, USA

e-mail: david.allie@cardio.com

Background Conventional diagnostic angiography (CDA) is considered the “gold standard” for peripheral vascular imaging (PVI) but data has shown correlation between CDA and 16-channel computed tomography angiography (CTA). No data exists correlating 64-channel CTA with CDA in PVI. Contrast induced nephropathy (CIN) has a reported incidence of 14.5% in coronary angiography and is reported to occur in 11–44% of patients with renal dysfunction (RD) with a 36% mortality with acute renal failure. CIN has been associated with diabetes, RD, and total contrast volume. Despite a known higher incidence of diabetes and RD in peripheral vascular disease (PVD), sparse data exists regarding CIN in CDA or 16–64 channel CTA in PVI. Therefore any modality designed to limit contrast use and retain imaging quality would be of clinical value.

Methods Between May 1 and December 31, 2005, 89 patients underwent 64-slice abdominal CT scan with CTA runoff of both legs utilizing a novel protocol A. A comparison was made to 89 similar patients but with a standard recommended protocol B (table). Variables analyzed included: imaging quality, post-processing time, and % stenosis correlation with CDA.

Results The resolution quality and post-processing imaging time were improved in Protocol A vs. B, especially in patients with significant infrainguinal PVD. The CDA vs. CTA correlation in protocol A were strong and included: carotid ($r^2 = 0.951$), renal ($r^2 = 0.939$), celiac ($r^2 = 0.910$), mesenteric ($r^2 = 0.919$), iliac ($r^2 = 0.947$), SFA ($r^2 = 0.916$), popliteal ($r^2 = 0.879$), peroneal ($r^2 = 0.888$), anterior tibial ($r^2 = 0.901$), and posterior tibial ($r^2 = 0.884$).

Conclusion Lower contrast volume (75 cc) 64-channel CTA with minor protocol changes enhance PVI in PVD.

Comparing standard and novel 64-slice PVI protocols

Settings	Protocol A (Novel)	Protocol B (Standard)
Contrast volume (ISOVUE 370-BRACCO)	75 cc	125 cc
Automated trigger (Hounsfield Units)	250 H	180 H
Injection rate	4 cc/s	4 cc/s
Scan delay	10 s	5 s
Bolus Chase	40 cc NS	30 cc NS
Slice thickness	0.5 mm	0.5 mm
Automated trigger position	*Check for distal aortic calcification	Start immediately above diaphragm
	*If calcium-start 2 cm above iliac bifurcation	
	*If no calcium-start 1 cm above iliac bifurcation	

06-A-113-NASCI

MDCT evaluation of congenital coronary to pulmonary artery fistulae: case series with coronary artery angiography and echocardiography correlation and review of literature

Giancarlo Savino, Marco Politi, Pierluigi Rinaldi, Carlo Liguori, Riccardo Marano, Paolo Zeppilli, Lorenzo Bonomo

Universita' Cattolica-Roma, Roma, Italy
e-mail: gsavino@sirm.org

Purpose To confirm the presence of Coronary Artery Fistula (CAF) diagnosed by transthoracic echocardiography (TTE) and to assess other anatomic anomalies by MDCT.

Methods We present a small series of young patient cases, clinically suspected for coronary to pulmonary fistulae, investigated with TTE and then evaluated by Angio-MDCT of thorax. Catheterization was also performed in positive cases. Ten patients presented to our sport health care department with clinical symptoms, EKG anom-

alies and TTE evaluation were enrolled in this study. CT-angiography (CTA) of thorax was performed on 16-slices scanner (Lightspeed, GE) during contrast medium administration (350 mgI/ml, Ultavist) and followed by saline chase using Smart Prep technique for bolus synchronization. Scan parameters were: 600 mAs, 150 kV, rotation time 0.4, TR 0.2, slice thickness 0.6, recon thickness 0.6, recon increment 0.6. All cases were reconstructed with retrospective EKG-gating, and evaluated on a dedicated workstation by specific cardiac software (advantage windows 4.2).

Results Four patients with a LAD to left main pulmonary artery fistula diagnosed by TTE were confirmed both by MDCT and coronary angiography. MDCT evaluation well-depicted all fistulae from the origin until the drainage site, and in two cases additional fistulae from the right coronary artery were identified and then confirmed by catheterization. In one case an incomplete 4-cuspid aortic valve was identified. In two cases other anomalies in origin and course of coronary arteries were well shown (one circumflex artery coming from the right sinus of Valsalva, and one right coronary coming from left sinus). In one case a persistent left superior vena cava draining in coronary sinus was also identified.

Conclusion Assessment of coronary artery fistulae by MDCT is feasible and may be useful for surgical planning or disease monitoring as well as to detect associated cardiac anomalies.

06-A-115-NASCI

Assessment of internal mammary-left anterior descending artery graft in coronary artery bypass graft (CABG) surgery with 16-slice multidetector CT angiography in early postoperative period: is there any finding that predicts mid-term graft failure?

Joon-Won Kang, Joon Beom Seo, Kyung-Hyun Do, Seong Ho Park, Hyun Song, Tae-Hwan Lim
Asan Medical Center, Seoul, Republic of Korea
e-mail: jwonkang@amc.seoul.kr

To determine significant findings on 16-slice multidetector-row coronary CT angiography (CTA) of

internal mammary artery (IMA)-left anterior descending artery (LAD) graft at immediate postoperative CTA that can predict graft failure at mid-term follow-up CTA, we analyzed 202 consecutive IMA-LAD grafts from whom underwent CABG surgery and coronary CTA with 16-slice multidetector CT (MDCT) at immediate postoperative period (within 7 days) and mid-term follow-up (5–7 months). Correlations between selected CT findings at immediate postoperative CTA and graft patency at mid-term CTA shows patients who showed poor opacification of IMA graft on CTA immediately after CABG are 25.01 times more likely to develop IMA graft failure at mid-term CTA than those who did not showed at immediate postoperative CTA.

06-A-116-NASCI

Cardiac CT before and after cardiac surgery in adults

Joon-Won Kang, Joon Beom Seo, Kyung-Hyun Do, Jin Seong Lee, Jae-Woo Song, Tae-Hwan Lim
Asan Medical Center, Seoul, Republic of Korea
e-mail: jwonkang@amc.seoul.kr

To give a general overview of various methods in cardiac surgery, review the role of cardiac CT in pre-surgical planning and post-operative evaluation, and illustrate typical pre- and post-operative cardiac CT findings and findings of various complications, we illustrated the technical considerations for CT, and the pre- and post-operative findings for selected cases: ischemic heart disease, valvular disease, constrictive pericarditis, and cardiac tumors.

06-A-117-NASCI

Detection of significant coronary artery stenosis using 64-slice computed tomography in heart transplant recipients: a comparative study with coronary angiography

Franz von Ziegler^{1,2}, Ingo Kaczmarek³, Alexander Becker², Alexander Leber², Bruno Reichart³, Marco Costa¹, Christoph Becker⁴, Norbert Wilke^{5,1}, Andreas Knez²

¹Department of Cardiology, University of Florida, Shands, Jacksonville, FL, USA

²Department of Cardiology, University of Munich, Grosshadern Campus, Munich, Germany

³Department of Cardiac Surgery, University of Munich, Grosshadern Campus, Munich, Germany

⁴Department of Clinical Radiology, University of Munich, Grosshadern Campus, Munich, Germany

⁵Department of Radiology, University of Florida, Shands, Jacksonville, FL, USA

e-mail: Franz.Ziegler@jax.ufl.edu

Cardiac allograft vasculopathy (CAV) still remains the major limiting factor of long-term positive outcome after heart transplantation. The current gold standard for detecting CAV is conventional coronary angiography (CCA). Multislice-Computed Tomography-Angiography (MSCTA) has recently proven effective in detecting coronary stenosis in non-transplanted patients. Therefore we sought to prove its ability in evaluating luminal obstruction due to CVA as a non-invasive alternative to CCA. Using a standardized protocol, 34 consecutive male heart transplant recipients underwent 64-slice-MSCTA (Sensation 64, Siemens, Germany) one day after annual routine CCA. Significant stenosis was defined as luminal diameter obstruction > 50% in quantitative coronary analysis (QCA). QCA analysis (Quantcor, Siemens, Germany) and interpretation of the CT dataset were performed by two blinded experienced readers. Due to renal insufficiency four patients did not undergo MSCTA and four studies had to be excluded because of inadequate image quality (motion artifacts, heart rate = 86 ± 7 bpm). Despite high heart rates (82 ± 14 bpm) diagnostic image quality was achieved in the remaining 26/30 (87%) patients. Twelve patients showed angiographic signs of CAV where of eight patients presented higher grade stenosis or total occlusion in CCA. All of them were detected by MSCTA. Two patients with CAV but without significant stenosis in QCA were overestimated by MSCTA and two further patients showed false positive results. A sensitivity of 100% (8/8) and specificity of 78% (14/18) for detecting significant stenosis with MSCTA on a patient-based analysis could be calculated. Negative predictive value and positive predictive value were 100% (16/16) and 67% (8/12),

respectively. Diagnostic accuracy was 85% (22/29). 64-slice-MSCT therefore is a reliable non-invasive diagnostic tool for detecting significant stenosis of coronary arteries in heart transplant recipients and may considered as an alternative to CCA in this specific population. Despite higher heart rates a diagnostic image quality could be achieved in most of the studies.

06-A-118-NASCI

Non-invasive assessment of coronary bypass grafts using 64-detector CT angiography

Amgad Makaryus, Sonia Henry, Michael Friedman, John Makaryus, Lawrence Boxt
North Shore University Hospital, Manhasset, NY, USA

e-mail: amakaryus@gmail.com

Background Significant narrowing of the coronary arteries requires coronary artery bypass graft surgery (CABG) for revascularization. Because the occlusion rates of CABG vary widely, coronary angiography (CA) is frequently used to evaluate their patency. However, repeated CA increases morbidity and mortality because of inherent catheterization-associated risks. Early experience with 64-CT demonstrates its utility for the evaluation of native coronary atherosclerosis. We evaluated the diagnostic value of 64-CT for the assessment of CABG disease.

Methods 1,317 consecutive patients were evaluated between April 2005 and April 2006 using 64-detector CT. 37(2.8%) of these patients had CABG. In 8 (22%) of these patients, CA was prompted based on 64-CT findings and completed within mean time of 23 ± 15 days. The bypass grafts as well as the native coronary arteries were evaluated and compared using CA as the gold standard.

Results A total of 94 bypass grafts (36 arterial; 58 venous) were evaluated by 64-CT in 37 patients (30 men, 7 women, ages 69 ± 9 years). 64-CT graft visualization was accomplished in 91%. In the eight who were subsequently evaluated with CA, 23/24 (96%) grafts and 32/34 (94%) of the native coronaries evaluated were correctly accessed by 64-CT. The overall sensitivity and

specificity of 64-CT compared to CA for the identification of graft patency was 89% and 100%, respectively. The negative predictive value (NPV) was 93% and the positive predictive value (PPV) was 100%. The overall sensitivity and specificity of 64-CT compared to CA for the identification of native vessel patency was 91% and 80%, respectively. The NPV was 80% and the PPV was 91%.

Conclusion 64-CT is a safe and accurate means of visualization of CABG and eliminates the inherent catheter-associated risks of CA. With its advanced spatial and temporal resolution, 64-CT should be considered in the noninvasive evaluation of bypass grafts as it provides diagnostic information comparable to that obtained with CA.

06-A-119-NASCI

64 MDCT : a guide to coronary stenting?

Jean-Louis Sablayrolles, Philippe Guyon,
Bernard Chevalier, Jacques Feignoux
Centre Cardiologique du Nord,
Saint Denis, France
e-mail: jl.sablayrolles@ccncardio.com

Background Cardiac CT allows assessment, not only of the artery lumen, but also of the artery wall, the plaque volume, its composition and its distribution within the coronary tree. We are testing the hypothesis that CT gives additional information about coronary lesions at the bifurcation compared to conventional coronary angiography (CA).

Method 22 patients with at least one coronary stenosis at a vessel bifurcation (17 men, mean age 61 ± 12 years) with atypical chest pain, stable or unstable angina, or non-ST elevation myocardial infarction scheduled for diagnostic CT and referred after for CA, were included in the study. The lesions were located on the Left Main trunk for three of the patients, on the LAD/Diagonal bifurcation for nine of them, on the Circumflex/Marginal in six cases and on the RCA crux for four patients. Two independent observers analyzed CT and CA in a blind study. Two patients were excluded for suboptimal quality of the CT acquisition. The bifurcation site was divided into

three segments: prior to the bifurcation for the main branch and after for the main and for the side branch. A binary classification was also used (0/1) to characterize the plaque distribution. Composition and other plaques in the 10 mm up or downstream to the lesion were analyzed.

Results In 70% of the cases, CA does not analyze clearly the plaque volume and its distribution at the bifurcation. CT modified and enhanced the visualization of the calcification (blooming effect), but not their location.

Conclusion In a selected population, CA highly underestimates the severity of lesions at the bifurcation and also lesions proximal and distal to the bifurcation. CT allows assessment of the plaque composition and also a 3D reconstruction of the plaque volume and its distribution. By improving lesion analysis at bifurcation, *CT guides (and facilitates) the revascularization strategy.*

06-A-120-NASCI

Coronary computed tomography angiography (CTA) for rapid disposition of low risk emergency department (ED) patients with chest pain syndromes

Woojin Kim, Judd Hollander, William Baxt,
Maureen Chase, Harold Litt
University of Pennsylvania Hospital,
Philadelphia, PA, USA
e-mail: KimWooji@uphs.upenn.edu

Purpose To assess the utility of coronary CTA for rapid evaluation and disposition of low cardiac risk patients presenting to the ED with chest pain.

Methods Seventy-five low risk patients with chest pain and Thrombolysis in Myocardial Infarction (TIMI) scores of 2 or less, without acute ischemia on ECG, had coronary CTA performed in the ED from January 2005 to May 2006. Patients with negative coronary CTA were discharged home from the ED. Thirty-day outcome data for mortality, myocardial infarction, and further cardiovascular testing were obtained for the first 59 patients by telephone contact. Subsequent patient cardiac enzymes, EKGs, stress tests and cardiac catheterizations, if obtained, were also documented.

Results Eight patients had positive findings on coronary CTA including six with > 50% stenosis: Two had positive stress tests and cardiac catheterizations revealing similar findings as coronary CTA; two had negative stress studies; four received no further workup. Other positive coronary CTA results included an anomalous RCA and myocardial bridging of the mid LAD. Two patients with negative coronary CTA were also admitted, but discharged without further cardiovascular testing. None of the patients admitted or discharged from the ED who were followed up had any 30-day cardiovascular events.

Conclusion The use of CTA in low risk patients presenting to the emergency department with chest pain may allow rapid discharge of those with negative studies and identify those with significant coronary stenosis.

06-A-121-NASCI

Significant dose reduction possibilities for coronary CTA using prospective gated contrast enhanced acquisition

Kevin Johnson¹, David Dowe²

¹Yale University, New Haven, CT, USA; ²AMI, Galloway, NJ, USA

e-mail: ddowe60@hotmail.com

Purpose Coronary CTA has high exposure due to the continuous ECG gated helical acquisition. Prospectively triggered acquisitions could enable a lower dose alternative (up to 80%) for imaging coronary arteries at a single cardiac phase location. Image quality was evaluated for the four main coronary vessels at a single diastolic phase to determine if diagnosis could be achieved for all vessels.

Method Contrast enhanced ECG gated helical CTA was performed on 100 consecutive patients in 10-days. Images at 75% phase location using a 64-slice CT scanner (LightSpeed VCT, GE Healthcare) were reconstructed. Images were evaluated for the LMA, LAD, LCX and RCA for all cases using curved reformat and MPVR views. IQ was rated according to clinical guidelines for diagnosis of each segment of the vessel to determine if the patient had normal coronaries, moderate disease or severe disease. Results were

tracked to assess percentage of the exams that would be diagnostic under the reduced dose scanning method.

Results Of the 100 patients analyzed, heart rate (HR) ranged from a minimum 38 bpm to a maximum 105 bpm. For 70/100 patients with max HR ≤ 60 bpm (up to 5 bpm variation) diagnosis of the coronaries at the 75% location was achieved with a success rate of 100%, 98.5%, 98.5%, and 97% for the LMA, LAD, LCX and RCA. When including HR ≤ 65 bpm (82/100) results were 100%, 95%, 95% and 91%, respectively. Remaining patients with HR ≤ 65 bpm (including some arrhythmias) results were 100%, 90%, 91% and 82%, respectively.

Conclusion A single 75% cardiac phase in assessed patients with HR ≤ 65 bpm is sufficient for accurate diagnosis in all main coronaries. This indicates that prospective triggered acquisition for coronary CTA may provide accurate diagnosis while reducing radiation exposure up to 80%. Next phase assessing prospective acquisition in clinical practice is underway.

06-A-122-NASCI

In vivo and ex vivo tissue characterization based on delayed contrast enhancement and R2-mapping in canine myocardial infarction

Pal Suranyi^{1,2}, Balázs Ruzsics¹, Pal Kiss^{1,2}, Brott Brigitta³, Tamas Simor^{1,2}, Nada Saab-Ismael², Baker Robert⁴, Gabriel Elgavish^{1,2}

¹Department of Biochemistry and Molecular Genetics, University of Alabama at Birmingham, Birmingham, AL, USA

²Elgavish Paramagnetics Inc., Hoover, AL, USA

³Division of Cardiovascular Disease, Department of Medicine, University of Alabama at Birmingham, Birmingham, AL, USA

⁴Animal Resources Program, University of Alabama at Birmingham, Birmingham, AL, USA

e-mail: psuranyi@uab.edu

Introduction Ischemic injury may result in edema, necrosis, hemorrhage and scar formation. Tissue-Characterization-Mapping (TCM) method is introduced here which combines delayed-contrast-enhancement (DCE) and Percent-Edema-Maps (PEM). The PEM is based on R2

(transverse relaxation rate) which is influenced by increased tissue water content (decreased R2) and intramyocardial hemorrhage (increased R2).

Methods In canine reperfused myocardial infarction ($n = 6$), four days after reperfusion, pixel-by-pixel R2-mapping was carried out. Conventional DCE images were acquired using 0.05 mmol/kg Gd(ABE-DTTA). Four dogs were immediately sacrificed. Two dogs were followed for eight weeks with repeat R2-maps and TCMs were generated at eight weeks using 0.2 mmol/kg Gd(DTPA). R2-maps were acquired using a double-IR fast-spin-echo sequence with varying echo-times (TE). Percent-edema(PE) = 100% was defined as the R2 of pure water (0.27 s^{-1}) and PE = 0% was defined as the R2 of intact myocardium (18.7 s^{-1}). A PE value was calculated for each voxel from the measured R2. Edema yielded positive PE values while mature scar yielded negative PE. In acute hemorrhage, in the center of the infarct normal PE values were obtained (Fig. 1). Postmortem, TTC-staining and hematoxylin-eosin microscopy was carried out. In two additional dogs, ex vivo TCMs (using Gd(DTPA)) were generated to allow better coregistration with histochemistry.

Results In vivo baseline myocardial R2 value was $18.7 \pm 1.2 \text{ s}^{-1}$. Injured tissue R2 values ranged from 7.4 s^{-1} (edematous) to 28.6 s^{-1} (scar). Quantitative comparison of the in vivo amount of myocardial hemorrhage determined using TCM yielded significant correlation ($R = 0.9$, $P < 0.05$, linear regression line: $y = 1.12x + 0.1$) with that determined with TTC-staining. Average overestimation of hemorrhage per slice was $0.2 \pm 0.4 \text{ ml}$ ($1.4 \pm 5.1\%$). **Conclusions** The TCM in vivo agrees well with TTC-staining in acute and chronic infarction regarding localization of acute necrosis, hemorrhage and mature scar. TCM is capable of quantifying myocardial hemorrhage.

06-A-123-NASCI

Transmural myocardial blood volume during dipyridamole and dobutamine stress: correlation between mri and radioactive measurements

Thomas Goldstein¹, Kyle McCommis¹, Haosen Zhang¹, Bernd Misselwitz², Jie Zheng¹
¹Washington University in St. Louis, St. Louis, MO, USA

²Schering AG, Berlin, Germany
 e-mail: zhengj@mir.wustl.edu

Purpose Measuring myocardial blood volume (MBV) may provide assessments of myocardial oxygen needs and viability. The aim of this study is to examine a MRI perfusion mapping method for the measurement of MBV distribution.

Methods Normal mongrel dogs ($n = 11$) were used in this study. Nine dogs were injected dipyridamole intravenously and three dogs were given dobutamine. MR first-pass perfusion imaging was performed at rest and during the pharmacological stress. An intravascular contrast agent, Gadomer (Schering AG), was injected (0.015 mmol/kg) as a bolus during the MR scans. For dipyridamole injection, MRI occurred at 10–30 min after the start of the injection. ^{99m}Tc-labeled-Red-Blood-Cell was injected at the end of study, when the dogs were randomly arranged with three states: at rest ($n = 5$), or during another injection of dipyridamole ($n = 3$) or dobutamine ($n = 3$). A perfusion quantification method was applied to obtain MBV maps. Region-of-interests ROI were drawn on the endo- and epi-myocardium of the entire left ventricle wall.

Results Table lists the results. MBV values measured by MRI were substantially larger than those measured by ^{99m}Tc method, but MRI data are in a good agreement with other reported values. Dipyridamole diminished the gradients of trans-

Table MBV data (ml/g) From MRI (**bold**) and ^{99m}Tc (in parenthesis)

	Epicardium	Endocardium	Ratio (Epi/Endo)
Rest	9.4 ± 2.6 (3.9 ± 0.7)	10.6 ± 3.2 (4.3 ± 0.7)	0.89 ± 0.07 (0.90 ± 0.02)
Dipyridamole	13.9 ± 2.2* (4.0 ± 1.4)	13.7 ± 2.8* (4.1 ± 1.6)	1.03 ± 0.12* (1.00 ± 0.04)*
Dobutamine	13.3 ± 4.9 (6.2 ± 0.6)*	16.0 ± 2.6* (7.0 ± 0.7)*	0.82 ± 0.17 (0.89 ± 0.01)

*Significant changes vs MBV at rest

mural MBV, but not for dobutamine, as consistently observed by both methods. Dobutamine also significantly increased MBV. However, ^{99m}Tc indicated there was no change in MBV during dipyridamole, which agreed with other reports, whereas MRI show significant increases in MBV.

Conclusion First-pass perfusion MRI with the injection of Gadomer is a promising approach for the assessment of MBV.

06-A-124-NASCI

Ex vivo percent infarct mapping using Gd(DTPA): R1-based MRI quantification of myocardial viability

Pal Kiss^{1,2}, Pal Suranyi^{1,2}, Balazs Ruzsics¹, Brigitta Brott³, Tamas Simor^{1,4}, Gabriel Elgavish^{1,2}

¹Department of Biochemistry and Molecular Genetics, University of Alabama at Birmingham, Birmingham, AL, USA

²Elgavish Paramagnetics Inc., Hoover, AL, USA

³Division of Cardiovascular Disease, Department of Medicine, University of Alabama at Birmingham, Birmingham, AL, USA

⁴Elgavish Paramagnetics Inc., Hoover, AL, USA
e-mail: pkiss@uab.edu

Introduction Our recently developed method for MRI quantification of myocardial viability, Percent-Infarct-Mapping (PIM), quantifies infarct content per voxel, based on the R1 value. This is made possible by the delayed accumulation of contrast agents (CA) into myocardial infarcts. The traditional analysis of delayed enhancement (DE) images results in either infarcted (bright) or viable voxels (dark) and therefore it tends to overestimate infarct size. PIM, however, allows the determination of the per-voxel percentage of infarcted tissue. The accuracy of the PIM method is shown here using high resolution ex-vivo R1-mapping using Gd(DTPA) and TTC-staining.

Methods In dogs ($n = 6$), 96 h following closed-chest, coronary-occlusion (180 min), Gd(DTPA) (0.2 mmol/kg) and after a 15-min waiting period the animals were euthanized. Ex vivo short-axis inversion-recovery (IR) fast-spin echo images were acquired with varying inversion-

time (10 TIs (50–1000 ms)) (Fig. 1A). Imaging parameters: FOV = 160 mm, matrix = 256×256 , slice = 3 mm, flip-angle = 90° , TE = 12.3 ms, ETL = 16, TR = 2000 ms. R1 and Percent-infarct values were calculated voxel-by-voxel. The IR image where viable myocardial signal was nulled (T1-weighted image, (T1w)), was also analyzed for using the remote SI+2SD threshold (2SD). During image analysis, the only manual input was tracing the endo- and epicardial contours in all slices. LV myocardial mass, total infarct mass (TIM) and infarction-fraction (IF) were calculated from PIMs, from thresholded T1w images, and from TTC-staining.

Results Excellent ($P < 0.01$ for all) pairwise correlations were obtained for TIM_{PIM} vs. TIM_{TTC} ($R^2 = 0.95$) and IF_{PIM} vs. IF_{TTC} ($R^2 = 0.94$). TIM_{PIM} slightly underestimated TIM_{TTC} by 1.1 ± 3.3 g and IF_{PIM} underestimated IF_{TTC} by $1.5 \pm 4.6\%$, while the traditional T1w method systematically overestimated IF by $22 \pm 21\%$. **Conclusions** From Gd(DTPA)-enhanced ex vivo R1-maps, voxel-by-voxel PIMs can be generated. PIM is more accurate to quantify myocardial viability than the traditional T1-weighted image thresholding method.

Figure represents ex vivo multislice short axis inversion-recovery MRI images and post-processed maps. From left to right, Shown a thresholded T1-weighted images, IR-images with multiple T1s, voxel-by-voxel R1 maps (calculated from the multi-TI IR images) and voxel-by-voxel Percent Infarct Maps (PIMs) based on the R1-map. R1 and Percent infarct value are shown on color scales. While thresholding (left) yields binary (infarcted or noninfarcted) assessment of viability, PIM (right) quantifies infarct in each voxel individually. Thus, PIM can visualize and quantify the patchyness of the infarct and is a more realistic representation of the tortuous infarct and yields highly accurate measurement of infarct size.

06-A-125-NASCI

Assessment of myocardial oxygenation by mri: comparing with PET

Kyle McCommis, Haosen Zhang, Pilar Herrero, Robert Gropler, Jie Zheng

Washington University in St. Louis, St. Louis, MO, USA

e-mail: zhengj@mir.wustl.edu

Introduction MRI has shown the capability to non-invasively image myocardial blood flow (MBF) and oxygen extraction fraction (OEF). We hypothesized that these MRI methods would provide comparable measurements with the PET. The aim of this work is to perform an initial study for the evaluation of previously developed MRI T_2 -BOLD methods to measure myocardial OEF and thus MVO_2 , in a comparison with PET in an acute coronary stenotic canine model.

Methods Three-dog study was completed and four more dogs are undergoing for this project. Single coronary artery stenosis was created in the proximal to middle portion of the LAD by an intracoronary Teflon ring. The diameter reduction in the LAD was approximately 70–80% to induce sufficient ischemia to impair myocardial perfusion reserve. The dogs were first scanned by PET and then transferred to MRI suite for imaging in the same day. During both imaging sessions, dobutamine was infused to alter MVO_2 and MBF. MR T_2 -weighted and T_1 -weighted images were obtained to calculate myocardial MBF and OEF, respectively. MVO_2 was calculated according to Fick's law.

Results Because of severe motion artifacts during dobutamine stress MRI session, MR data

(MBF or OEF) in one dog was excluded for further analysis, resulting in two comparable (MRI vs. PET) data sets for MVO_2 . Both PET and MRI shows comparable decreases in MBF and MVO_2 reserve in stenotic perfusion segments, but changes in the OEF remain the same between stenotic and normal perfused myocardial beds, as consistently observed by both modalities.

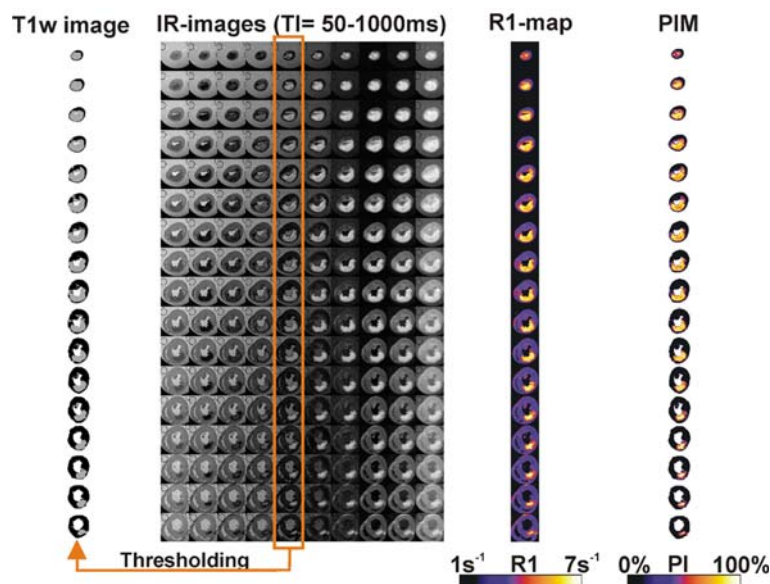
In conclusion, the MBF and MVO_2 assessed by MRI appear to correlate well with PET results. Our results indicate it is possible to perform relatively accurate measurements by our MRI methods. As this is a work in progress, further effort to improve the accuracy of OEF and MVO_2 measurement is warranted.

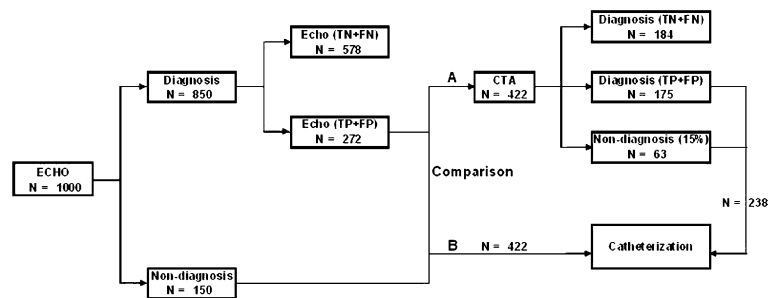
06-A-126-NASCI

Cost savings of a strategy using coronary CTA vs. cardiac catheterization to evaluate patients with an abnormal stress echocardiogram or nuclear study

Srikanth Sola, Zhenghong Alex Fu, Michael Lieber, Nancy Obuchowski, Mario Garcia
Cleveland Clinic Foundation, Cleveland, OH, USA

e-mail: solas@ccf.org





Background We sought to evaluate cost savings associated with the use of coronary CTA in patients with an abnormal or non-diagnostic exercise stress nuclear scintigraphy (ESN) or stress echocardiogram (ESE) study.

Methods We developed a mathematical model to evaluate total cost/patient in 1,000 patients referred for either an ESN or ESE (Fig. 1). The model was designed so that the prevalence of CAD could be varied from 0 to 100%. Patients with an abnormal or non-diagnostic stress study would undergo either 1 of 2 strategies: a conventional strategy, consisting of cardiac catheterization; or coronary CTA. In the coronary CTA arm, only patients with an abnormal or non-diagnostic coronary CTA study were referred for cardiac catheterization. Sensitivity and specificity for ESN, ESE, and coronary CTA were obtained from the published literature. Costs for each procedure were determined using actual costs from Medicare part B and a private insurer.

Results A strategy utilizing coronary CTA for the primary evaluation of patients with either an abnormal or non-diagnostic ESE was cost saving when compared with cardiac catheterization only for disease prevalence rates of $\leq 63\%$ when using private insurer costs for each procedure. Cost savings of a coronary CTA strategy in these patients were limited to a disease prevalence rate $\leq 31\%$ when using Medicare part B costs, reflecting varying costs for the different procedures used in the model. Similar levels of cost savings were seen for patients with abnormal or non-diagnostic exercise ESN with a coronary CTA strategy.

Conclusions A strategy utilizing coronary CTA as the primary modality to evaluate patients with an abnormal or non-diagnostic ESN or ESE study is cost savings for a population with low-intermediate prevalence of disease.

06-A-127-NASCI

Gadofluorine M helps to monitor advanced plaques during progression: a MRI study in rabbits

Jie ZhenG¹, Elizabeth Ochoa¹, Bernd Misselwitz², Pamela Woodard¹, Dana Abendeschein¹

¹Washington University In St. Louis, St. Louis, MO, USA

²Schering AG, Berlin, Germany

e-mail: zhengj@mir.wustl.edu

Purpose Non-invasive MR imaging allows monitoring of atherogenic process consecutively. The aim of this study is to exam the hypothesis that a molecular MR contrast agent Gadofluorine M will help to monitor the progression of advanced plaques.

Methods Six New Zealand White rabbits were used and focal femoral atherosclerosis was induced in right femoral arteries using a double-injury model. MR imaging with three contrasts (T1, T2, and PD) were performed one month after the injury and then be repeated after another month. Gadofluorine M was given intravenously to the rabbits ($n = 6$) at 24 h before the 1st MR scans, and then 24 h before the 2nd MR scans ($n = 3$) or during the 2nd MR scans ($n = 3$). The left femoral arteries were used as the control groups. Histopathological images were used to determine the plaque components.

Results The compound selectively enhanced advanced plaque areas, but was not seen in control left arteries. The compound enhanced mostly in the areas with loose matrix and foam cells, with 92% increase in signals and 210% increases in image contrast, in comparison with the left normal arteries. Three image contrasts

offers similar enhancement patterns, but combination of three contrasts helps to delineate total plaque and lumen boundaries. With improved visualization of MR images, progression of the plaque areas within one month could be assessed: lumen reduced 11%, fibrous tissue increased 4%, and loose matrix with foam cells increased 12%. Furthermore, Gadofluorine M was found to stay within the plaques for one month.

Conclusion MR contrast agent Gadofluorine M provides specific enhancements on components associated with plaque instability and may help to monitor the progression of these plaque components. Enhancement of plaque signals at one month after the injection of Gadofluorine M may reduce the cost for monitoring the progression of the plaques.

06-A-128-NASCI

Z-score Mapping technique for visualization of perfusion deficits in coronary CT angio exams

Tracy Callister¹, Jason Cole², Amy Broadie³, Hugo Arques Aquilo⁴, Bernice Hoppel³

¹Tennessee Heart and Vascular Institute, PC, Hendersonville, TN, USA; ²Cardiology Associates, Mobile, AL, USA

³GE Healthcare, Waukesha, WI, USA

⁴GE Healthcare, Buc, France

e-mail: bernice.hoppel@med.ge.com

Coronary CT Angiography (CTA) allows for noninvasive visualization of the coronary arteries, while potentially providing data on functional importance of obstructive coronary disease. Injection of contrast agents provides information concerning the myocardial microvasculature. Injured myocardium shows delayed or decreased intake of contrast agent with resultant decrease in signal intensity. Microvasculature obstruction maybe caused by factors such as obstructive CAD, embolisms, or spasm, which decrease signal intensity. To visualize these defects we developed a tool that produces a 3D Z-score transform which maps the myocardium to a color scale with a selectable confidence interval. The myocardium is segmented out of the volume, and the Z-score is calculated by a fit of the pixels within the myocardial region to a Gaussian distribution.

Pixels falling outside the confidence interval are mapped to a separate color. Sixteen patients scanned with both SPECT perfusion and 64 slice CTA (*LightspeedVCT*, GE Healthcare). A mean value of 67 ± 67 HU was calculated for normal myocardium and 20 ± 28 HU was calculated in ischemic region with a significant ($P < 0.05$) difference between defects and normal myocardium. Three patients showed no defects on their coronaries, nuclear or Z-score images. Seven patients had visible defects in the coronary images, visualized on the both the SPECT and Z-score images. Three patients without evidence of obstructive coronary disease on CTA showed defects on the SPECT and on the Z-score. This finding could be lysis of previous obstructing thrombus or microvascular disease in the coronary circulation. Two patients had SPECT with possible defects but CTA showed normal variant decrease flow in apical region. One patient showed ischemia on SPECT but a noisy CTA scan limited the Z-score map. The Z-score allows better visualization of perfusion defects with higher spatial resolution than SPECT imaging without attenuation artifacts misinterpretation.

06-A-129-NASCI

Congenital coronary artery fistulas: evaluation of 64-slice MDCT appearances in seven adults

Jonathan Dodd, Maros Ferencik, Koen Nieman, Udo Hoffmann, Richard Liberthson, Ricardo Cury, Tom Brady, Suhny Abbara

Massachusetts General Hospital, Boston, MA, USA

e-mail: jddodd@partners.org

Purpose To evaluate the cardiac 64-slice multi-detector computed tomography (MDCT) appearances of congenital coronary artery fistula (CCAF) in seven adults.

Material and methods Two readers prospectively evaluated the 64-slice cardiac MDCT appearances in seven adults diagnosed with CCAF in consensus (five male/two female, mean age 54, range 32–72). The proximal vessel, subsequent course and distal vessel entry site of the CCAF were evaluated. Maximal receiving

chamber/vessel dimensions were recorded in end-ventricular systole using retrospective multisegment reconstructions at 10% increments of the cardiac cycle. Images were also evaluated for the presence of a contrast shunt sign secondary to the CCAF.

Results The origin of all CCAF was clearly outlined in all patients and involved the right coronary artery in one case, the right sinus of valsalva in one case, the left circumflex artery in one case, multiple origins from the left anterior descending artery in two patients, and multiple origins from the left and right coronary systems in two patients. The subsequent anatomical course of all CCAF was clearly visualized on MDCT. Site of entry of the distal vessel involved multiple small entry vessels in three patients, a single entry vessel in two patients and division into multiple tiny vascular lakes in one case. Receiving right-sided heart chambers were enlarged in all patients. The contrast shunt sign was present in two patients indicating the site and patency of shunt flow.

Conclusion Cardiac 64-slice MDCT provides excellent visualization of the origin, course and distal vessel entry site of CCAF as well as the size of the receiving chamber. In select patients in whom precise anatomical and physiological information cannot be obtained from other modalities, MDCT may provide definitive clarification allowing optimal interventional decision-making.

06-A-130-NASCI

Impact of 64-Detector CT coronary angiography on volume of diagnostic cardiac catheterization

Bruce Rutkin, Amgad Makaryus, Jason Freeman, Lawrence Boxt
North Shore University Hospital, Manhasset, NY, USA
e-mail: brutkin05@yahoo.com

Background We examined if 64-slice cardiac CT (64-CT) impacted the volume of patients undergoing coronary angiography (CA) or nuclear stress testing at our institution.

Methods The volume of cardiac catheterizations, nuclear stress tests, and 64-CT at our institution in the year prior to initiation of our 64-CT program (year A, 4/1/04 to 3/31/05) and the first year during its use (year B, 4/1/05 to 3/31/06) was tracked. We were interested in the ratio of coronary interventions to the total number of cardiac catheterizations performed, possibly suggesting that the number of CA not requiring intervention were reduced with the advent of the 64-CT.

Results 13,716 cardiac catheterizations were performed at North Shore University Hospital in year A and 13,665 in year B. Of the total CA performed during year A, 9,767 (71.2%) required no coronary intervention. During year B, 9,730 of the CA (71.2%) required no intervention. The ratios of coronary interventions to total catheterizations performed was 28.8% and identical in years A and B. Additionally, there was no significant reduction in the number of nuclear stress tests performed during year B.

Conclusion We performed 1,200 64-slice cardiac CT angiograms at our institution in the past year. While we had expected to see a decrease in the number of diagnostic cardiac catheterizations and/or nuclear stress tests performed, we did not in either case. The absolute consistency in the ratio of diagnostic CA and interventions over the two years raises several points. First, it may be too nascent in our 64-CTA experience to have influenced the volume of traditional cardiac imaging modalities. Second, while we are likely selecting the appropriate group of patients for the 64-CTA (only 4.2% have been referred for CA), we may be identifying a new population of patients at risk for CAD who were previously unscreened and undertreated.

06-A-131-NASCI

Smaller pulmonary Vein ostia area is associated with recurrent arrhythmia following pulmonary venous antral isolation for atrial fibrillation

Subramanya Prasad, Andre Natale, Milind Desai, Dhanunjaya Lakkireddy, Tamer Fahmy, Luigi Dibise, Rong Bai, Dimpi Patel, Lucie Popova, Mandeep Bhargava, Srikanth Sola

Cleveland Clinic Foundation, Cleveland, OH, USA

e-mail: prasads@ccf.org

Background Pulmonary vein antral isolation (PVAI) using radiofrequency ablation is increasingly used for the treatment of atrial fibrillation (AF). We hypothesized that pulmonary vein ostia area, as determined by multi-detector computed tomography (MDCT), would predict recurrent atrial fibrillation after PVAI.

Methods We prospectively evaluated 129 consecutive patients with symptomatic AF resistant to > 2 antiarrhythmics referred for PVAI. Patients who had previously undergone PVAI were excluded from the study. All patients underwent MDCT study of the pulmonary veins using a 16- or 64-slice Siemens Sensation scanner prior to the PVAI procedure. The number and total ostial area of all pulmonary veins, indexed to body surface area, were determined by two independent blinded observers. Left atrial and left atrial appendage volumes were also determined. Patients were followed with transtelephonic monitoring for 6 months, and clinically at 3 months and one year for recurrent AF.

Results We followed 129 patients (85% male, age 56 ± 11 years) for an average of 9 ± 2 months following PVAI for AF. Recurrent AF occurred in 22 patients (17%) during the follow-up period. Mean total area of the pulmonary venous ostia was lower in patients with recurrent AF than in patients who maintained normal sinus rhythm during the follow-up period (total area $357 \pm 13 \text{ mm}^2/\text{m}^2$ vs. $442 \pm 19 \text{ mm}^2/\text{m}^2$; $p = 0.02$). A smaller ostial area of the left superior (LSPV) and left inferior pulmonary veins (LIPV) was also associated with recurrent AF (LSPV $65 \pm 4 \text{ mm}^2/\text{m}^2$ vs. $88 \pm 5 \text{ mm}^2/\text{m}^2$; $P = 0.007$; LIPV $66 \pm 4 \text{ mm}^2/\text{m}^2$ vs. $82 \pm 4 \text{ mm}^2/\text{m}^2$; $P = 0.006$). There was no relationship between left atrial volume, left atrial appendage volume, the number of pulmonary veins, or the right sided pulmonary venous ostia area and recurrent AF.

Conclusions A smaller total pulmonary vein ostia area, particularly of the left sided pulmonary veins, as measured by MDCT is associated with recurrent AF in patients undergoing PVAI.

06-A-132-NASCI

Effects of an intravenous pre-medication regimen on image quality and heart rate prior to coronary CT angiography

Micky Mishra, Michael Militello, Antonette Turay, Phyllis DeSantis, Paul Schoenhagen, Srikanth Sola
Cleveland Clinic Foundation,
Cleveland, OH, USA
e-mail: mishram@ccf.org

Background Pre-medication with beta-blockers or calcium channel blockers is used routinely prior to coronary CT angiography (CTA) to slow heart rate (HR) and reduce cardiac motion at the time of study acquisition. We evaluated the effect of an intravenous-only pre-medication regimen on image quality and heart rate in patients undergoing coronary CTA.

Methods We prospectively evaluated 249 consecutive subjects who underwent coronary CTA on a Siemens Sensation 64- or Philips Brilliance 64-slice multi-detector CT scanner. Subjects were given either intravenous metoprolol (maximum 30 mg) or, for patients with pulmonary disease, diltiazem (maximum 20 mg) to achieve a target HR of 60–70 bpm. Sublingual nitroglycerin was given when tolerated. Image quality was scored on a 3-point scale using a standard 16-segment model by two investigators blinded to the patients' clinical status.

Results 249 subjects (64% male, 53 ± 12 years) underwent coronary CT angiography. 166 subjects (67%) received intravenous metoprolol ($11.6 \pm 8.4 \text{ mg}$); 14 subjects (5%) required intravenous diltiazem ($15.8 \pm 6.6 \text{ mg}$). In the remaining subjects, intravenous pre-medication was not given either because the subject's heart rate was already < 65 bpm (67 subjects) or due to severe aortic insufficiency (two subjects). HR decreased from $72 \pm 13 \text{ bpm}$ to $65 \pm 8 \text{ bpm}$ after medication ($P < 0.001$). A target HR was achieved in 88% of study subjects. Patients in the highest quartile of image quality scores had a lower final HR than those in the lowest quartile ($69 \pm 3 \text{ bpm}$ vs. $80 \pm 10 \text{ bpm}$; $P = 0.02$) although there was

no difference in pre-medication type or dose between the different quartiles. There were no adverse events related to study pre-medication.

Conclusions A pre-medication regimen of intravenous-only metoprolol or diltiazem safely reduces heart rate to 60–70 bpm in 88% of study subjects prior to coronary CTA. However, image quality is dependent on the final HR achieved, rather than the type or dose of medication used.

06-A-133-NASCI

Influence of somatotype on left ventricular mass

Abdullahi Adamu, Mikhail Babaev, Alexander Kondrashev, Nikolai Nelasov, Olga Yeroshenko
Rostov State Medical University, Rostov-on-Don, Russian Federation
e-mail: scorpion68kd@yahoo.com

Background Left ventricular mass is known to be dependent upon several constitutional factors like height, body weight and body composition. The influence of somatotype on LVM needs to be evaluated as it is sometimes necessary to delineate between higher limit of normality and early manifestation of disease. This study aimed to examine the effect of body habitus on left ventricular mass in healthy individuals.

Materials and methods –165 healthy individuals in the age range 17–23 years (85 females and 80 males) underwent anthropometry and M-mode echocardiography. Using the method of R.N.Dorokhov and V.G.Petrukhin (1989), the individuals were grouped according to somatotype into nanosomic (I), microsomic (II), micromesosomic (III), mesosomic (IV), mesomacrosomic (V), macrosomic (VI) and megalosomic (VII). Left ventricular mass was calculated using the ASE-recommended method.

Results In this study, no individuals with types I and VII somatotypes were found. Left ventricular mass is considerably higher in males than in females (140.49 and 108.40 g respectively). In females the values obtained for the different somatotypes are 109,86 g (II), 109,50 g (III), 104,13 g (IV), 106,59 g (V) and 109,67 g (VI). No apparent difference was observed in LVM amongst females. However, in males we observed

a progressive rise in LVM with increasing body habitus –123.90 g (II), 125.07 g (III), 134,40 g (IV), 142,00 g (V) and 162,28 g (VI).

Conclusions Left ventricular mass increases with increasing body size in males but not in females.

06-A-134-NASCI

Precontrast detection of myocardial infarction using T1 weighted imaging

James Goldfarb
St. Francis Hospital, Roslyn, NY, USA
e-mail: James.Goldfarb@chsli.org

Background Although contrast enhanced techniques are typically used to identify myocardial infarction, precontrast T1 weighted MR imaging can readily identify recent myocardial infarcts (MIs) due to local edema and chronic MIs due to their increased fat content.

Method and materials Thirty-one patients with documented prior MIs underwent MR imaging on a clinical 1.5 T MR scanner using both pre- and post-contrast inversion recovery SSFP CINE imaging. 22 patients had MIs older than 6 months (11.6 ± 10.3 years) and nine patients had infarcts within 6 months of the MR scan (0.9 ± 12 years). Images from each patient were selected with the lowest signal from epicardial fat (fat nulled) and functional myocardium (muscle nulled). To quantify the contrast between the MI and adjacent tissue, signal difference to noise ratios between the infarct and adjacent myocardium were performed. Precontrast infarct location and detection was compared with post contrast delayed hyperenhanced imaging.

Results Fat nulled imaging was useful in identifying older myocardial infarct. Older myocardial infarct were seen as hypointense regions. Muscle nulled images were better for detecting recent myocardial infarcts and showed hyperintense regions due to myocardial edema of the region at risk.

Conclusion Precontrast T1 sensitive MR imaging is a new technique for imaging of myocardial infarction. It has the ability to identify and discriminate between recent and chronic myocardial infarcts.

06-A-135-NASCI**Screening of asymptomatic coronaropathy with adenosine stress myocardial perfusion MRI: a pilot study**

Denis Brisbois, Alain Nchimi, Bruno Raskinet, Julien Djekic, Adrian Morar, Thomas Brouseaud, Isabelle Mancini, Paul Magotteaux
CHC, Liege, Belgium
e-mail: denis.brisbois@chc.be

Objectives (1) Evaluate the prevalence of the myocardial perfusion abnormalities in asymptomatic patients with high cardiovascular risk factors. (2) Evaluate the diagnostic value of myocardial perfusion MRI as systematic screening test in these patients.

Material and methods A retrospective study of 103 consecutive asymptomatic patients (F/M = 54/49) with high cardiovascular risk factors explored from 01/2004 to 06/2005 was performed. The MRI exams were a part of a clinical protocol including a study of perfusion with a first passage at rest and during a maximal stress (adenosine). Ninety-seven patients do not underwent a coronarography but they were clinically followed (mean follow-up = 15 months). The diagnostic value of myocardial perfusion MRI was calculated using the results of coronarography and/or clinical follow-up as gold standard.

Results The percentage of significant stenoses detected by coronarography was 2/103 (1.9%). The values of sensibility, specificity, positive predictive value, negative predictive value of the myocardial perfusion MRI in the target population were, respectively, of 100%, 92%, 40% and 97%.

Conclusion Myocardial perfusion MRI at rest and during a perfusion stress is an efficient screening test for the detection of asymptomatic coronaropathy.

06-A-137-NASCI**Impact of cardiac motion on assessment of coronary artery stenosis using multidetector CT angiography**

Yves Provost, Narinder Paul, Andre Pereira,

Dyrdre Doyle, Mark Hansen
UHN-Toronto General Hospital, Toronto, ON, Canada
e-mail: yves.provost@uhn.on.ca

Cardiac motion remains one of the most frequent technical limitations to assess the degree of coronary artery stenosis during CT Angiography. Previous studies using 16- or 64-slice multidetector CT Angiography have focused on the ability to detect and quantify coronary artery stenosis using conventional invasive coronary angiography as the gold standard in the absence of cardiac motion. We will present the results of 50 consecutive patients suspected of significant coronary artery disease and undergoing 64-slice multidetector CT Angiography. All patients will receive appropriate premedication to lower the heart rate below 70 beats per minute and to achieve maximal vasodilatation using sublingual nitrates. The volumetric data will be obtained using a multisegment reconstruction technique to optimize the temporal resolution. The image display that best enhances visual inspection of coronary artery anatomy and appreciation of potential stenoses will be evaluated. The degree of cardiac motion that precludes evaluation of the coronary arteries will be assessed by comparing the results to conventional invasive coronary artery angiography performed within less than 14 days following the multidetector CT Angiography study.

06-A-138-NASCI**Pulmonary embolism—important CT findings besides the clots**

Pierre Maldjian
University Hospital, UMDNJ-New Jersey Medical School, Newark, NJ, USA
e-mail: maldjipd@umdnj.edu

Computed tomography angiography has become the study of choice for the workup of suspected pulmonary embolism. In addition to visualization of the pulmonary clots, other findings with significant cardiopulmonary implications may also be present on CT pulmonary angiograms. This presentation will review the appearances on CT

pulmonary angiography of important conditions that may be associated with pulmonary embolism. These include: right ventricular dysfunction (strain), pulmonary artery hypertension, intracardiac thrombi, intracardiac shunts and paradoxical embolism. Correlation with echocardiography will also be shown demonstrating the complimentary nature of these two modalities.

06-A-139-NASCI

Evaluation of cardiac chamber enhancement during 64-slice coronary CT angiography using a triphasic contrast injection protocol and automated bolus tracking

William Boonn, Harold Litt, Sridhar Charagundla
University of Pennsylvania Health System, Philadelphia, PA, USA
e-mail: william.boonn@uphs.upenn.edu

Purpose 64-slice coronary CTA is possible using short-lived boluses of contrast with high flow rate and automated bolus tracking, however, enhancement of all cardiac chambers is needed for complete assessment of cardiac morphology and function, particularly in patients with congenital heart disease. The purpose of this study was to evaluate enhancement of all four cardiac chambers as compared to the interventricular septum using a triphasic injection protocol, and determining influence of automated delay time on scan performance.

Method and materials 24 subjects underwent coronary CTA on a 64-slice MDCT scanner using a triphasic injection of contrast. Scan timing was determined by automated bolus tracking in the descending thoracic aorta. Using reformatted images created retrospectively, enhancement was measured within regions of interest in the left and right ventricles (LV and RV), in the interventricular septum (IS), and in the left and right atria (LA and RA). The delay between start of contrast injection and ventricular image acquisition was recorded.

Results All studies were of diagnostic quality for coronary CTA. Mean chamber enhancement measured as follows (mean \pm SD in HU): RA 185 ± 47 , RV 190 ± 52 , LA 311 ± 83 , and LV

296 ± 72 . Mean IS attenuation measured 116 ± 17 HU. All 24 cases showed greater than 50 HU difference between the LV lumen and IS, whereas 16/24 cases showed greater than 50 HU difference between the RV lumen and IS. There was a significant negative correlation between right ventricular enhancement and delay time ($R = -0.64$, $P < 0.001$).

Conclusion The triphasic injection protocol resulted in optimal LV chamber enhancement in all cases and adequate RV chamber enhancement in 2/3 of cases. Suboptimal RV enhancement occurred with increased scan delay. When cardiac CT is used to evaluate the morphology and function of both ventricles, injection protocols must be modified to achieve consistent RV enhancement.

06-A-140-NASCI

Prospective ECG gating in cardiovascular CT imaging achieves 70% dose reduction while maintaining image quality

John Londt, Melissa Vass, Jiang Hsieh, Erdogan Cesmeli, Uri Shreter
GE Healthcare, Waukesha, WI, USA
e-mail: john.londt@ge.com

Purpose Developing imaging methods that maintain diagnostic image quality in cardiovascular CTA exams while substantially reducing radiation dose is highly desirable. Limiting X-ray exposure to only those cardiac phases required for diagnosis has a potential for dramatic dose reduction. The purpose of this work was to evaluate the image quality and dose performance of a new prospective ECG gating scanning method in comparison to retrospectively gated helical scans.

Method New advancements in X-ray and table-motion control were used to achieve fast and precise timing with minimal delays, which enable prospective ECG gated acquisition for contrast enhanced coronary CTA. A new reconstruction algorithm was developed to optimize image quality for this acquisition mode. The technique was used on an image quality phantom,

with simulated ECG signal of 40–65 bpm, measuring noise, slice profile, in-plane resolution and dose using a volume scanner with 64×0.625 mm slices (GE LightSpeed VCT, Waukesha, WI USA). Prospectively gated axial scans were acquired with a halfscan plus 20% of the heart cycle duration to accommodate changes in heart rate during the acquisition. Both methods used 0.35 s rotation speed, covered 14 cm of scanned length and used tube current settings from 300 mA to 600 mA. Helical scans were done with and without ECG modulation.

Results In-plane spatial resolution and slice sensitivity profiles across the scanned volume were equivalent between the two scanning modes when reconstructed with the same kernels. Ten percent higher mA was used for prospectively gated scans as compared to helical scans to maintain equivalent image noise level. This prospectively gated technique demonstrates 75–78% dose reduction compared to non-modulated mA helical scans and 54–60% compared to aggressively modulated mA helical scans.

Conclusion Prospectively gated acquisitions can provide up to 78% dose reduction without degrading image quality for contrast enhanced coronary CTA. Clinical evaluations are underway.

06-A-141-NASCI

Identification of small atrial septal defect on coronary CTA studies

Nina So, Chi Wong
St. Teresa's Hospital, Hong Kong, China
e-mail: ninamc_so@yahoo.com.hk

Objective Identify small atrial septal defects on coronary CTA

Materials and methods Coronary CTA scans of 75 consecutive patients obtained between 26 Feb 2006 and 7 Mar 2006 were reviewed. The studies were performed on a 64-MDCT scanner (Sensation 64, Siemens) using Carebolus technique and retrospective ECG gating. Scans were reviewed interactively using multiplanar reconstructions. Presence of atrial septal defect was defined as either presence of a jet of contrast from

the well opacified left atrium to the much less opacified right atrium through the interatrial septum or presence of a definite contrast filled track between the left and right atria. The size of the defect was defined either as the largest diameter of the jet or size of the defect measured at the right atrial side of the septum.

Result 9 patients showed positive evidence of atrial septal defect. Six of these were fossa ovalis defects, which measured 3.5, 2.8, 3.8, 6.5 and 6.8 mm. The other three defects were sinus venosus defects and opened in the right atrium just below the superior vena cava with contrast filled tracts originated from the high left atrium. The sizes of these three defects measured on the right atrial side of the septum were 2.8, 3.6 and 5.2 mm.

Conclusion and discussion Atrial septal defects could be identified on coronary CTA studies. CTA studies with similar contrast enhancement in the right and left atrium precluded assessment of small septal defect. There was no reference test available to exclude false negative results. Further studies will be required to evaluate whether MDCT studies of the heart with a good washout of the contrast from the right atrium will become a comparable test to ultrasound in the detection of small atrial septal defects.

06-A-142-NASCI

Dr Robert Kelly, Clinical Instructor in Medicine

Robert V. Kelly, Mauricio G. Cohen, Walter A. Tan, David Tate, George A. Stouffer
UNC, Chapel Hill, NC, USA
e-mail: rkelly@med.unc.edu

There is greater in-stent restenosis in the proximal LAD compared to other coronary arteries. Stent sizing is determined by lumen opacification with angiographic contrast (CM) of which Iohexol is the most commonly used. Iohexol causes vasoconstriction in animals but effects on human coronary arteries are poorly understood. Since undersizing of stents is a major risk-factor for restenosis, we examined whether iohexol causes vasoconstriction of the proximal LAD in patients with atherosclerotic disease.

Methods The effects of iohexol were studied in 12 patients referred for PCI of proximal LAD. Lesions were assessed by quantitative coronary angiography (QCA) and intravascular ultrasound (IVUS). Fractional Flow Reserve (FFR) was measured using a pressure wire.

Results There were seven men and five women, with a mean age of 63 years (range 37–86). The reference vessel diameter was 2.9 mm with QCA and 4.0 mm with IVUS ($P < 0.05$). The mean % lesion stenosis was 72% on QCA. The IVUS-measured mean lumen diameter at the level of the lesion was 2.36 mm (2.26–2.45) at baseline and 2.19 mm (2.11–2.33) during administration of iohexol ($P = 0.002$). The cross sectional area decreased from 4.21 mm² at baseline to 3.87 mm² with iohexol ($P = 0.017$). The proximal reference vessel diameter (RVD) decreased from 4.35 mm to 4.31 mm and CSA from 15.8 mm² to 14.7 mm² ($P = 0.017$), while the distal RVD changed from 3.84 mm to 3.64 mm and CSA from 11.54 mm² to 10.54 mm² ($P = 0.017$) after injection of iohexol. The mean FFR was 0.80 at baseline, 0.69 with adenosine, 0.67 with iohexol, 0.67 with a mixture of iohexol and adenosine and 0.99 after stenting.

Conclusion Iohexol has significant effects on coronary vasomotor tone causing vasoconstriction of atheromatous segments of the proximal LAD artery with a significant reduction in mean lumen diameter. It also induces maximal hyperemia presumably through an effect on the microvasculature.

06-A-143-NASCI

Infarct size and microvascular obstruction are related to duration of ischemia prior to thrombolysis

John Younger¹, John Greenwood¹, Sven Plein¹, Jullian Barth¹, Mohan Sivananthan², John Ridge-way¹, Steven Ball¹

¹Leeds University, Leeds, UK

²Leeds General Infirmary, Leeds, UK

e-mail: jonnyyounger@hotmail.com

Objectives The aims of this study were to relate the ischemic time prior to thrombolysis to both infarct size and presence of MVO as assessed by LGE-CMR. Additionally, infarct mass by LGE-CMR was compared with creatine kinase, 12- and 72-h troponin-I concentrations. **Background** The prevalence of microvascular injury in medically treated acute coronary syndromes is unknown. Late gadolinium hyper-enhancement cardiac magnetic resonance imaging (LGE-CMR) accurately quantifies infarct size and demonstrates microvascular obstruction (MVO).

Methods Ninety-seven patients underwent LGE-CMR at 3.7 ± 1.4 days after medically treated first acute myocardial infarction (AMI). Areas of hypoenhancement surrounded by hyper-enhanced myocardium were identified as MVO. Serum troponin-I concentrations were measured at 12 and at 72 h after admission, in addition to serial creatine kinase (CK) levels.

Results Ninety-three patients, of whom 71 had received thrombolysis, completed the CMR study and 25 demonstrated MVO. Time to thrombolysis related both to mass of MVO ($r = 0.48$, $P < 0.0001$), and to total infarct mass ($r = 0.26$, $P < 0.027$). Door-to-needle time showed no association with either infarct mass or MVO. Infarct size was larger in patients with MVO compared to those without (mean 37.6 g vs. 15.3 g respectively, $P < 0.0001$). Peak CK, 12-h troponin-I, and 72-h-troponin-I were related to acute infarct size ($r = 0.74$, $P = 0.0001$; $r = 0.56$, $P = 0.0003$; $r = 0.62$, $P < 0.0001$, respectively).

Conclusion In medically treated AMI patients, acute infarct size and the presence of MVO are related to duration of pain prior to thrombolysis. Infarct size is better reflected by peak CK and 72-h-troponin-I than by 12-h-troponin-I.

06-A-144-NASCI

Coronary CTA with conventional angiographic correlation: anatomy, normal variants and anomalies

Cylen Javidan-Nejad¹, Brian Seeck², Fernando Gutierrez¹, Sanjeev Bhalla¹, Pamela Woodard³

¹Mallinckrodt Institute of Radiology, Washington University School of Medicine, St.Louis, MO, USA

²Cardiovascular Laboratory, Washington University School of Medicine, St.Louis, MO, USA

³Cardiovascular Laboratory, Mallinckrodt Institute of Radiology, Washington University School of Medicine, St.Louis, MO, USA

e-mail: javidanc@mir.wustl.edu

Coronary artery disease (CAD) is associated with high annual mortality and morbidity in the United States. The need for early diagnosis and treatment results in the need for faster and less invasive ways of CAD diagnosis. Conventional angiography has been the gold standard for imaging the coronary arteries, however being an invasive procedure it has risks of its own. High temporal and spatial resolution required to image the coronary arteries of a beating heart has been achieved with 16- and 64-multidetector row computed tomography (MDCT). Post-processing software available to create 3-dimensional CT angiography is currently used by radiologists to evaluate the vasculature and their relationship with the cardiac chambers. As coronary CTA becomes more widely available, it is essential for the radiologist to become familiar with normal coronary anatomy and variants and the conventional nomenclature currently used in cardiology literature to describe these vessels. Such will result in accurate communication with clinicians when describing atherosclerotic disease. Similarly the same terminology should be used when describing coronary artery anomalies, as an accurate description guides the clinician towards an appropriate treatment plan. Since traditionally the coronary arteries have been depicted by angiography, both CTA and conventional angiography appearance of normal, variant, and anomalous coronary arteries will be shown. This exhibit will educate the reader of normal anatomy and variants of coronary arteries as depicted on axial and CTA images. Anomalies of coronary arteries will be described, while explaining their clinical significance and possible pitfalls of CTA diagnosis.

06-A-145-NASCI

Left ventricular aneurysm and pseudoaneurysm: imaging features and clinical implications

Cylen Javidan-Nejad, Fernando Gutierrez, Sanjeev Bhalla, Pamela Woodard
Mallinckrodt Institute of Radiology, Washington University School of Medicine, St.Louis, MO, USA

e-mail: javidanc@mir.wustl.edu

Left ventricular aneurysms are complications of myocardial infarctions. They usually require no treatment other than anticoagulation, as they can be a source of thrombotic emboli. Surgical repair, such as the Dor procedure, is advocated when the aneurysm is large enough to compromise cardiac function. Contrarily, pseudoaneurysms of the left ventricle require immediate intervention due to their unstable nature. So it is imperative to differentiate true from false ventricular aneurysms.

Computed tomography and magnetic resonance imaging are reliable means to identify cardiac aneurysms and differentiate true from false aneurysms. By knowing the imaging features of the two and other mimickers, the radiologist can play a key role in diagnosis and directing appropriate management.

06-A-146-NASCI

Step-by-step approach to MDCT of adults with congenital heart disease

Cylen Javidan-Nejad¹, Sanjeev Bhalla¹, Pamela Woodard¹, Joseph Billadello², Fernando Gutierrez¹

¹Mallinckrodt Institute of Radiology, Washington University School of Medicine, St. Louis, MO, USA

²Section of Cardiology, Department of Internal Medicine, Washington University School of Medicine, St. Louis, MO, USA

e-mail: javidanc@mir.wustl.edu

The diagnosis and treatment of congenital heart disease has markedly improved in the past few decades. This has resulted in an increasing number of such patients reaching adulthood with both repaired and unrepaired lesions. Many are imaged by computed tomography for noncardiac complaints and frequently the radiologist is not provided by an accurate history describing the underlying cardiac disease and past surgical repairs. Having a systematic approach is essential to evaluate for underlying congenital heart disease and to identify the various repairs and possible surgical complications.

06-A-147-NASCI

Determination of the optimal concentration of a gadolinium and iodinated contrast mixture for coronary angiography and ventriculography

Sean Javaheri, Bernard Rubal, John Ward, Terry Bauch

Brooke Army Medical Center, Ft Sam Houston, TX, USA

e-mail: sean.javaheri@amedd.army.mil

Objective To determine the ideal concentration of a gadolinium and iodinated contrast mixture for coronary angiography and ventriculography in a swine model. *Background* Case reports have described the use of gadolinium based coronary angiography and ventriculography in patients at high risk for contrast induced nephropathy, although the ideal concentration of a gadolinium and iodinated contrast mixture has yet to be determined.

Methods Ex vivo and in vivo comparisons of various concentrations of gadolinium and iodinated contrast were compared to 100% iodinated contrast. In vivo quantitative and qualitative comparisons of coronary angiography and ventriculography were performed in a swine model. The hemodynamic effects of gadolinium ventriculography were monitored for 30 s after performance of ventriculography.

Results Qualitative comparisons of coronary angiography and ventriculography revealed that a 50:50 mixture was best and most comparable to 100% iodinated contrast. In this limited swine model, there were no adverse hemodynamic

effects associated with the use of gadolinium during ventriculography.

Conclusions The ideal concentration of gadolinium and iodinated contrast appears to be a 50:50 mixture for both coronary angiography and ventriculography. It appears adequate coronary angiography and ventriculography can be performed without a significant decrease in image quality. Further investigation of a mixture of gadolinium and iodinated contrast should be undertaken in order to find a safer contrast agent for various angiographic and radiologic procedures in the prevention of contrast induced nephropathy.

06-A-148-NASCI

Delayed enhancement MRI of myocardial damage: correlation with electroanatomic mapping

Benoit Desjardins, Thomas Crawford, Frank Bogun, Fred Morady

University of Michigan, Ann Arbor, MI, USA

e-mail: benoitd@umich.edu

Introduction Delayed enhanced MRI (DE-MRI) provides precise imaging of the distribution of myocardial damage. The purpose of this study is to assess the electrical properties throughout areas of infarcted myocardium on DE-MRI, using endocardial electroanatomic mapping by catheter (EM).

Methods Six patients with ventricular tachycardia post-infarct (mean age 69, mean LVEF 36%) were imaged by DE-MRI on a 1.5 T GE magnet. The patients then underwent EM prior to ablation therapy, using the CARTO system (Biosense-Webster) and intra-vascular catheters with a 4 mm tip electrode. A total of 2026 EM measurements were performed, and classified by electrical potential amplitude and signal duration. Areas of infarct on DE-MRI in the left ventricle were segmented manually, displayed as a bullseye map, and correlated with EM measurements.

Results Areas of infarct as demonstrated by DE-MRI correlated well with areas of low voltage on EM (red circles on Fig. 1d), with optimal cutoff voltage < 1.0 mV ($R = 0.92$, $P = 0.02$). Areas of normal voltage were only found in areas of normal signal on DE-MRI, and areas of high signal on DE-MRI had a

lower bipolar voltage than areas of normal signal on DE-MRI (0.57 ± 0.6 mV vs. 2.0 ± 1.7 mV; $P < 0.0001$), as well as broader signals (117 ± 60 ms vs. 78 ± 13 ms; $P < 0.0001$).

Conclusion Areas of myocardial infarct as demonstrated by EM measurements correlate well with areas of high signal on DE-MRI. DE-MRI can therefore be used to facilitate EM and ablation in patients with arrhythmia post-infarct.

Figure represents an inferior myocardial infarct is demonstrated by high signal on DE-MRI (a, b) and low (red) signal on ME (c). A bullseye map (d) shows that areas of infarct (black) on DE-MRI correlate well with areas of abnormal signal on EM (red circles).

06-A-149-NASCI

Thrombembolic myocardial infarction in patients with coronary artery ectasia—detection with MR imaging

Peter Fries, Heiko Kilter, Ingrid Kindermann, Michael Böhm, Jörn Balzer, Günther Schneider
University of Saarland, Homburg, Germany
e-mail: drpeterfries@googlemail.com

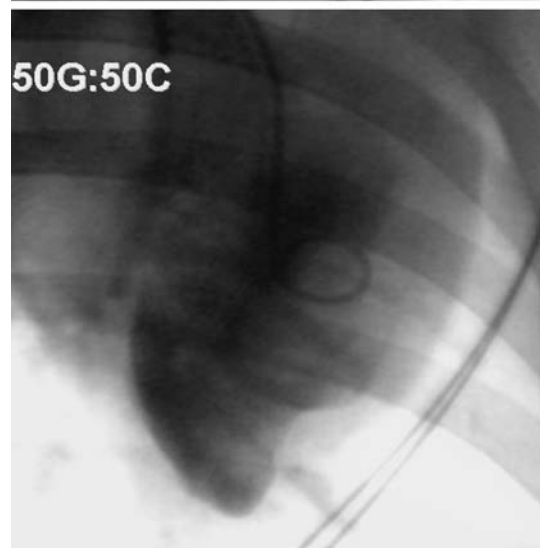
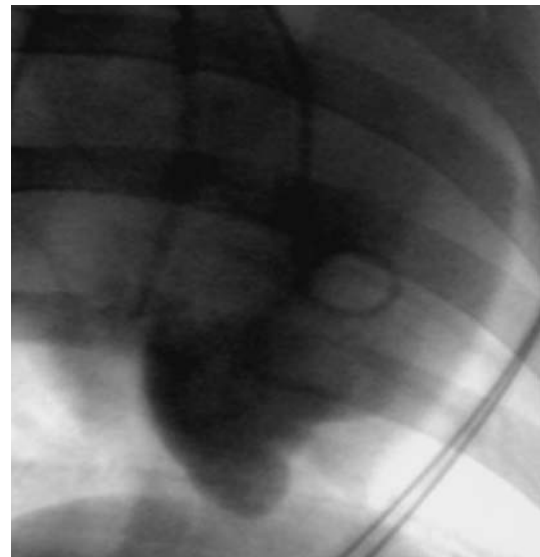
Introduction Coronary artery ectasia (CAE) represents a rare pathology of the coronary arteries, defined as a distension of a coronary vessel 1.5–2 times the diameter or coronary aneurysms with more than 2 times the diameter of adjacent not dilated vessel segments. Fifty percent of cases occur as concomitant pathology in coronary atherosclerosis. Twenty to thirty percent are considered to be congenital in nature, while about 10–20% are associated with inflammatory or connective tissue diseases, the incidence of CAE is 0.3–4.9% in coronary angiography studies. Myocardial ischemia may occur in patients with CAE as a result of coronary artery stenosis or thrombembolic infarctions.

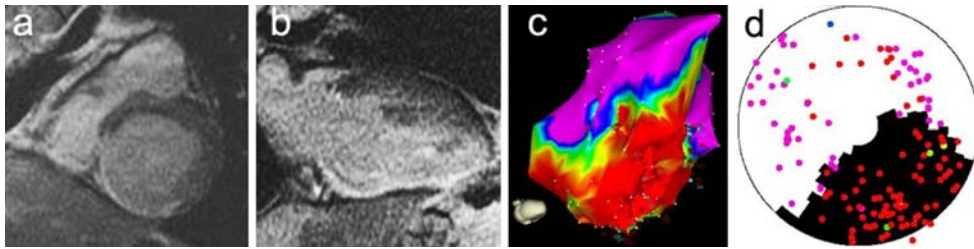
Material and methods Between January and November 2005 approx. 0.3% of patients (16 patients) with suspected coronary artery disease that underwent coronary angiography showed CAE. These patients underwent MRI of the heart to evaluate global and regional function (CINE SSFP-sequences) as well as dynamic T1w IR perfusion studies and T1w inversion recovery

sequences for detection of late hyperenhancement as an indicator of myocardial ischemia after the application of 0.1 mmol/kg body weight Gd-BOPTA.

Results Five patients (31%) showed small circumscribed areas of late hyperenhancement with diffuse left ventricular distribution and reduced wall motion representing areas of thrombembolic infarction. These findings did not correlate with typical ECG-findings, elevated serum levels of MB-CPK or troponin or typical clinical symptoms like angina pectoris or dyspnea.

Conclusion Thrombembolic infarctions in patients with CAE may occur as “silent” infarctions





without typical findings on ECG, increased serum levels of CPK or troponin. Contrast enhanced cardiac MRI represents the only tool to evaluate thrombotic infarctions in patients with CAE, since the size of infarcted areas is rather small and only MRI is able to provide a sufficient spatial resolution. In these patients, consequent anticoagulation has to be considered in order to avoid further events.

06-A-150-NASCI

MR imaging and contrast enhanced MR angiography in diagnosis and follow-up of congenital heart disease

Günther Schneider, Peter Fries, Ingrid Kindermann, Angelika Lindinger, Alexander Massmann, Hans-Joachim Schäfers
University of Saarland, Homburg, Germany
e-mail: ragsne@uniklinikum-saarland.de

Magnetic resonance imaging (MRI) is generally considered as well-established imaging modality for evaluation of congenital and acquired heart disease. Accurate determination of cardiac and vascular anatomy and the underlying function is essential for patient management at initial diagnosis as well as for follow-up studies after operative repair of cardiovascular malformations. The presented exhibit will review the application of functional and contrast-enhanced MRI for the diagnosis of different forms of congenital and acquired disease of the heart and great vessels. Imaging procedures and protocols including unenhanced and contrast enhanced cardiac MRI in addition to the application of multiphase MR angiography studies after application of 0.1 mmol/kg bodyweight Gd-BOPTA will be discussed. Special interest will be taken on protocol optimization as well regarding unenhanced

studies as contrast enhanced MRA. Typical imaging findings in patients with congenital heart disease that underwent corrective surgical procedures together with a review of typical postoperative complications will be presented. Cases are discussed in context with clinical findings together with other imaging modalities such as echocardiography and catheter angiography. The role of MRI in the work-up of patients with congenital heart disease will be discussed critically and results of MRI will be compared with the results of MDCT studies.

06-A-151-NASCI

MRI of impaired right ventricular function

Günther Schneider, Alexander Massmann, Ingrid Kindermann, Michael Böhm, Peter Fries
University of Saarland, Homburg, Germany
e-mail: ragsne@uniklinikum-saarland.de

Right ventricular (RV) dysfunction is generally underestimated as a significant cause of acute and chronic heart disease. Because of the anatomic location, the complex shape and the pronounced trabecular structure of the RV echocardiography only allows an orientating analysis of RV function and thus in the past only a limited number of studies have attempted to evaluate RV dysfunction. With MRI it is possible to perform reliable determinations of RV masses and volumes and to analyze the underlying and concomitant diseases. The aim of this study is to demonstrate typical and rare pathologies which may lead to a right ventricular dysfunction. Topics to be covered include different causes of pulmonary hypertension, pulmonary and tricuspid valve disease, septal defects, functional left to right shunts, structural disorders such as arrhythmogenic RV dysplasia and RV involvement in ischemic heart

disease as well as common and rare congenital disorders and post surgical findings. Common and uncommon right atrial and ventricular tumors and pericardial disease will be presented and muscular hypertrophy or infiltrative disease such as amyloidosis in differential diagnosis will be discussed.

Learning objectives To understand the different primary and secondary pathologic conditions leading to RV dysfunction and to appreciate the possible strategies for further work-up of different etiologies on MRI. To gain a detailed understanding of techniques for the morphologic and functional evaluation of RV function, for the evaluation of flow measurements in great vessels and for the quantification of shunts.

06-A-152-NASCI

Visual semiquantitative assessment of delayed enhancement (DE) and first pass (FP) perfusion defects: correlation with planimetric data and global functional outcome at follow up

Luigi Natale, Agostino Meduri, Stefano Palmucci, Antonella Lombardo, Lorenzo Bonomo
Catholic University of Sacred Heart, Rome, Italy
e-mail: lnatale@rm.unicatt.it

Background MRI DE has a strong correlation with infarct size (IS) determined in autoptic studies. However, exact “planimetric” quantification of IS is time-consuming, requiring ROIs tracing on several images using dedicated software.

Purpose to use a visual semiquantitative method to quantify IS and FP and to correlate these data with planimetric measures and global functional indexes assessed 4–6 months after myocardial infarction.

Methods 22 patients with AMI, treated with PTCA, were studied by 1.5 T MRI within 7 days to assess end-diastolic (EDV) and end-systolic (ESV) volumes and ejection fraction (EF). SSFP for contractile function, FGRET for first pass and IR-prep-FGRE sequences for DE were obtained. A dose of 0.1 mmol/Kg of Gd-DTPA was injected at 3 ml/s for FP study, immediately followed by equivalent dose for DE. Additional 4 patients with

chronic infarction were studied with the same protocol. Out of 26 patients, 24 were studied after 4–6 months to assess functional recovery. FP and DE were first scored on a visual scale, based on number of segments involved and on transmural extent (FP-Score, DE-Score), then compared with planimetric-FP and DE measurements, expressed as percentage of myocardial mass.

Results DE Score had good correlation with planimetric-DE ($R = 0.68$, $P < 0.001$), often underestimating IS in large infarcts (mean difference -3.4 ± 21). FP score had less strong correlation with planimetric-FP ($R = 0.46$, $P = 0.015$), overestimating small defects (mean difference 4.9 ± 15). At follow up, DE Score had significant correlation with global function (EDV: $R = 0.75$; ESV: $R = 0.67$; EF: $R = -0.54$) even accounting for initial volumes (EDV: beta = 0.46; ESV: beta = 0.46; EF: beta = -0.6 , $P < 0.05$). FP-score did not show any significant correlation.

Conclusion Visual semiquantitative assessment of DE is feasible and has good correlation with global function at follow-up.

06-A-153-NASCI

CMR evaluation in patients with high grade ventricular arrhythmias

Luigi Natale, Agostino Meduri, Stefano Palmucci, Riccardo Fenici, Lorenzo Bonomo
Catholic University of Sacred Heart, Rome, Liechtenstein
e-mail: lnatale@rm.unicatt.it

Purpose To assess by cardiac-MR the prevalence of myocardial alterations in arrhythmic patients. *Materials and methods* We examined 63 patients with non ischemic ventricular arrhythmias. Premature ventricular complexes had left bundle branch block morphology (LBBB) in 43 cases, in 10 a right bundle branch block contour (RBBB) and 10 had polymorphic patterns (PV). US was negative in 77.6% of patients, while CMR was negative in only 11% of patients. Studies were performed on a 1.5 MR scanner with Cine sequences (Fastcard or FIESTA), bb-FSE and IR-prep FGRE 15 min after injection of 0.2 mmol/kg of Gd-DTPA.

Results CMR found a high prevalence of morphological, signal intensity and functional myocardial abnormalities. RV dilatation was found in 87% of patients with PV arrhythmias, 51% of patients with LBBB morphology, 12% of patients with RBBB morphology. LV dilatation was present in 27%, 26% and 24% of patients with LBBB, PV and RBBB type arrhythmias, respectively. RV wall motion abnormalities were identified in 52% and 37% of patients with PV and LBBB pattern, respectively; LV wall motion abnormalities in 26% and 11% of patients with PV and LBBB pattern, respectively. Free wall RV signal/thickness abnormalities were found in 24.3% of patients (19.6% with LBBB pattern and 4.7 with PV pattern); LV signal abnormalities were found in 13.2% of patients (10.3% with LBBB pattern and 2.9% with PV pattern). Twelve patients underwent myocardial biopsy: eight positive for myocarditis, three positive for ARVD, one had a negative biopsy.

Conclusions In patients with primary ventricular arrhythmias MR documented high prevalence (86%) of morphological, signal intensity and wall motion abnormalities even with negative echocardiogram.

06-A-154-NASCI

Evaluation by MRI of left ventricular remodelling and global functional recovery in patients treated with granulocyte-colony stimulating factor (G-CSF) after acute myocardial infarction (AMI)

Luigi Natale, Agostino Meduri, Stefano Palmucci, Antonella Lombardo, Lorenzo Bonomo
Catholic University of Sacred Heart, Rome, Italy
e-mail: lnatale@rm.unicatt.it

Background Recent data suggest better outcome and functional recovery in patients with AMI treated with stem cells therapy, both with intracoronary delivery or hematopoietic precursor mobilization by G-CSF.

Purpose To assess by MRI the effect of i.v. administration of G-CSF on global myocardial function after AMI.

Methods eight patients with anterior AMI, treated with primary PTCA (TIMI 3) and i.v.

administration of G-CSF (5 mcg/kg for 5 days), were studied by 1.5 T MRI within 7 days and after 3–5 months. Functional, perfusion (FP) and delayed enhancement (DE) studies were obtained. Values were compared with eight control patients (anterior AMI, primary PTCA). FP and DE were scored basing on number of segments involved and on transmural extension. Correlation of FP and DE with functional outcome and differences between the two groups, accounting for FP and DE extent, were assessed with Univariate (LR) and Multivariate Linear Regression (MLR) and Covariance Analysis (ANCOVA).

Results LR showed significant correlation between DE-score and follow-up EDV (FU-EDV), ESV (FU-ESV), and EF (FU-EF). No significant linear correlation with FP-Score was found. MLR and ANCOVA showed a positive trend in G-CSF group for all functional indexes, accounting for differences in DE (effect of G-CSF, expressed as LS-Means: FU-EDV = -22.19 ± 41.54 ml; FU-ESV = -25.13 ± 37.37 ml; FU-EF = $+5.43\% \pm 10.07$). Anyway, the effect of G-CSF approached statistical significance only for FU-ESV ($P = 0.06$).

Conclusion We found a positive trend with partial statistical significance regarding global functional recovery in patients treated with iv G-CSF after AMI. These data need however to be confirmed in larger series.

06-A-155-NASCI

Prediction of regional functional improvement after acute myocardial infarction: comparison between dobutamine echocardiography and contrast enhanced magnetic resonance

Luigi Natale, Agostino Meduri, Stefano Palmucci, Antonella Lombardo, Lorenzo Bonomo
Catholic University of Sacred Heart, Rome, Italy
e-mail: lnatale@rm.unicatt.it

Purpose To predict segmental functional recovery after acute myocardial infarction (AMI) with dobutamine stress echocardiography (DSE) and contrast enhanced magnetic resonance (CE-MRI).

Materials and methods 25 consecutive patients with first AMI (65 ± 8 years) underwent DSE and CE-MRI (GE Signa Excite 2) within 7 days after successful PTCA. Dobutamine was infused stepwise from 10 mcg/kg to 40 mcg/kg. Cine-MRI was performed in short axis (6–8 slices, FIESTA sequences) with additional HLA or VLA slices; delayed imaging (IR-prep FGRE) was obtained in short axis 15 min after 0.2 mmol/kg Gd-DTPA. Regional function was evaluated using a 16-segments LV model (total 240 segments). Delayed Enhancement (DE) was classified as: absent or transmural extent < 50% (Pattern 1) and transmural extent > 50% (Pattern 2). Segmental function was visually assessed with DSE and cine-MR. After 6-months echocardiography and cine-MRI assessed functional recovery

as improvement of segmental WMSI. Segments without functional improvement after DSE and without recovery of WMSI at follow up were considered as necrotic.

Results There was a significant agreement between DSE and CE-MRI in prediction of functional LV improvement. Specificity of DSE in the evaluation of necrosis was 82% and negative predictive value (NPV) was 89%; specificity of DE with transmural extent > 50% was about 88% and NPV was 88%.

Conclusion Functional improvement after DSE and absent or < 50% delayed enhancement are highly predictive of functional improvement at follow up. Both techniques showed significant specificity and NPV in the assessment of myocardial necrosis and showed a significant concordance.